
OXYGENASE ACTIVITIES FOR THE BIOSYNTHESIS OF AROMATIC ANTIOXIDANTS

Giuliana Donadio

Dottorato in Scienze Biotecnologiche – XXVI° ciclo
Indirizzo Biotecnologie Industriali e Molecolari
Università di Napoli Federico II



Dottorato in Scienze Biotecnologiche – XXVI° ciclo
Indirizzo Biotecnologie Industriali e Molecolari
Università di Napoli Federico II



OXYGENASE ACTIVITIES FOR THE BIOSYNTHESIS OF AROMATIC ANTIOXIDANTS

Giuliana Donadio

Dottorando: Giuliana Donadio

Relatore: Prof. Alberto Di Donato

Coordinatore: Prof. Giovanni Sannia

"Vorrei tanto vedere un tramonto.. Ordinate al sole di tramontare..." disse il Piccolo principe.

Rispose il re: "Se ordinassi a un generale di volare da un fiore all'altro come una farfalla, o di scrivere una tragedia, o di trasformarsi in un uccello marino; e se il generale non eseguisse l'ordine ricevuto, chi avrebbe torto, lui o io?"

"L'avreste voi", disse con fermezza il piccolo principe.

"Esatto. Bisogna esigere da ciascuno quello che ciascuno puo' dare", continuo' il re.

"L'autorita' riposa, prima di tutto, sulla ragione...."

INDEX

Abstract	PAG 5
Riassunto	7
Chapter 1 - Introduction	13
1.1 Oxidative stress in biological systems	14
1.2 Phenols and catechols as antioxidants	17
1.3 Microbial biotransformations for the production of phenolic antioxidants	21
1.4 Bacterial Multicomponent Monooxygenases: ToMO as a case study	22
1.5 Baeyer-Villiger monooxygenases as biocatalysts	27
1.6 <i>Bacillus subtilis</i> in industrial biotransformations	30
1.7 Aim of the PhD project	32
Chapter 2 - Materials and methods	35
2.1 Bacterial strains	36
2.2 Bacterial culture media	36
2.3 Antibiotics	36
2.4 Proteins	36
2.5 Plasmids	36
2.6 Plasmidic DNA Purification	36
2.7 Purification of DNA fragments from agarose gel	36
2.8 Preparation of competent cells and transformation of <i>E. coli</i>	37
2.9 Preparation of competent cells and transformation of <i>Bacillus subtilis</i>	37
2.10 Genomic DNA extraction from <i>Bacillus subtilis</i>	37
2.11 Restriction endonucleases	37
2.12 Isolation of plasmid DNA from <i>Bacillus subtilis</i>	37
2.13 SDS-PAGE.	37

2.14 Whole-cell assays	37
2.15 Catalytic assay on crude extract for identification of ToMO activity	38
2.16 Total RNA purification and RT-PCR	38
2.17 Identification of the reaction products of ToMO-catalyzed hydroxylation of non-natural aromatic substrates	39
2.18 Purification of reaction products	39
2.19 NMR and mass spectrometry analysis of catechols	39
2.20 DPPH assay	40
2.21 Cell cultures and extracts	40
2.22 Immunofluorescence	40
2.23 MTT Assay	41
2.24 Ethidium bromide and acridine orange assay	41
Chapter 3 - Results and discussion Section I	43
3.1.1 ToMO from <i>Pseudomonas</i> sp. OX1 for the biosynthesis of phenolic antioxidants	44
3.1.2. Identification and characterization of the products obtained from the ToMO-catalyzed hydroxylation	44
3.1.3 In vitro assessment of the antioxidant potential: the DPPH assay	51
3.1.4 Cytotoxicity studies on H9c2 cell line	55
Chapter 3 – Results and discussion Section II	61
3.2.1 The Industrial scale-up of ToMO-catalyzed hydroxylation: use of <i>Bacillus subtilis</i> as a GRAS host for the heterologous expression of oxygenase activities	62
3.2.2 Cloning the <i>tou</i> gene cluster: integration into the genome of <i>Bacillus subtilis</i>	63
3.2.3 Cloning of <i>tou</i> gene cluster: the use of the non-integrative plasmid pHT01	68

3.2.4 Total RNA purification and RT-PCR	77
Chapter 3 – Results and discussion Section III	79
3.3.1. 3,6 diketocamphane 1,6-monooxygenase, a type II Baeyer-Villiger Monooxygenases from <i>Pseudomonas putida</i> NCIMB 10007	80
3.3.2. Expression and purification of 3,6-diketocamphane 1,6 monooxygenase (3,6 DKCMO)	82
3.3.3 Crystallization of 3,6-diketocamphane 1,6 monooxygenase (3,6 DKCMO)	85
3.3.4 ThermoFluor Assay on 3,6-DKCMO	88
3.3.5 Cloning, expression and purification of the flavin reductase component of 3,6-DKCMO	90
Conclusions	95
References	99
Appendices	105

Abstract

Reactions in which organic compounds are oxygenated or hydroxylated are of great value for organic synthesis. The “oxyfunctionalization” of aromatic compounds is a modification of primary interest for the pharmaceutical and food industries allowing to obtain high-value-added compounds, characterized by a wide array of biological activities, starting from cheap and commercially available molecules. Selective oxyfunctionalization of organic substrates, however, can be a significant problem in organic synthesis, as these reactions are often carried out with strong oxidizing agents and occur with little chemo-, regio-, and enantio- selectivity. Thus, growing attention has been dedicated in the last years to the development of biotransformations, also known as bioconversions, which make use of the metabolic versatility of either purified enzymes or whole microorganisms to perform the oxyfunctionalization of organic substrates of industrial interest. These methodologies, compared with already established chemical processes, are appealing alternatives to obtain active aromatic compounds under mild experimental conditions and without employing toxic reagents. In this thesis project several aspects of this kind of biotransformation were analyzed; more in detail the attention was focused on:

- **The use of the bacterial multicomponent monooxygenase ToMO from *Pseudomonas* sp. OX1 for the production of novel hydroxylated antioxidants starting from commercially available aromatic precursors such as 2-phenoxyethanol, 2,3-dihydrobenzofuran, 2-indanol and phthalan.** The antioxidant potential of the hydroxylated compounds obtained in ToMO-catalyzed bioconversion was assessed both *in vitro*, by using the DPPH assay, and *ex vivo* on the embryonic rat cardiomyoblast cell line H9c2 subjected to oxidative stress induced by sodium arsenite. Not all compounds showed antioxidant potential in the DPPH assay; however, when cells were incubated with any of them, a differential protective effect towards the oxidative stress induced by sodium arsenite was observed.

- **The recombinant expression of ToMO in the GRAS host microorganism *Bacillus subtilis* to analyze the potential use of this bacterium for the industrial scale-up of ToMO-catalyzed hydroxylation of aromatic substrates of interest.** To this purpose, ToMO gene cluster was cloned in two different shuttle vectors, a non-integrative plasmid indicated as pHT01, and Pr19, a vector that allows instead the direct integration of the recombinant gene in *B.subtilis* chromosomal DNA through single crossing-over. In this latter case, no integration was observed. When using a non-integrative shuttle vector, the ToMO system was efficiently expressed in *E.coli*, but RT-PCR experiments showed that almost no mRNA corresponding to the *tou* gene cluster appeared to be transcribed when the plasmid was inserted in *B.subtilis*.

- **The expression and purification of the Baeyer Villiger 3,6-diketocamphane 1,6 monooxygenase (3,6 DKCMO) and its flavin reductase component from *Pseudomonas putida* NCIMB 10007.** The optimization of the expression and the purification of these proteins will pave the way to the future biochemical characterization of this flavoenzyme and to its biotechnological use for the oxyfunctionalization of aromatic compounds of industrial interest.

Riassunto

Attività enzimatiche microbiche per la biosintesi di nuovi antiossidanti fenolici e catecolici.

Gli antiossidanti sono un gruppo di sostanze piuttosto eterogenee dal punto di vista chimico in grado di agire come *radical scavengers* e di proteggere cellule e tessuti dai danni ossidativi dei radicali liberi. Questi ultimi interagiscono con DNA, proteine e lipidi causando, rispettivamente, mutazioni, alterazione dell'attività enzimatica e riduzione della fluidità di membrana (*Reactive oxygen species: metabolism, oxidative stress, and signal transduction*. Apel K., Hirt H.. Annu. Rev. Plant. Biol. 2004; 55:373-399).

In questo panorama rivestono un ruolo particolarmente importante gli antiossidanti di origine vegetale, molecole che, seppur caratterizzate da una notevole varietà chimica, condividono la comune struttura polifenolica. Gli anelli aromatici ossidrilati in generale sono molto sensibili all'ossidazione e reagiscono velocemente con vari tipi di agenti ossidanti, tra cui i radicali liberi, comportandosi come donatori di elettroni (*Transmitting biological information using oxygen: Reactive oxygen species as signaling molecules in cardiovascular pathophysiology*. Shah M.A., Sauer H. Cardiovascular Research 2006; 71:191–194). Ad esempio, uno fra i più abbondanti e potenti antiossidanti nelle olive è l'idrossitirosolo –ovvero il 2-(3,4-diidrossifenil)-etanolo– che contiene un anello catecolico. Il tirosolo, il 2-(4-idrossifenil)-etanolo, secondo composto antiossidante delle olive in ordine di abbondanza, contiene invece un anello fenolico. Tirosolo ed idrossitirosolo, essendo composti idrosolubili, sono presenti come tali nell'acqua di vegetazione delle olive e come esteri liposolubili nella frazione oleosa.

Anche se una alimentazione varia e corretta può fornire un adeguato apporto di tali molecole in condizioni normali, la ridotta disponibilità degli antiossidanti più efficaci in forma pura ne impedisce attualmente l'impiego come veri e propri farmaci in quelle patologie che coinvolgono fenomeni ossidativi e danni da radicali liberi come aterosclerosi, diabete, eventi ischemici e cancro.

Purtroppo, sia la purificazione degli agenti antiossidanti dalle fonti naturali che la loro sintesi chimica risulta attualmente difficoltosa.

La purificazione degli antiossidanti dal materiale vegetale è resa infatti ardua dalla loro elevata reattività chimica, dalla termolabilità e dalla presenza di miscele complesse di composti simili e dei loro derivati esterificati, glicosilati ecc. La sintesi chimica permette agevolmente di convertire anelli fenolici in anelli catecolici, ma la prima reazione di ossidrilazione di un anello aromatico richiede condizioni di reazioni drastiche e non ecocompatibili. Inoltre, a causa della maggiore reattività dei prodotti monoossidrilati rispetto ai composti aromatici di partenza, è difficile controllare la reazione di ossidrilazione e ottenere un singolo prodotto. Di conseguenza le rese sono basse e il prodotto desiderato va comunque purificato a partire da miscele racemiche complesse.

Le problematiche descritte hanno spinto diversi gruppi di ricerca a mettere a punto per i composti aromatici ossidrilati procedure di sintesi alternativa che sfruttano la versatilità e l'efficienza dell'attività catalitica degli enzimi batterici (*A Comparative Study of the Synthesis of 3-Substituted Catechols using an Enzymatic and a Chemoenzymatic Method*, J Advanced Synthesis & Catalysis Berberian, et al 2007.349 4-5 p: 727-739). Tali procedure prendono il nome di bioconversioni (o biotrasformazioni) e sono processi che sfruttano l'azione di catalizzatori biologici, enzimi e sistemi cellulari, per la sintesi di composti di interesse industriale. Tali

metodiche si basano sulla versatilità ed efficacia delle componenti biologiche per la trasformazione di molecole organiche, anche su substrati diversi da quelli convenzionali. Le tecniche di bioconversione, differentemente dai processi di sintesi chimica che utilizzano reagenti tossici e producono scorie spesso inquinanti, permettono di produrre composti puri ed enantiopuri, in maniera semplice ed in condizioni ecocompatibili (*Monooxygenases as biocatalysts: Classification, mechanistic aspects and biotechnological applications* Torres Pazmino, D.E., et al., J Biotechnol, 2010. 146(1-2): p. 9-24).

Nel laboratorio presso il quale è stato svolto il presente progetto di dottorato è già disponibile, in forma ricombinante ed espresso nel ceppo JM109 di *E.coli*, il complesso multienzimatico della toluene/o-xilene monossigenasi (ToMO) da *Pseudomonas* sp. OX1, enzima in grado di catalizzare l'aggiunta di gruppi ossidrilici a diversi substrati aromatici convertendoli in molecole mono- e diossidrilate. Questo enzima rappresenta un sistema molto versatile da utilizzare nelle biotrasformazioni; studi condotti finora dimostrano infatti che impiegando le metodiche della biologia computazionale e dell'ingegneria proteica è possibile alterare in maniera mirata sia la specificità di substrato che la regioselettività della ToMO allo scopo di creare catalizzatori ossidrilasici dotati delle proprietà desiderate (*Regiospecificity of two multicomponent monooxygenases from Pseudomonas stutzeri OX1: molecular basis for catabolic adaptation of this microorganism to methylated aromatic compounds*. Cafaro, V., et al., Appl Environ Microbiol, 2005. 71(8): p. 4736-43).

Diversi mutanti dell'enzima ToMO sono stati recentemente realizzati per effettuare con elevata efficienza la bioconversione di una molecola economica e facilmente reperibile quale il 2-feniletanolo in tirosolo e idrossitirosolo. Questi ultimi sono composti dalla comprovata efficacia nei confronti di diverse patologie cardiovascolari. Nel caso specifico dell'idrossitirosolo è stato ad esempio dimostrato *in vivo* ed *in vitro* che questa molecola esercita un'azione protettiva che previene l'ossidazione delle LDL, contrastando così uno dei passaggi chiave alla base dei fenomeni di aterosclerosi (*Antioxidants in health and disease*. Young IS, Woodside JV. J Clin Pathol. 2001;54(3):176-86.; *Antioxidant relevance to human health*. Wahlqvist MLAsia Pac J Clin Nutr. 2013;22(2):171-6.), (*The antioxidative protecting role of the Mediterranean diet*. Hadziabdić MO, Bozikov V, Pavić E, Romić Z. Coll Antropol. 2012;36(4):1427-34).

Fra i mutanti della ToMO messi a punto recentemente, la variante E103G/F176T espressa nel ceppo di *E.coli* JM109 ha consentito di ottenere, a partire dal 2-feniletanolo e in esperimenti di bioconversione condotti in *batch*, una resa di tirosolo pari a ca. il 50%. Nel terreno di coltura esausto è stata inoltre verificata la presenza anche di una piccola percentuale di idrossitirosolo (*Tuning the specificity of the recombinant multicomponent toluene o-xylene monooxygenase from Pseudomonas sp. strain OX1 for the biosynthesis of tyrosol from 2-phenylethanol*. Notomista, E., et al., Appl Environ Microbiol, 2011. 77(15): p. 5428-37).

La particolare versatilità della monoossigenasi multicomponente ToMO e le strategie bioinformatiche sviluppate recentemente per questo sistema, basate sul docking nel sito attivo della struttura cristallografica della ToMO degli intermedi della reazione di ossidrilazione, hanno quindi incoraggiato l'utilizzo di tale sistema enzimatico per la conversione di nuclei aromatici che non sono substrati naturali dell'enzima allo scopo di sintetizzare nuovi composti ossidrilati antiossidanti per l'industria alimentare e farmaceutica.

Come sottolineato precedentemente, il sistema ricombinante utilizzato attualmente per l'espressione dell'enzima ToMO è l'ospite batterico Gram-negativo *E.coli*. Ai fini

di uno *scale-up* industriale delle bioconversioni operate tramite questa monoossigenasi multicomponente va però ricordato che tale microorganismo non rappresenta un ospite eterologo ideale per l'espressione ricombinante a causa della presenza, nella sua membrana esterna, del lipopolisaccaride (LPS), una endotossina che può provocare shock anafilattico e che sicuramente pone seri problemi negli eventuali processi di purificazione dei prodotti di interesse ed in generale in tutte le fasi di *downstream processing* del processo biotecnologico. Una buona alternativa ad *E.coli* è *Bacillus subtilis*, un batterio Gram-positivo, endo-spirogeno, aerobico, designato come organismo GRAS (**G**enerally **R**ecognized **A**s **S**afe) e non patogeno per l'uomo (*Production of recombinant proteins in Bacillus subtilis*. Schumann, W., Adv Appl Microbiol, 2007. 62: p. 137-89). *B. subtilis* presenta condizioni di crescita simili a *E. coli* ed è inoltre caratterizzato da un efficiente apparato di secrezione. Un'altra caratteristica di questo ceppo batterico è la resistenza a condizioni ambientali estreme attraverso il differenziamento della spora e della cellula madre che la produce. Va inoltre sottolineato che è ormai disponibile una vasta gamma di informazioni sulla fisiologia e la genetica di *B.subtilis*, il che facilita il futuro sfruttamento di tale microorganismo e l'ottimizzazione del suo utilizzo nell'ambito delle bioconversioni industriali (*Developments in the use of Bacillus species for industrial production*. Schallmeyer M, Singh A, Ward OPCan J Microbiol. 2004 Jan;50(1):1-17).

Le reazioni di ossidrilazione catalizzate dalle Monoossigenasi Multicomponente Batteriche (BMM) quali l'enzima ToMO non rappresentano sicuramente le uniche reazioni di "ossifunzionalizzazione" di molecole per la produzione di composti ad alto valore aggiunto di interesse industriale. Le reazioni di ossidazione di "Baeyer-Villiger" sono delle reazioni in cui i chetoni vengono convertiti nei corrispondenti esteri. L'inserimento di un atomo di ossigeno in una ampia varietà di chetoni ciclici ed alifatici per la produzione di esteri o lattoni chirali puri è di fondamentale importanza nella chimica organica poiché tali molecole vengono utilizzate come intermedi e/o precursori per la sintesi di composti importanti per la chimica fine e di composti farmacologicamente attivi (*Investigating the coenzyme specificity of phenylacetone monooxygenase from Thermobifida fusca*. Dudek HM, Torres Pazmlno DE, Rodríguez C, de Gonzalo G, Gotor V, Fraaije MW. Appl Microbiol Biotechnol. 2010 Nov;88(5):1135-43).

Nella sintesi organica tale reazione è condotta in presenza di perossiacidi, agenti ossidanti molto forti e tossici il cui utilizzo presuppone l'impiego di laboriosi passaggi di protezione e di de-protezione per evitare la formazione di prodotti secondari (*Investigating the coenzyme specificity of phenylacetone monooxygenase from Thermobifida fusca*. Dudek HM, Torres Pazmlno DE, Rodríguez C, de Gonzalo G, Gotor V, Fraaije MW. Appl Microbiol Biotechnol. 2010 Nov;88(5):1135-43). Le Monoossigenasi Baeyer Villiger (BVMOs) sono flavoenzimi e rappresentano una ottima alternativa da utilizzare in ambito biotecnologico; tali enzimi, infatti, sono in grado di catalizzare l'ossigenazione di chetoni lineari, ciclici o aromatici a esteri e lattoni in maniera regio- ed enantioselettiva (*Cloning, expression and characterization of a Baeyer–Villiger monooxygenase from Pseudomonas putida KT2440*. Rehdorf, J., Kirschner, A., and Bornscheuer, U.T. Biotechnol. 2007.Lett. 29, 1393–1398; *Functional expression, purification, and characterisation of the recombinant Baeyer–Villiger monooxygenase MekkA from Pseudomonas veronii MEK700*. Völker, A., Kirschner, A., Bornscheuer, U.T., and Altenbuchner, J. Microbiol. Biotechnol. 2008 77, 1251–1260). Tali enzimi rappresentano quindi, insieme alle BMM, dei biocatalizzatori di primaria importanza per le biotecnologie industriali. Ad oggi solo

pochi geni codificanti per le BVMOs sono stati clonati ed espressi e ciò ha rappresentato sicuramente un grosso ostacolo verso l'applicazione industriale di questa classe di enzimi.

Il presente progetto di ricerca ha avuto tre obiettivi principali:

- 1) Utilizzo della BMM ToMO da *Ps. sp.OX1* per la biosintesi di nuovi composti ossidrilati antiossidanti;
- 2) Clonaggio dell'enzima ToMO in un vettore compatibile con l'espressione ricombinante di tale sistema in un ospite eterologo GRAS quale *B.subtilis*.
- 3) Espressione e purificazione della BMVO 3,6-diketocamphane 1,6 monooxygenase (3,6 DKCMO) e della sua componente flavin reduttasica da *Pseudomonas putida* NCIMB 10007.

1) Utilizzo della BMM ToMO da *Pseudomonas sp.OX1* per la biosintesi di nuovi composti ossidrilati antiossidanti.

Nell'ambito di tale obiettivo i composti di partenza sono stati scelti per la loro somiglianza con i substrati naturali di ToMO ed in funzione della diversa natura del sostituente legato all'anello aromatico. La presenza di gruppi differenti legati agli anelli aromatici può influenzare aspetti quali la reattività dei derivati ossidrilati di tali composti nei confronti delle specie ossidanti, la loro farmacocinetica e la distribuzione tissutale e cellulare.

I substrati di partenza individuati sono stati: il 2-fenossietanolo, il 2,3 diidrobenzofurano, il 2-indanolo e lo ftalano. Tali composti sono stati utilizzati in esperimenti di bioconversione in *batch* utilizzando cellule di *E.coli*, ceppo JM109 trasformate con il plasmide pGEM3Z/*wt* ToMO. Per tutti i substrati, eccetto il 2-indanolo, è stata verificata la presenza di prodotti ossidrilati nel mezzo di coltura esausto. Nel caso del 2-indanolo, non convertito dall'enzima *wt*, è stato utilizzato il mutante E103G/F176A, precedentemente realizzato nel laboratorio in cui il presente progetto è stato svolto, che mostra una cavità del sito attivo più ampia rispetto all'enzima *wt*. Tutti i prodotti di ossidrilazione presenti nel terreno di coltura esausto sono stati purificati su HPLC, singolarmente raccolti e identificati mediante NMR e spettrometria di massa. La loro analisi ha evidenziato la presenza di tre derivati monoossidrilati nel caso del 2-fenossietanolo, di un unico derivato fenolico nel caso dello ftalano e di un derivato fenolico e di uno catecolico nella bioconversione dell'indanolo. Nel caso del 2,3 diidrobenzofurano non è stato possibile identificare in maniera univoca il prodotto di ossidrilazione ottenuto. I composti ossidrilati ottenuti e debitamente purificati sono stati utilizzati in un saggio *in vitro* che utilizza un catione radicale cromoforo stabile, come il DPPH (difetilpicrilidrazile), e che consente di valutare la capacità antiossidante della molecola in esame in base alla diminuzione di assorbanza che si osserva in seguito alla "cattura" del radicale DPPH. Prodotti ossidrilati quali il 2-(2'-idrossifenossi)-etanolo, il 2-(4'-idrossifenossi)-etanolo e il 5,6-idrossi-2-indanolo hanno dimostrato in questa tipologia di saggio una efficacia antiossidante comparabile a quella di antiossidanti naturali quali l'idrossitirosolo ed i

carotenoidi. Tutti i nuovi composti ossidrilati sono stati successivamente utilizzati in saggi di attività antiossidante *ex vivo* utilizzando la linea cellulare eucariotica H9c2 soggetta a stress ossidativo indotto da arsenito di sodio. In questo caso è stata innanzitutto stimata la vitalità cellulare in presenza dei nuovi composti ossidrilati mediante saggio MTT e valutazione dell'apoptosi. I composti utilizzati hanno dimostrato di non influenzare la vitalità cellulare in maniera significativa e di poter essere quindi utilizzati nell'analisi più specifica di protezione dal danno ossidativo effettuata analizzando la formazione di quelli che vengono comunemente indicati come granuli da "stress". I nuovi composti ossidrilati, aggiunti alla linea cellulare eucariotica prima dell'induzione dello stress, hanno dimostrato un significativo effetto protettivo, riducendo la formazione dei granuli.

2) Espressione ricombinante di ToMO in un microorganismo GRAS: *Bacillus subtilis*

Una buona alternativa ad *E.coli*, utilizzato attualmente per l'espressione dell'enzima ToMO, è *B. subtilis*, un batterio GRAS non patogeno per l'uomo. *B. subtilis* mostra condizioni di crescita simili a *E. coli* e presenta un efficiente apparato di secrezione. Un'altra caratteristica di questo ceppo batterico è la resistenza a condizioni ambientali estreme attraverso il differenziamento della spora e della cellula madre che la produce.

A questo scopo il *cluster* genico *tou* è stato clonato in due differenti vettori,

A) Pr19, un plasmide che permette l'integrazione diretta del gene ricombinante in *B. subtilis* mediante singolo *crossing-over*.

B) pHT01, un plasmide non integrativo IPTG-inducibile.

Per quanto riguarda il punto **A)**, il *cluster* genico *tou* è stato clonato all'interno del vettore Pr19, ottenendo un nuovo costrutto, indicato con la sigla NIC11, a partire dal quale è possibile ottenere l'espressione funzionale del complesso proteico ricombinante nell'ospite eterologo *E.coli*, ceppo JM109. Quando trasferito in *B.subtilis*, tale vettore non ha purtroppo consentito la corretta integrazione del *cluster* genico *tou* all'interno del genoma, come evidenziato da analisi PCR e da saggi di attività enzimatica condotti sia su cellule integre che sugli estratti cellulari dei cloni trasformati di *B.subtilis*.

Le attività sperimentali del punto **B** hanno avuto come scopo l'inserimento del *cluster* genico *tou* nel vettore non-integrativo pHT01; il costrutto ottenuto è stato indicato come pDAM10. Anche in questo caso, come nel caso del plasmide NIC11, è stato possibile avere l'espressione funzionale del complesso multienzimatico ToMO all'interno dell'ospite eterologo *E.coli*, ceppo JM109. Il plasmide pDAM 10 è stato successivamente utilizzato per la trasformazione di *B.subtilis*; nonostante l'elevata efficienza di trasformazione, prove di espressione del complesso ToMO nel nuovo ospite non hanno dato esito positivo. Analisi di RT-PCR hanno evidenziato, in questo caso, che la mancata espressione di ToMO in *B.subtilis* è probabilmente dovuta ad una quasi totale mancanza del corrispondente mRNA.

3) Espressione e purificazione della BMVO 3,6-diketocamphane 1,6 monooxygenase (3,6 DKCMO) e della sua componente flavin reduttasica da *Pseudomonas putida* NCIMB 10007.

Questa parte del mio progetto di dottorato è stata svolta nei laboratori della Prof.ssa Jennifer Littlechild presso il centro di biocatalisi e bioscienze dell'università di Exeter (UK).

Come sottolineato precedentemente, le Monoossigenasi Baeyer-Villiger rappresentano una classe di enzimi di particolare interesse nell'ambito della biosintesi di molecole organiche funzionalizzate per le industrie farmaceutica ed alimentare. Le BVMOs possono essere classificate in due gruppi. Quelle appartenenti al gruppo I contengono FAD e utilizzano il NADPH come donatore di elettroni, laddove gli enzimi del gruppo II utilizzano FMN come cofattore ed il NADH come donatore di elettroni. La maggior parte delle BVMOs caratterizzate fino ad ora appartiene al gruppo I, ma sono gli enzimi del gruppo II a rivestire un particolare interesse per le biotecnologie industriali grazie alla loro ampia specificità di reazione. Il microorganismo *Pseudomonas putida* NCIMB 10007 è in grado di crescere utilizzando la canfora quale unica fonte di carbonio ed energia. Ciò avviene grazie alla presenza di due BMVOs, la 2,5-diketocamphane monoossigenasi (2,5-DKCMO) e la 3,6-diketocamphane 1,6 monoossigenasi (3,6-DKCMO). Quest'ultima è una BMVO di gruppo II che ha recentemente attratto un notevole interesse da parte di numerosi gruppi di ricerca.

In questo contesto si è inserito il mio lavoro sperimentale i cui obiettivi sono stati:

- Espressione, purificazione e cristallizzazione della componente ossigenasica della 3,6-diketocamphane 1,6 monoossigenasi (3,6 DKCMO).
- Clonaggio, espressione e purificazione della componente flavin reduttasica della 3,6-diketocamphane 1,6 monoossigenasi (3,6 DKCMO).

L'ottimizzazione delle procedure di espressione e purificazione della componente ossigenasica ha consentito di ottenere discreti quantitativi di proteina purificata utilizzata successivamente in esperimenti di cristallizzazione. I pattern di diffrazione raccolti, ottenuti da diversi cristalli di buona qualità, sono attualmente in analisi presso il laboratorio della Prof.ssa Littlechild.

La disponibilità di entrambe le proteine purificate, che *in vivo* si associano a formare un complesso la cui dinamica strutturale non è ancora nota, consentirà di effettuare nell'immediato futuro studi di co-cristallizzazione che permetteranno di acquisire nuovi dettagli sul meccanismo enzimatico responsabile della degradazione della canfora in questo microorganismo. Con una visione completa e dettagliata della struttura, della specificità di substrato e del meccanismo catalitico, si potrà valutare in modo più critico il potenziale utilizzo della 3,6-diketocamphane 1,6 monoossigenasi per applicazioni biotecnologiche.

1.1 Oxidative stress in biological systems

In living organisms, aerobic metabolic processes such as respiration and photosynthesis entail the generation of reactive oxygen species (ROS) in specific organelles such as mitochondria, chloroplasts, and peroxisomes. ROS are not the only free radical species generated, as cell metabolism produces also reactive nitrogen species usually referred to as RNS.

In cells, both ROS and RNS are unstable and highly reactive. They become stable by acquiring electrons from nucleic acids, lipids, proteins, carbohydrates causing a sequence of chain reactions that might be responsible for cellular damage and disease (Fig.1) **(1)**.

More specifically, the different sources of ROS and RNS include the mitochondrial respiratory chain and enzymes such as the NADPH oxidases, xanthine oxidase, uncoupled nitric oxide (NO) synthases, 5-lipoxygenase, and cyclooxygenases **(2)**.

Decades of dedicated studies have shown that an overproduction of either ROS and/or RNS is implicated in several pathologies such as atherosclerosis, cardiovascular diseases, Parkinson and Alzheimer diseases, and some types of cancer.

However, ROS and RNS should not be considered as being only detrimental as they can specifically modulate diverse intracellular signaling pathways and induce distinct changes in cell phenotype that are important in many physiological processes **(2)**. Indeed, some ROS such as H_2O_2 are ideal as signaling molecules because they are small, highly diffusible, and can be rapidly generated and degraded. Moreover ROS and RNS have been suggested to be involved, among others, in host defense against invading pathogens **(3)**.

The three major types of ROS are superoxide ($O_2^{\bullet-}/HO_2^{\bullet}$) anions, hydrogen peroxide (H_2O_2), and hydroxyl radical (OH^{\bullet}) **(4)**. Superoxide radicals are mainly formed when electrons “leak” from the electron transport chain.

Dismutation of superoxide leads to the formation of hydrogen peroxide. Hydrogen peroxide, although more oxidizing than superoxide, is biologically less toxic **(3)**. Hydroxyl radical is highly reactive and can modify purines and pyrimidines causing strand breaks and thus DNA damage. OH^{\bullet} is nonselective and can react with a wide array of biological molecules.

Nitric oxide (NO) and nitrogen dioxide are the most common RNS. NO is synthesized during the conversion of L-arginine to L-citrulline catalyzed by nitric oxide synthase (NOS). NO regulates in many tissues a diverse range of physiological processes, but an excess of NO can be toxic. As a matter of fact, RNS have been associated with asthma, septic shock and atherosclerosis **(3)**.

The complicated “ménage à trois” between the cell from one side and the reactive species of both oxygen and nitrogen on the other is maintained in a delicate equilibrium thanks to a complex array of non-enzymatic and enzymatic detoxification mechanisms whose role is to guarantee inside the cell the correct balance between prooxidants and antioxidant species.

An imbalance in favor of the prooxidants is usually indicated as “oxidative stress” and can potentially lead to cellular damage. Evidence has been accumulating which shows that oxidative stress is not merely responsible for the aging process, as previously thought, but might represent a common element linking diverse mechanisms responsible for the initial onset of several diseases such as cancer, neurodegenerative and cardiovascular diseases, arthritis and inflammation **(5-8)**. Antioxidants are compounds or enzymatic systems that reduce, neutralize and

prevent the damage induced in cells by free radicals **(9-10)**. In the human body there are two types of antioxidants, either enzymatic or non-enzymatic. The first type consists of enzymes such as superoxide dismutase, catalase, glutathione peroxidase and glutathione reductase. Non-enzymatic antioxidants are antioxidant vitamins and minerals such as vitamin C, vitamin E, selenium, zinc, taurine, hypotaurine, glutathione, β -carotene and carotene **(3)**. It is now evident that regular consumption of vegetables, fruits, red wine and tea, which contain antioxidants, is associated with lower incidences of many chronic diseases, including cancer **(11-12)**. Although a varied and healthy diet can provide an adequate intake of these molecules in normal conditions, the reduced availability of more effective antioxidants in pure form currently precludes the use of real drugs in those diseases directly depending on oxidation and damage caused by free radicals such as atherosclerosis, diabetes, ischemic events and cancer **(13)**.

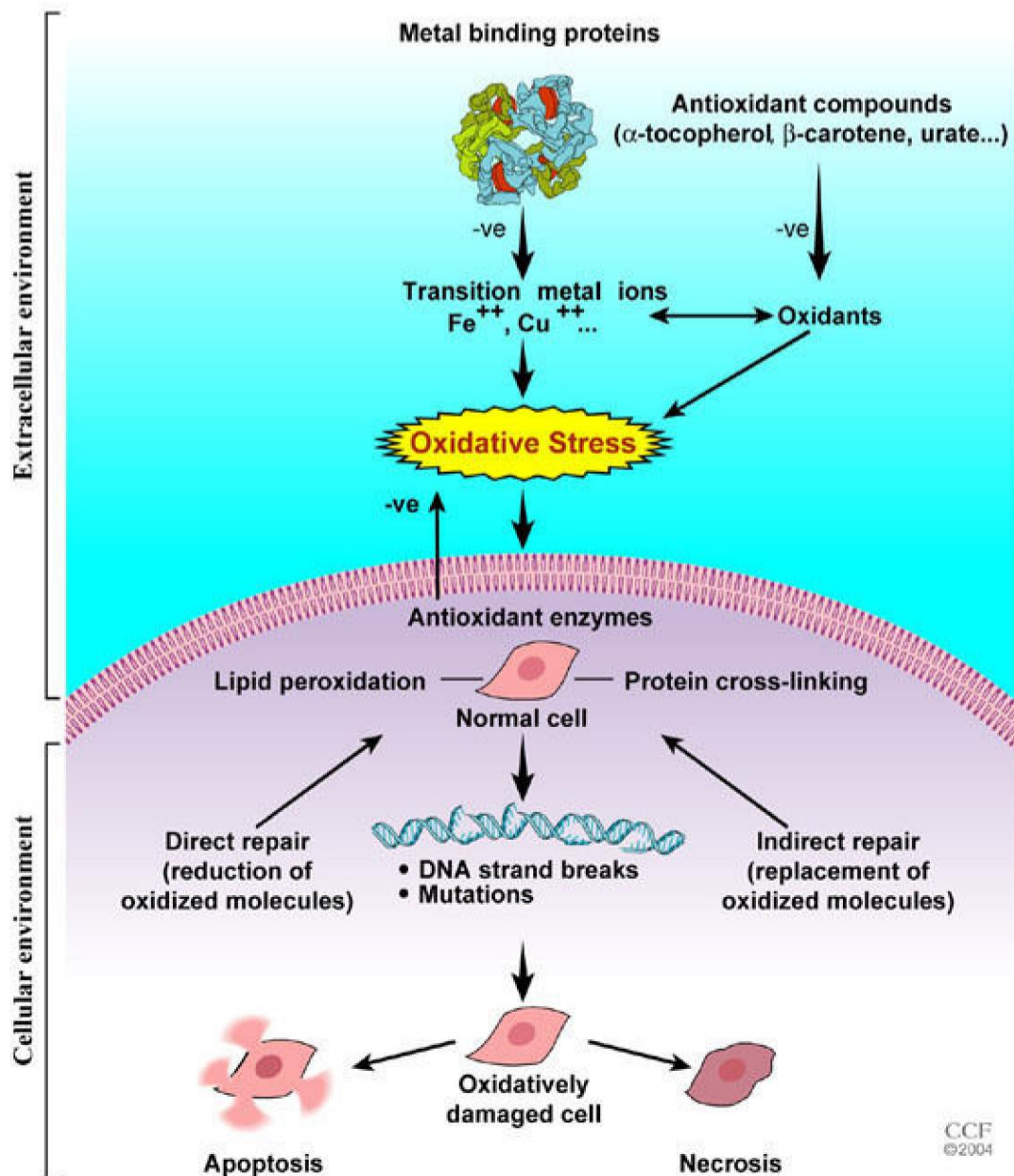


Figure 1: Mechanisms of oxidative stress-induced cell damage (Image from Agarwal *et al. Reproductive Biology and Endocrinology* 2005 **3**:28).

The demand for natural and synthetic antioxidants to strengthen endogenous defenses has undoubtedly grown in recent years. Antioxidants must react with radicals and other reactive species faster than biological substrates, thus protecting biological targets from oxidative damage.

However, much caution should be taken into account in the validation of antioxidants as pharmacological molecules. In fact, although vitamin E, ascorbate and β -carotene are excellent antioxidants in model systems, supplements of these compounds in clinical trials do not seem to have generated the expected beneficial effects on patients. Therefore, the challenge for the future is to gain further information on the effective role of antioxidant molecules inside the cell to efficiently prevent and treat diseases related to oxidative stress.

1.2 Phenols and catechols as antioxidants

Phenols are endowed with the property of suppressing or delaying spontaneous autoxidation of organic molecules **(14)**. Therefore, these compounds might be useful to prevent *in vivo* the consequences of the autoxidation of biomolecules.

Plants have been the main suppliers of molecules analyzed as potential antioxidant drugs, due to their high content of phenolic compounds such as phenolic acids and flavonoids. Indeed, as underlined in the previous paragraph, the consumption of fruits and vegetables, which contain plenty of phenolic antioxidants, has been demonstrated to significantly reduce the risk of cancer. These properties have generated in the last decades a great interest in phenolic antioxidants, particularly after the discovery that the main lipid-soluble antioxidant present in human blood is a phenol, namely α -tocopherol **(15)**. Therefore, the design and production of novel phenolic antioxidants has recently attracted much interest in the scientific community. Indeed, the most popular synthetic antioxidants currently used are phenolic compounds such as butylated hydroxyanisole (BHA), butylated hydroxytoluene (BHT), tert-butylhydroquinone (TBHQ) and propyl gallate (PG) (Fig. 2), even though BHA and BHT have been restricted by legislative rules due to doubts of their toxic and carcinogenic effects **(16)**.

Despite all the interest towards phenolic antioxidants, there are still many details to unravel concerning their biological activity. The analysis of kinetic and thermodynamic data available so far in the literature indicates that the efficiency of phenols as inhibitors of the autoxidation of organic matter depends on a variety of factors, and this becomes particularly challenging in complex systems such as living organisms. The design of new phenolic antioxidants must therefore take into consideration most of these physical/chemical constraints. Among the possible mechanisms proposed to explain the antioxidant potential of phenols, one hypothesis might be that these molecules chelate and inactivate free metal ions that are an important intracellular source of free radicals.

Phenols have other interesting biological activities of pharmacological interest, as it has been described for example for 4-hydroxyanisole (4-OHA). Several reports have

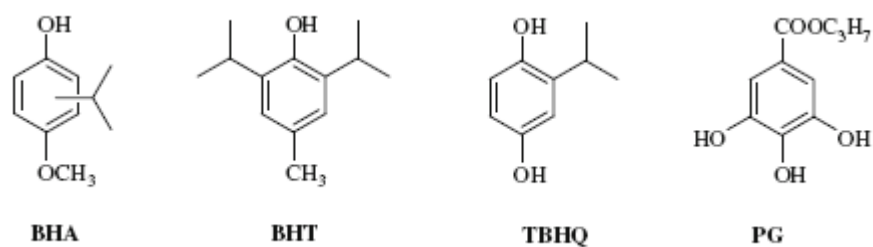


Figure 2: The most popular synthetic antioxidants. BHA, butylated hydroxyanisole; BHT, butylated hydroxytoluene; TBHQ, tert-butylhydroquinone; (Image from Gülçin I. *Antioxidant activity of food constituents: an overview* Arch Toxicol (2012) **86**:345-391).

indicated highly specific antitumor activity of 4-OHA against melanoma cells both *ex vivo* and *in vivo*.

This specific antitumor activity has been proposed to be due to the oxidation of 4-OHA by tyrosinase, an abundant enzyme found in melanocytes, to form catechol and then *o*-quinone which is highly cytotoxic **(17)**.

In this framework, other antioxidant pharmacophores have been identified, among which catechols, 1,2-dihydroxybenzenes, have been given much attention **(18)** as they are very susceptible to oxidation and react quickly with various oxidizing agents, including free radicals, acting as electron donors. For these molecules it is commonly accepted that the key factor underpinning the antioxidant effect depends on the fact that the semiquinone radical derived from H-atom donation of catechol can be stabilized by both an intramolecular hydrogen bond and the electron-donating properties of the *ortho*-OH (Fig.3) **(19-21)**.

The Comprehensive Medicinal Chemistry (CMC) database shows the presence of many drugs containing the catechol moiety for which several pharmacological effects have been described such as antioxidant, adrenergic, antihypertensive, bronchodilator, and antiparkinsonian activity **(22)**. The diverse range of potential pharmacological effects as well as the need to find approaches to overcome the potential toxicity frequently described for these molecules **(18,22)** have recently encouraged the use of catechols as scaffolds for designing novel bioactive molecules. Indeed, the different nature of the substituents bound to the catechol ring may influence, among others, the reactivity towards oxidizing agents, the pharmacokinetics, the tissue and cellular distribution of these compounds **(18)**.

In addition to their medical applications, catechols and their substituted derivatives are employed in many industrial processes, such as the manufacture of photographic developers, inks, insecticides, rubber, plastics, and are essential precursors for the production of a large number of fine-chemicals, and synthetic flavor compounds **(23)**.

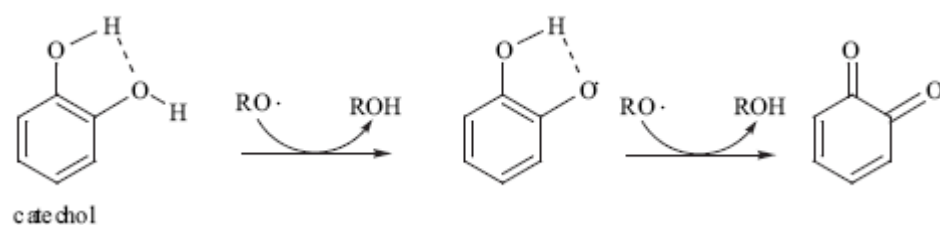


Figure 3: H-atom abstracting reactions occurring in catechol (Image from Zhang H.I. *Structure-activity relationships and rational design strategies for radical-scavenging antioxidants* Curr. Comput.-Aided Drug Des. (2005) 1:257-273).

1.3 Microbial biotransformations for the production of phenolic antioxidants

Reactions in which organic compounds are oxygenated or hydroxylated are of great value for organic synthesis; several hydroxylated aromatic intermediates are in fact widely used in the industrial production of polymers and drugs **(24,25)**. Selective oxyfunctionalization of organic substrates, however, can be a significant problem in organic synthesis, as these reactions are often carried out with strong oxidizing agents and occur with little chemo-, regio-, and enantio- selectivity. As a consequence, the synthesis of phenols and catechols by chemical methods is often complex, resulting in low yields and the formation of racemic mixtures **(26,27)**. Thus, growing attention has been dedicated in the last years to the development of biotransformations, also known as bioconversions, which make use of the metabolic versatility of either purified enzymes or whole microorganisms to perform oxyfunctionalization of organic substrates of industrial interest. These methodologies, compared with already established chemical processes, are appealing alternatives for obtaining active aromatic compounds under mild experimental conditions and without employing toxic reagents **(25)**.

Purified enzymes and whole-cell biocatalysts **(28)** have several attractive properties which make them privileged catalysts for organic synthesis. In fact, they show high chemo-, regio- and stereoselectivity and require mild reaction conditions. Therefore, biocatalysis offers great chances and advantages for successful industrial applications, also in cases where either substrates or products of a reaction are chemically labile. The complex organization of specific enzymes combined with aspects such as cofactor dependency and low stability in isolated form, often favors the use of whole cells over that of isolated enzymes. Whereas whole cells generally offer a simple and effective option for cofactor regeneration and enhanced enzyme stability, protein engineering and the use of single enzymes is sometimes considered more economic and practical **(29)**.

The biocatalysis industry has currently high potential and resources **(30-32)** according to the increasing availability of sequenced genomes and the existence of a huge unexplored microbial diversity. In addition, it should be noted that, through recombinant DNA technologies, the number of enzyme variants available continues to increase steadily.

1.4 Bacterial Multicomponent Monooxygenases: ToMO as a case study

The complications experienced in the chemical synthesis of substituted monocyclic aromatic compounds from more readily available precursors have boosted the research for alternative enzymatic or chemoenzymatic routes to phenols and catechols. Among others, Bacterial Multicomponent Monooxygenases (BMMs), a diverse group of non-heme diiron enzymes able to catalyze a variety of complex oxidation reactions on aromatic compounds, have several attractive properties which make them privileged catalysts for oxyfunctionalization reactions on aromatic compounds such as benzenes and phenols to produce the corresponding catechols (33-34,25). In recent years both directed evolution and rational design have been successfully used to identify the molecular determinants responsible for BMMs regioselectivity and to improve their activity towards natural and non-natural substrates. Monooxygenase biocatalysts are already used in the chemical industry to obtain additives for agriculture, synthones, drugs, and plastics and due to their catalytic properties, these multicomponent enzymes, either wild type (*wt*) or engineered, are a versatile biosynthetic tool for the preparation of different active aromatic compounds (25). Toluene *o*-xylene monooxygenase (**ToMO**) from *Pseudomonas* sp. OX1 (Fig.4) is a BMM that belongs to the subfamily of the four component aromatic/alkene monooxygenases (group 2 BMMs) (33).

ToMO is endowed with a broad spectrum of substrate specificity and, among others, is able to oxidize *o*-, *m*-, and *p*-xylene, 2,3- and 3,4-dimethylphenol, toluene, cresols, benzene, naphthalene, and styrene. The ToMO multicomponent system has been thoroughly investigated to identify the molecular determinants responsible for its regioselective hydroxylation of aromatic compounds (35,36).

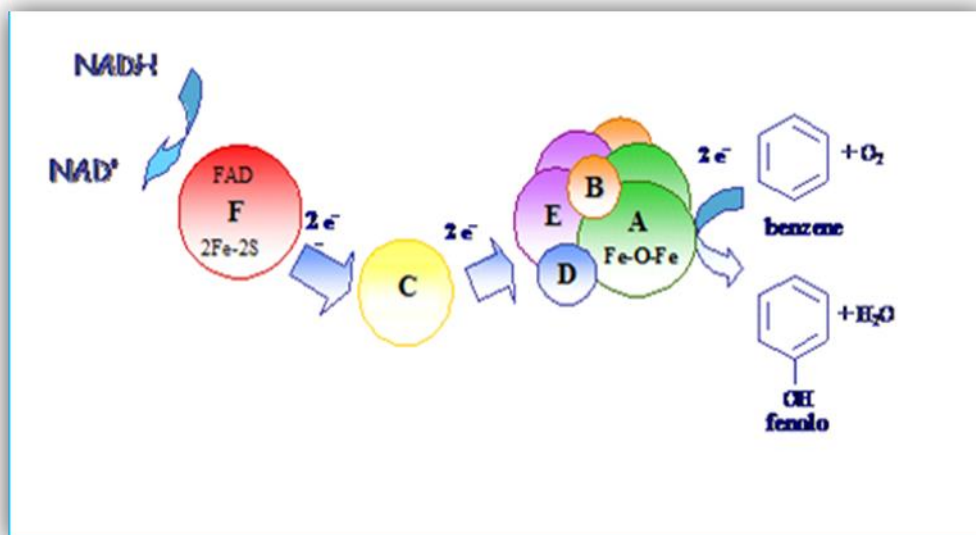
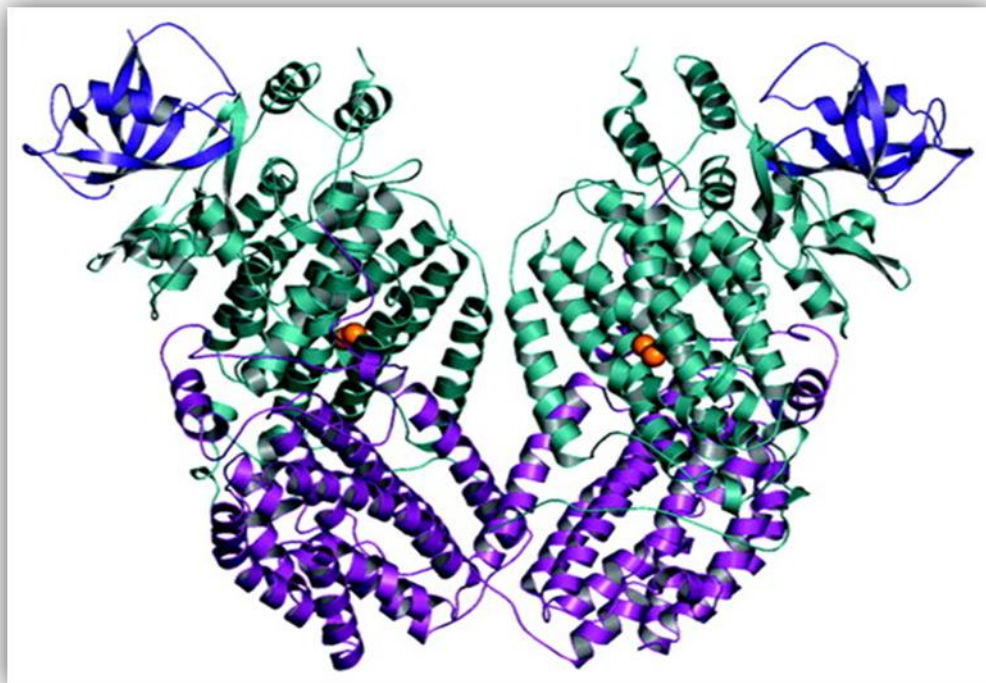


Figure 4:

A) 3-D structure of the hydroxylase component ToMOH of the ToMO multicomponent system. In the ribbon diagram, subunits A, B and E are in green, blue and violet, respectively; iron atoms are in red.

B) Scheme of the ToMO electron transport chain that shuttles electrons from NADH to oxygen through subunits F and C and the hydroxylase complex ToMO H with quaternary structure (BEA)₂.

Moreover, a computational model has been recently developed that quantitatively predicts the effects of mutations into the active-site pocket of ToMOA (Fig.4), thus allowing the rational design of variants of the enzyme endowed with the desired regioselectivity **(37)**. The biocatalytic potential of ToMO has been recently confirmed by its use for the production of tyrosol and hydroxytyrosol, strong antioxidants commonly found in extra virgin olive oil, starting from a low-added-value, commercially available aromatic precursor such as 2-phenylethanol (Fig.5) **(38)**. Tyrosol and hydroxytyrosol belong to a class of natural phenolic antioxidants, commonly referred to as “nutraceuticals” **(39-41)** whose role in the prevention of diseases such as cancer and cardiovascular diseases is rapidly emerging **(42-49)**. Hydroxytyrosol is one of the most abundant and powerful antioxidant catechol found in olive fruits and in extra-virgin olive oil. Tyrosol and hydroxytyrosol are compounds of proven efficacy against various cardiovascular diseases and of particular interest in food and pharmaceutical industries. In the case of hydroxytyrosol it has been demonstrated *in vivo* and *in vitro* that this molecule exerts a protective action that prevents oxidation of LDL, thus counteracting one of the key underlying phenomena of atherosclerosis **(46-49)**.

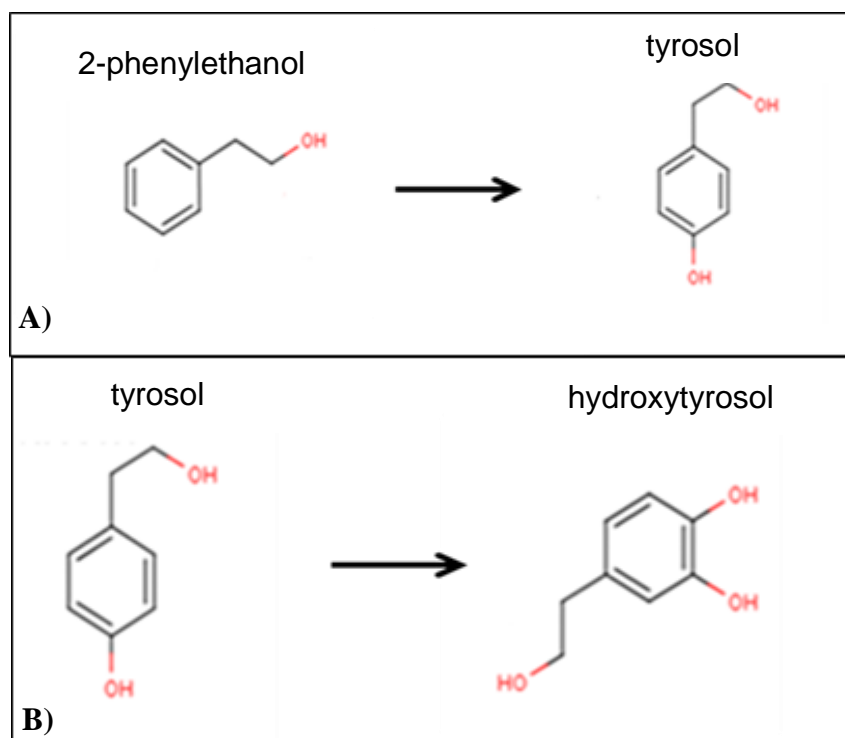


Figure 5:
ToMO-catalyzed conversion of **A)** 2-phenylethanol to tyrosol
and **B)** tyrosol to hydroxytyrosol.

There are many protocols for the chemical synthesis of tyrosol and hydroxytyrosol, which are currently mainly produced by extraction from oil mills wastewaters. However, either the purification of antioxidants from natural sources or their chemical synthesis is difficult. The former is made difficult by the high chemical reactivity of these molecules, the thermolability and the presence of complex mixtures of similar compounds and of their esterified derivatives. On the other hand, chemical synthesis can easily convert phenolic rings into catechol rings, but the first reaction of an aromatic ring hydroxylation requires harsh conditions of reaction. In addition, because of the increased reactivity of mono-hydroxylated products compared to the starting compound, it is difficult to control the hydroxylation reaction and to obtain a single product. Consequently, yields are low and the desired products need to be purified from complex mixtures.

Due to the inability of *wt* ToMO to produce tyrosol as the sole isomer from the hydroxylation of 2-phenylethanol, a non-natural substrate of this enzyme, a computational model which provides a molecular explanation for this outcome was developed. To validate the computational model, several ToMO variants were designed and tested for their ability to transform 2-phenylethanol into tyrosol **(38)**. More specifically, it was shown that variants E103G/F176T and E103G/F176I were the most efficient catalysts in the bioconversion of 2-phenylethanol to tyrosol and hydroxytyrosol.

In conclusion, all the experimental data gathered so far on this enzymatic system concur in suggesting that ToMO is a versatile candidate for the development of enzymatic oxyfunctionalization processes of industrial interest using both natural and non-natural substrates.

1.5 Baeyer Villiger monooxygenases as biocatalysts

The “Baeyer-Villiger” oxidation reaction was first discovered by Adolf von Baeyer and Victor Villiger more than a hundred years ago (50). In this reaction, ketones are converted into the corresponding esters (Fig.6). The insertion of an oxygen atom in a range of aliphatic and cyclic ketones to produce optically pure chiral esters or lactones is of fundamental importance in organic chemistry as these molecules serve as primary intermediates and/or precursors for the synthesis of industrially important fine chemicals and pharmacologically active compounds (51-54).

In organic chemistry, peroxy acids are commonly used as catalyst to perform this atypical oxidation reaction that results in oxygen insertion into a carbon-carbon bond. However, the chemical Baeyer-Villiger reaction shows several drawbacks such as poor regio- and enantioselectivity, environmentally unfriendly reaction parameters (use of halogenated reagents and solvents) as well as the use of toxic peroxy acids. These latter are powerful oxidative agents; therefore, laborious protection and deprotection steps are requested in order to prevent by-product formation.

These drawbacks have encouraged a great deal of interest in the use of enzymes referred to as Baeyer Villiger monooxygenases (BVMOs) that are endowed with the ability to catalyze the nucleophilic oxygenation of linear, cyclic or aromatic ketones to esters or lactones in a region and enantio-selective manner.

Microorganisms have been found to use BVMOs in order to grow on aliphatic methyl ketones (55), alicyclic hydrocarbons (56) aromatic compounds (57), and terpenes (58) as carbon source.

All BVMOs characterized to date are NAD(P)H-dependent flavoproteins that use flavin cofactors to catalyze the insertion of an oxygen atom into ketone substrates to generate esters and/or lactones. These enzymes are endowed with the ability to catalyze regio- and enantioselective Baeyer-Villiger oxidations of a wide range of carbonylic compounds, as well as epoxidations, and enantioselective sulfoxidations. These conversions are of great biotechnological interest because they produce high-added value intermediates and allow transformations that are otherwise difficult to achieve using chemical approaches, as underlined above (59). A special feature of these atypical monooxygenases is that they do not only catalyze Baeyer-Villiger oxidations but also sulfoxidations and a number of other oxidation reactions.

BVMOs are actually considered very promising targets for biocatalytic applications in synthetic and pharmaceutical chemistry.

Most importantly, BVMOs such as for example the 4-Hydroxyacetophenone monooxygenase from *Pseudomonas fluorescens* ACB, perform Baeyer-Villiger oxidation reactions of aromatic compounds (60). Thus, these enzymes can be considered, along with BMMs, another important element in the toolbox of biocatalysts of industrial interest capable of performing oxyfunctionalization reactions of aromatic substrates.

Several different mechanisms have been proposed for the O₂-driven reactions catalyzed by BVMOs which share a dependence of these enzymes for a reduced nicotinamide coenzyme such as NAD(P)H for the reduction of the FAD cofactor. This latter, once reduced, rapidly reacts with molecular oxygen to form a reactive peroxyflavin intermediate. After the oxygenation of the substrate, the enzyme reverts to the oxidized state; subsequently, the oxidized NAD(P)⁺ coenzyme is released (61). A key feature of BVMOs and related monooxygenases is the dual role of NADP(H) in catalysis. It acts in fact as the electron donor to reduce the flavin, and it is also required for the stabilization of the essential flavin-peroxide intermediate (62). The recently elucidated BVMO crystal structures, that have allowed a detailed insight into

the complex mechanism of these flavin-containing enzymes, and the recent identification of several novel members of this family of enzymes, have boosted the research efforts towards the study and engineering of these unique oxidative biocatalysts to understand their effective potential for future industrial applications **(63)**. By using random mutagenesis and site directed evolution approaches, it has been highlighted the possibility to expand the substrate specificity, as well as to improve and change the stereoselectivity of BVMOs such as, for example, the cyclopentanone monooxygenase **(64)**. Moreover, the designing of chimeric BVMOs, which has provided the recombinant enzymes produced with the novel selectivities of other BVMOs, has been also recently developed **(65)**.

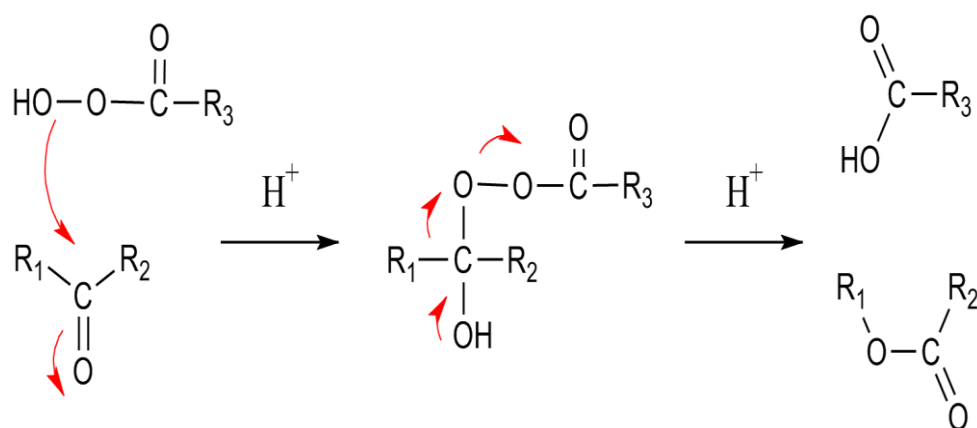


Figure 6: The reaction mechanism hypothesized for the Baeyer Villiger oxidation reaction.

1.6 *Bacillus subtilis* in industrial biotransformations

Escherichia coli is the preferred host for the heterologous expression and production of recombinant proteins. This microorganism is in fact well known for its ease of handling, its short time of generation and its ability to accumulate high amount of recombinant protein in the cytosol. Nevertheless, *E. coli* expression systems show several limits such as low expression rates, formation of inclusion bodies, improper protein-folding and inability to produce complex disulfide bonds. This is due, among others, to the lack of fundamental molecular mechanisms for an efficient secretion, the low chaperone and foldase levels and the high concentration of periplasmic proteases (66).

One of the main alternative to *E.coli* for the heterologous expression of recombinant proteins is *Bacillus subtilis*, a non-pathogenic, GRAS (Generally Recognized As Safe) microorganism.

B. subtilis is generally free of endotoxins, and, compared with *E. coli*, offers high biosynthetic capacity and an efficient secretion apparatus that directs expressed proteins directly into the culture supernatant. *Bacillus* species are attractive industrial organisms for a variety of reasons, including their high growth rates that allow short fermentation cycle times. In addition, much information is now available on the biochemistry, physiology, and genetics of *B. subtilis*, which facilitates further development and a future greater exploitation of this microorganism in industrial processes (67).

Furthermore, *B. subtilis* shows several advantages over fungal expression systems such as smaller process times, cultivation techniques for the production of industrial enzymes already standardized, and a greater variety of tools for its genetic manipulation (68).

Nonetheless, several technical drawbacks have been described in the use of *B. subtilis* such as plasmid instability, and low yields of heterologous protein production, which currently limit the biotechnological potential of this microorganism (68). Plasmid instability can be overcome with the use of integration vectors, characterized by the presence of chromosomal regions of *B. subtilis* (100-200 bp), which virtually allow the integration of any gene in a specific site through homologous recombination. The integration can be mediated through a single or a double crossing over (Fig. 7). Low yields of recombinant protein expression are frequently due to the presence of proteases that cleave proteins expressed in *Bacillus*; this aspect has been overcome with the use of specific protease deficient strains (68). In conclusion, *B. subtilis* might represent an ideal host for the recombinant expression of enzymes used in industrial biocatalysis such as BMMs and BVMOs. However, up to now, there is a fundamental lack in the scientific literature concerning the use of this microorganism for the recombinant expression of proteins belonging to both these families of enzymes.

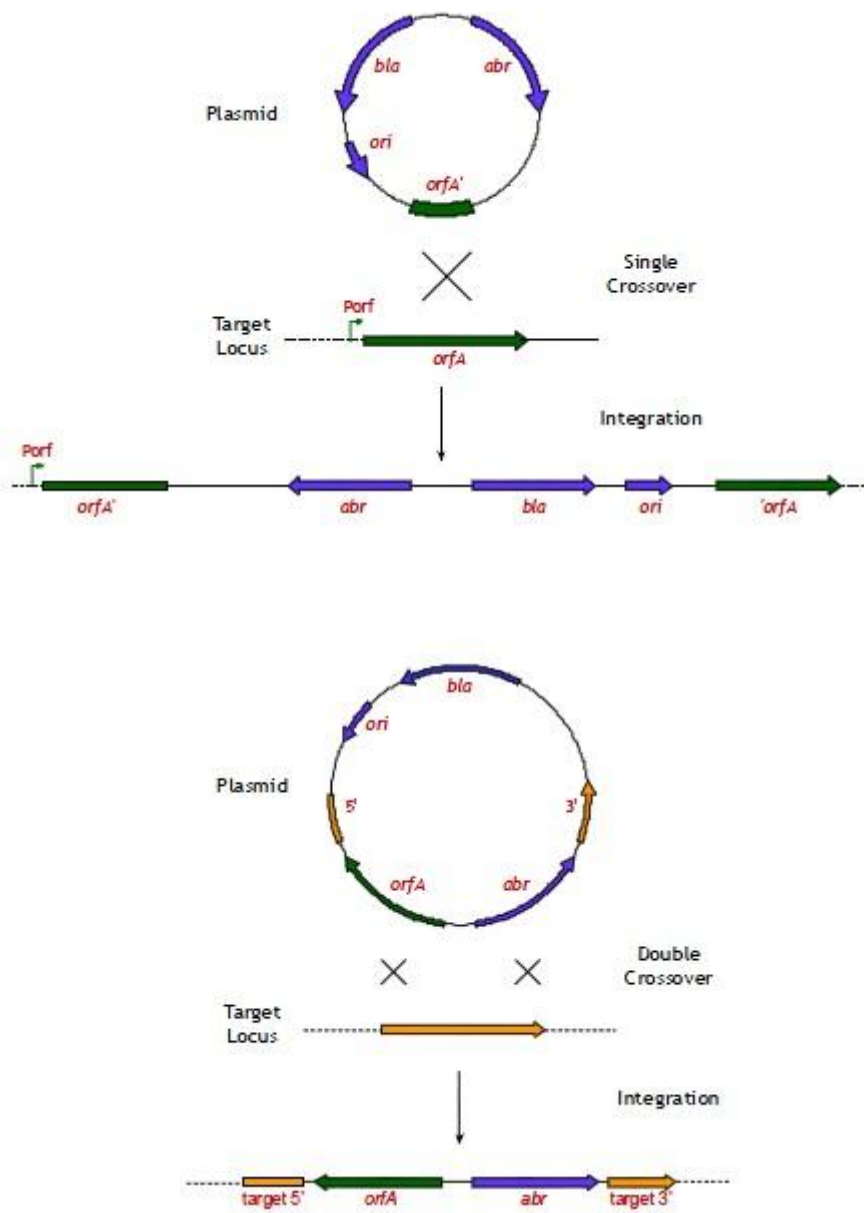


Figure 7: Models for single or double crossing-over strategies to insert a specific gene in *Bacillus subtilis* genome.

1.7 Aim of the PhD project

Main objectives of my PhD project have been:

1) The production of new antioxidant phenols and catechols using the catalytic activity of ToMO on non-natural substrates.

The model compounds for this study were chosen on the basis of their similarity with the natural aromatic substrates of ToMO (Fig.8):

- 2-phenoxyethanol, a compound in which a group $\text{-O-(CH}_2\text{)}_2\text{-OH}$ is attached to an aromatic ring;
- 2,3-dihydrobenzofuran, a compound in which a $\text{-(CH}_2\text{)}_2\text{-O-}$ substituent is linked to two adjacent carbons of the benzene ring, forming a five atoms ring;
- 2-indanol, characterized by the presence of an -OH group which gives the molecule a more polar character compared to other substrates.
- phthalan, an isomer of 2,3-dihydrobenzofuran, in which the linked substituent is the group $\text{-(CH}_2\text{)-O-(CH}_2\text{)-}$.

The antioxidant potential of these molecules was evaluated both *in vitro*, using the DPPH assay, and *ex vivo* on cardiomyoblast cell line H9c2 subjected to oxidative stress induced by sodium arsenite.

2) The recombinant expression of ToMO in the GRAS host microorganism *Bacillus subtilis*.

To this purpose ToMO gene cluster was cloned in two different shuttle vectors, a non-integrative plasmid indicated as pHT01, and Pr19 that allows instead the direct integration of the recombinant gene in *B.subtilis* chromosomal DNA through single crossing-over.

3) Expression and purification of the Baeyer Villiger 3,6-diketocamphane 1,6 monooxygenase (3,6 DKCMO) and its flavin reductase component from *Pseudomonas putida* NCIMB 10007.

This part of my project was performed in the Laboratory of Prof. Jennifer Littlechild at the Exeter Biocatalysis Centre, Biosciences, College of Life and Environmental Sciences at the University of Exeter, UK.

The biochemical characterization of this multicomponent enzyme is important to understand the future biotechnological potential of this protein for the oxyfunctionalization of aromatic compounds of industrial interest.

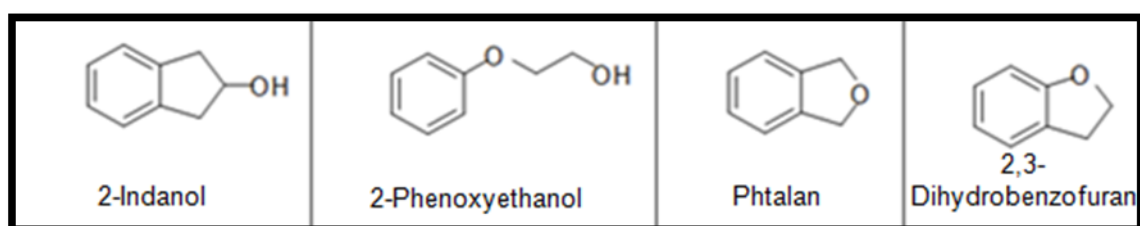


Figure 8: The aromatic compounds selected as substrates for the ToMO-catalyzed hydroxylation reaction to produce novel antioxidant phenols and catechols.

2.1 Bacterial strains

Escherichia coli strain JM109 was from Novagen and was used for the recombinant expression of ToMO. The genotype is: *recA1 supE44 endA1 hdsR17 gyrA96 relA1 thi Δ(lac-proAB)*.

Escherichia coli strain Top10 was purchased from Invitrogen. The genotype is *F-mcrA Δ(mrr-hsdRMS-mcrBC) φ80lacZΔM15 ΔlacX74 nupG recA1 araD139 Δ(ara-leu)7697 galE15 galK16 rpsL(Str^R) endA1 λ⁻*.

Bacillus subtilis strain AZ54 (*w.t.*) and strain **MW10 (protease deficient)** were a kind gift of Dr. Rachele Isticato (Department of Structural and Functional Biology, University Federico II of Naples). The genotypes are respectively: *PY79 trpC2 metC3 and apr his hpr eglSΔ(102) bglT/bglSΔEr*.

BL21(DE3) were purchased from Novagen, genotype: *95 F- ompT hsdSB (rB-mB-) gal dcmrne131 (DE3)*.

2.2 Bacterial culture media

LB (Luria Bertani), was prepared as described by (69)

M9 minimal salt medium was prepared as described by (69)

TY (Tryptone yeast medium): this medium was used for agar plates of *B. subtilis* and prepared as described in (69).

TB (Terrific both): for this medium 12g of tryptone, 24 g of yeast extract, 4g of glycerol were added in a final volume of 1L.

2.3 Antibiotics

Ampicillin (Amp) was purchased from Sigma and used at a concentration of 100 μg/mL.

Chloramphenicol (CF) was purchased from Sigma and used at a concentration of 5μg/mL.

2.4 Proteins

Catechol 2,3 dioxygenase was purified (Department of Structural and Functional Biology, University Federico II, Naples, Italy) according to the procedure described in Viggiani *et al* (70).

2.5 Plasmids

pGEM3Z/tou wt and mutants. These plasmids were prepared as previously described (36,37).

pHT01 was supplied by Dr. Rachele Isticato (Department of Structural and Functional Biology, University Federico II, Naples, Italy).

Pr19. Plasmid Pr19 was supplied by Dr. Rachele Isticato (Department of Structural and Functional Biology, University Federico II, Naples, Italy).

2.6 Plasmidic DNA Purification

Plasmidic DNA was purified using the QIAprep spin miniprep kit for mini preparation.

2.7 Purification of DNA fragments from agarose gel.

The Wizard PCR Preps DNA Purification System from Promega was used.

2.8 Preparation of competent cells and transformation of *E. coli*.

A single, well-isolated colony was picked, inoculated into 5 mL of LB/amp and incubated at 37°C up to 0.6 OD₆₀₀. 1 mL was then withdrawn and centrifuged for 3 min at 4°C at 12,000 rpm. The pellet was suspended into 100 µL of TSS (10% PEG, 5% DMSO, 50 mM MgCl₂ in LB). 50 ng of purified plasmidic DNA was added to the cell suspension and put on ice for 30 min. 1 mL of LB was then added and the sample was incubated for 1h at 37°C. After centrifugation, 1mL of supernatant was removed, the pellet suspended in 100 µL and plated on ampicillin containing LB/agar plates. The plates were incubated at 37°C, overnight.

2.9 Preparation of competent cells and transformation of *Bacillus subtilis*.

Competent cells of *B. subtilis* were thawed by incubating for 5 minutes the frozen tubes in a 37°C water bath. One volume of SpII (0.3% potassium acetate, pH 7.0 + 2mM EGTA) was added to the thawed cells.

In a sterile test tube competent cells (0.2–0.5 mL) were added to a purified plasmidic DNA preparation (ca. 1µg) and incubated in a roller drum at 37°C for 45 minutes. The cell suspension was plated on selective agar plates.

2.10 Genomic DNA extraction from *Bacillus subtilis*.

A colony of *B. subtilis* was inoculated in 4 mL of LB containing cloramphenicol (5 µg /mL) and incubated overnight at 37°C. The cell suspension was then centrifuged for 15 min at 3,500 rpm at 4°C and the supernatant was discarded.

The cell pellet was suspended in 1.6 mL of Lysis Buffer (0.5 M NaCl, 5 mM EDTA pH 8.0). A spatula tip of lysozyme powder was added; the sample was mixed by inversion and incubated at 37° for 10 minutes.

45 µl of 20% Sarcosyl were added to the sample which was then incubated for 5 min at 37°C. The sample was extracted twice with phenol/chloroform. The resulting aqueous phase was transferred to a clean tube; 50 µl of 3M NaAc pH 6.0 and 1.5 mL of 96% Ethanol were added and the genomic DNA was precipitated by centrifugation at 13,000 rpm for 10 min at 4°C. The resulting pellet was dried for 10 min at 37°C and suspended in 200 µL in nuclease-free water.

2.11 Restriction endonucleases

Restriction endonucleases were purchased from New England Biolabs (NEB).

2.12 Isolation of plasmid DNA from *Bacillus subtilis*

Plasmidic DNA was purified using the QIAprep spin miniprep kit for mini preparation.

2.13 SDS-PAGE.

Electrophoresis was performed as proposed by Leammli (71). The percentage of polyacrylamide was 18% in resolving gel and 6% for the stacking gel.

2.14 Whole-cell assays

Whole-cell assays were performed using *E. coli* JM109 cells transformed with the plasmid of interest. Recombinant strains were routinely grown in LB medium supplemented with 100 µg/mL ampicillin at 37°C to an optical density at 600 nm of 0.6. Expression of the recombinant proteins was induced with 0.1 mM IPTG at 37°C in the presence of 0.2 mM Fe(NH₄)₂(SO₄)₂; this latter was necessary for the assembly of the iron-containing catalytic center of the recombinant ToMO.

One hour after induction, cells were collected by centrifugation and suspended in M9 minimal medium containing 0.4% glucose, from here on indicated as M9-G. The hydroxylase activity of cells was measured using phenol as the substrate and monitoring the production of catechol in a continuous coupled assay with recombinant C2,3O from *Pseudomonas* sp. OX1, which cleaves the catechol ring and produces 2-hydroxymuconic semialdehyde. This can be monitored spectrophotometrically at 375 nm. The specific activity of cells on phenol was determined by their incubation at an OD₆₀₀ of 0.1 to 0.5 in a quartz cuvette in a final volume of 600 µL of M9-G, 1 mM phenol, and saturating amounts of C2,3O (3 U). The rate of formation of catechol ($\epsilon_{375} = 29,100 \text{ M}^{-1} \text{ cm}^{-1}$) was measured. Specific activity was expressed as the number of mU/OD₆₀₀, with one milliunit being defined as the amount of catalyst that oxidized 1 nmol of phenol per minute.

2.15 Catalytic assays on crude extracts of *Bacillus subtilis*

To verify the effective expression of the ToMO recombinant system in *B. subtilis*, a single clone of this microorganism was picked from the transformation plate and grown at 37°C in a final volume of 250 mL of LB containing chloramphenicol. 60 mL of cell suspension were withdrawn from the growing culture at 1.5h, 3h and 16h after the addition of 0.2 mM Fe(NH₄)₂(SO₄). The culture was supplemented with iron at an optical density of 0.9 OD₆₀₀. At specific time intervals cells were collected by centrifugation and the resulting pellets were suspended in 50 mM Tris HCl pH 7.5 and disrupted by sonication (10 min effective: 30 sec ON, 30 sec OFF).

The cell suspension was centrifuged for 20 min at 4°C at 12,000 rpm and the supernatant filtered through a 0.45 µm filter. The assay mixture contained, in a final volume of 600 µL, variable amounts of cell extract, 1mM phenol and 500 µM NADH. Discontinuous coupled assays were performed; After 15, 30, 120 and 240 minutes of incubation, 3 U of catechol 2,3-dioxygenase were added to each sample in order to convert the catechol, the product of the ToMO-catalyzed hydroxylation of phenol, to 2-hydroxymuconic semialdehyde, a product whose formation can be monitored at 410 nm.

2.16 Total RNA purification and RT-PCR

Total RNA was extracted with the TRI-Reagent kit (Sigma), using the manufacturer's protocol. Samples were then incubated with 10 U µL⁻¹ DNaseI (Boehringer) at 37°C for 30 min and subjected to an acid phenol:chloroform extraction. RNA was recovered from the aqueous phase by precipitation with 3 M sodium acetate pH 5.3.

Total RNA was dissolved in 60 µL of diethylpyrocarbonate-treated H₂O and stored at -80°C. RNA concentration was estimated spectrophotometrically by measuring the absorbance at 260 nm ($1 \text{ OD}_{260\text{nm}} = 40 \text{ µg mL}^{-1}$) (69). The integrity of RNA was verified on a denaturing 1.5% agarose gel. RT-PCR reactions were performed using the "Access RT-PCR System" kit (Promega), using 200 ng of RNA as template for each reaction and amplification products were examined on 1% agarose gels.

RT-PCR reactions were performed using the following primers:

5-GATTATTACACGCCACTGGAAT-3 (upstream); 5-GTCGCCATGTCCACCTC-3 (downstream) for the amplification of *orf touA*.

2.17 Identification of the reaction products of ToMO-catalyzed hydroxylation of non-natural aromatic substrates.

Cells of *E. coli* strain JM109 transformed with either plasmid pBZ1260 or variant E103G/F176A, were routinely grown in LB to which ampicillin was added to a final concentration of 100 µg/mL (LB/amp). Three well-isolated colonies were picked from LB/amp agar plates, inoculated into 12.5 mL of LB/amp in a sterile 50 mL Falcon Tube and incubated in constant shaking at 37°C up to 0.6 OD₆₀₀; the preinoculum was diluted 50-fold in two 500 mL Erlenmeyer flasks containing each 250 mL of LB/amp, and incubated in constant shaking at 37°C up to 0.7-0.8 OD₆₀₀. Expression of the recombinant ToMO proteins was induced with 0.2 mM IPTG at 37°C in the presence of 0.2 mM Fe(NH₄)₂(SO₄)₂; this latter was necessary for the assembly of the iron-containing catalytic center of the recombinant ToMO. After 1 hour of induction, cells were collected by centrifugation (1,880 x g for 15' at 4°C), resuspended in M9 medium containing 0.4% glucose (M9-G) at a final concentration of 6 OD₆₀₀ and incubated with 2 mM of either phthalan, 2-phenoxyethanol, 2,3 dihydrobenzofuran or 2-indanol dissolved in methanol (final methanol concentration is of 2%). After a 14h incubation at 28°C at 230 rpm, cells were collected by centrifugation at 1,880 x g for 15' at 4°C; an aliquot of the cell-free supernatants was loaded on HPLC to check for the presence of hydroxylated products before their purification. To this purpose, an HPLC system equipped with a Waters 1525 binary pump coupled to a Waters photodiode array detector was used. Hydroxylated products and substrates were separated using a Ultrasphere C₁₈ reverse-phase column (4.6 by 250 mm; pore size, 5 µm). Separation was carried out at a flow rate of 1 mL/min by using a two-solvent system consisting of a 0.1% formic acid solution in water (solvent A) and a 0.1% formic acid solution in methanol (solvent B). Compounds were separated using a 3-min isocratic elution with 10% solvent B, followed by a 20-min linear gradient from 10 to 75% solvent B and an isocratic 5-min step at 98% solvent B.

2.18 Purification of reaction products

Cell-free supernatants prepared as described above were extracted twice with ethyl acetate added in a 1:2 ratio compared to the aqueous phase. The organic phase was recovered, dried with a Rotavapor apparatus, and the pellet is dissolved in 100% methanol and stored at -20°C. For further purification the sample is first diluted to a final 10% concentration of methanol and then loaded on HPLC. In this case an Econosil C18 reverse-phase column (250 by 10 mm) is used. Separation is carried out at a flow rate of 2 mL/min by using a two-solvent system consisting of a 0.1% formic acid solution in water (solvent A) and a 0.1% formic acid solution in methanol (solvent B). Compounds are separated using a 10-min isocratic elution with 10% solvent B, followed by a first 10-min linear gradient from 10 to 40%, a second 10-min linear gradient from 40% to 75%, a third 5-min gradient from 75% to 90% and a final isocratic 10-min step at 90% of solvent B. Each peak of interest was individually collected, concentrated, and stored at -20°C.

2.19 NMR and mass spectrometry analysis of catechols

For NMR analysis (performed by Dr. Alessandro Pezzella at the Department of Chemistry, University Federico II of Naples) aliquots of the purified cell-free supernatants prepared as described in paragraph 2.3 were lyophilized. The residues

obtained were directly used for NMR analysis in deuterated methanol. Chemical shifts are reported in δ values (ppm) downfield from tetramethylsilane. ^1H NMR spectra were recorded at 600, 400, or 300 MHz, and ^{13}C NMR spectra were recorded at 75 MHz. ^1H and ^{13}C distortion less enhancement by polarization transfer heteronuclear single-quantum correlation and ^1H and ^{13}C heteronuclear multiple-quantum correlation (HMBC) experiments were run at 600 and 400 MHz, respectively, on instruments equipped with a 5 mm ^1H /broadband gradient probe with inverse geometry using standard pulse programs. The HMBC experiments used a 100-ms long-range coupling delay. Hydroxyl group positions were deduced on the base of the spin-coupling pattern in the aromatic region of the ^1H NMR spectra.

2.20 DPPH assay.

α,α -diphenyl- β -picrylhydrazyl (DPPH) free radical scavenging method is generally the first approach to evaluate the antioxidant potential of a compound (**72**). DPPH is a stable free radical with λ_{max} at 515 nm (purple, ϵ_{517} in methanol = $12 \text{ mM}^{-1}\text{cm}^{-1}$). Its conversion to DPPH (yellow) is used as a readout of radical scavenging of an antioxidant compound. In a final volume of 1 mL of 100% methanol, different concentrations of our phenolic compounds and 0.1 mM of a freshly prepared DPPH solution in 100% methanol were added. It is important to note that, as recommended by Kedare and coauthors (**72**), the initial DPPH concentration should give absorbance ≤ 1.0 . The reaction was allowed to proceed for a maximum time of 30 minutes at RT, in any case till completion, and followed at $\lambda = 515 \text{ nm}$.

2.21 Cell cultures and extracts

H9c2 cells were maintained in Dulbecco's modified Eagle medium supplemented with 10% fetal bovine serum, 2 mM L-glutamine, 1% v/v penicillin/streptomycin solution (100 U/ml) (Sigma-Aldrich, Milano, Italy) at 37°C in 5% CO_2 incubator. To induce oxidative stress, cells were treated with 250 μM of an aqueous solution of sodium arsenite (Sigma Aldrich).

2.22 Immunofluorescence

Cells were seeded onto coverslips (25,000 cells in 300 μL of DMEM for each coverslip), grown for 48 hours, incubated for 3h with different concentrations of the novel catechols, and subsequently treated with 250 μM of sodium arsenite for 1.5h. As negative and positive control of the stress effect, cells were treated with either buffer or 250 μM of sodium arsenite, respectively. Cells were then fixed in 4% paraformaldehyde in PBS 1X for 15 min at room temperature and rinsed three times with PBS 1X. Quenching was performed with 50 mM NH_4Cl in PBS 1X. After washing, cells were permeabilized using 0.1% Triton X100 in PBS 1X for 30 min and blocking was performed by adding 5% albumine bovine serum in PBS 1X for 1h at room temperature. PABP monoclonal antibody (Sigma Aldrich) was diluted (1 $\mu\text{g/mL}$) in blocking buffer and incubated overnight at 4°C . After washing in PBS 1X, cells were incubated with secondary antibody Cy3 conjugated goat anti-mouse IgG (1:1,000 dilution) (Jackson Immuno Research Laboratories). For nuclear counterstaining, cells were incubated with DAPI in PBS 1X 0.1 $\mu\text{g/mL}$ for 10 min at room temperature. After washing, coverslips were mounted in 50% glycerol in PBS 1X. Images were captured using a Zeiss confocal laser-scanning microscope LSM 510 using suitable lasers. Image analyses on stress granules was performed using "Stress granule counter" and "Analyze particles" ImageJ (<http://rsbweb.nih.gov/ij/index.html>) plugins. Nuclear

counterstaining was used to count the total number of cells. Statistical analyses were performed using GraphPad (Prism) software ver. 5.0.

2.23 MTT Assay

Cells were seeded on 96-wells plates (2,500 cells in 100 μ L of DMEM) and grown at 37°C overnight. Catechols were added at the same concentrations used for immunofluorescence experiments. After 72 h of incubation, 10 μ L of a MTT stock solution in PBS 1X were added to the cells to a final concentration of 0.5 mg/mL in Dulbecco's modified Eagle's medium without red phenol (final volume 100 μ L). After 4h of incubation, the MTT solution was removed and MTT formazan salts were dissolved in 100 μ L of 0.1 N HCl in anhydrous isopropanol. Cell survival was expressed as the absorbance of blue formazan measured at $\lambda=570$ nm with an automatic plate reader (Victor ³TM Multilabel Counter; Perkin Elmer, Shelton, CA, USA). Standard deviations were always <5% for each experiment.

2.24 Ethidium bromide and acridine orange assay

An ethidium bromide and acridine orange (EB/AO) staining assay was performed to identify and quantify apoptotic cells **(73)**.

AO is a nucleic acid selective fluorescent dye that permeates all living cells highlighting the nuclei by green fluorescence, while EB is only taken up by cells when cytoplasmic membrane integrity is compromised, staining red apoptotic nuclei. Cells were seeded in 6-wells plates (200,000 cells in 2 mL of DMEM) and grown for 48h. Cells were incubated with the appropriate concentrations of antioxidant catechols for 3h, before or after treatment with sodium arsenite (250 μ M for 1.5 h) and then trypsinized, collected by centrifugation, and washed with ice cold PBS 1X. Then, cells were re-suspended in 100 μ L of cold PBS 1X and incubated with 5 μ L of the EB/AO dye mixture (100 μ g/mL each of AO and EB in PBS 1X) at 37°C for 20 min. Stained cells were placed on a microscope slide and covered with coverslips. Images were taken at 200 X magnification. Both apoptotic (red) and live (green) cells were counted in five microscopic fields, to obtain the percentage of apoptotic cells.

3.1.1 ToMO from *Pseudomonas* sp. OX1 for the biosynthesis of phenolic antioxidants.

Oxidative stress is a consequence of the imbalance between the production of reactive oxygen species (ROS) and the ability of cells to counterbalance this physiological event through the action of antioxidants (74,75). Much attention has been dedicated by the scientific community to both antioxidant phenols and catechols, molecules -that among others- can be easily functionalized. Particular interest has also been devoted to the set-up of biocatalytic processes to produce these compounds to avoid the problems encountered with the chemical synthesis.

The biocatalytic potential of the ToMO multicomponent monooxygenase from *Ps.* sp. OX1 has been recently confirmed by its use for the production of tyrosol and hydroxytyrosol, strong antioxidants commonly found in extra virgin olive oil, starting from a low cost, commercially available aromatic precursor such as 2-phenylethanol (38).

The versatility of ToMO and the bioinformatic strategy recently developed for this system, allow the use of this enzyme not only for the optimization of the bioconversion of 2-phenylethanol in hydroxytyrosol, but also for the hydroxylation of other monocyclic aromatic compounds, which are not natural substrates of this enzyme, in order to synthesize novel antioxidant phenols and catechols for food and pharmaceutical industries.

Therefore, it was decided to investigate the potential use of ToMO for the hydroxylation of the following molecules: 2-phenoxyethanol, 2,3-dihydrobenzofuran, phthalan and 2-indanol (Fig.8). As underlined in the Introduction section these substrates were chosen on the basis of *i*) their similarity with ToMO natural substrates and *ii*) the different nature of the substituents bound to the aromatic ring which may influence the biological activity of their hydroxylated derivatives obtained from the ToMO-catalyzed reaction.

3.1.2 Identification and characterization of the products obtained from the ToMO-catalyzed hydroxylation.

2-phenoxyethanol, 2,3-dihydrobenzofuran, phthalan and 2-indanol were purchased from Sigma. Their purity was checked by HPLC, as described in Materials and Methods. For each compound the corresponding UV-Vis spectrum was recorded. λ_{max} for each substrate is reported in Fig.9.

In order to verify the stability at room temperature of these aromatic compounds their evaporation rate was checked (Fig. 10 and Table 1) under experimental conditions that simulated the typical biotransformation assays, *i.e.* using a final concentration of 1 mM of each substrate of interest dissolved in M9 medium containing 0.4% glucose

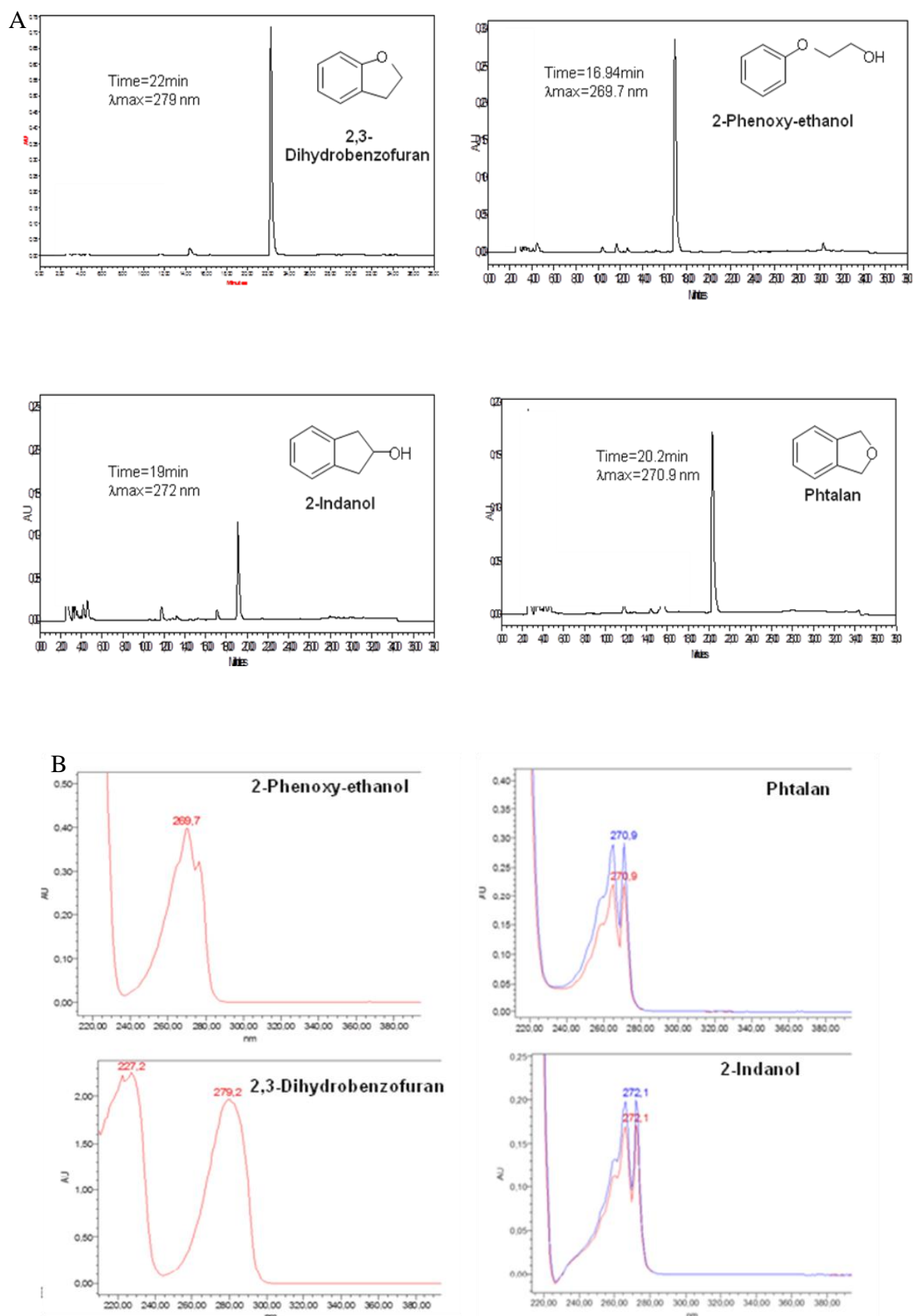


Figure 9:
A) HPLC elution profiles of each substrate
and B) the corresponding UV-vis spectrum.

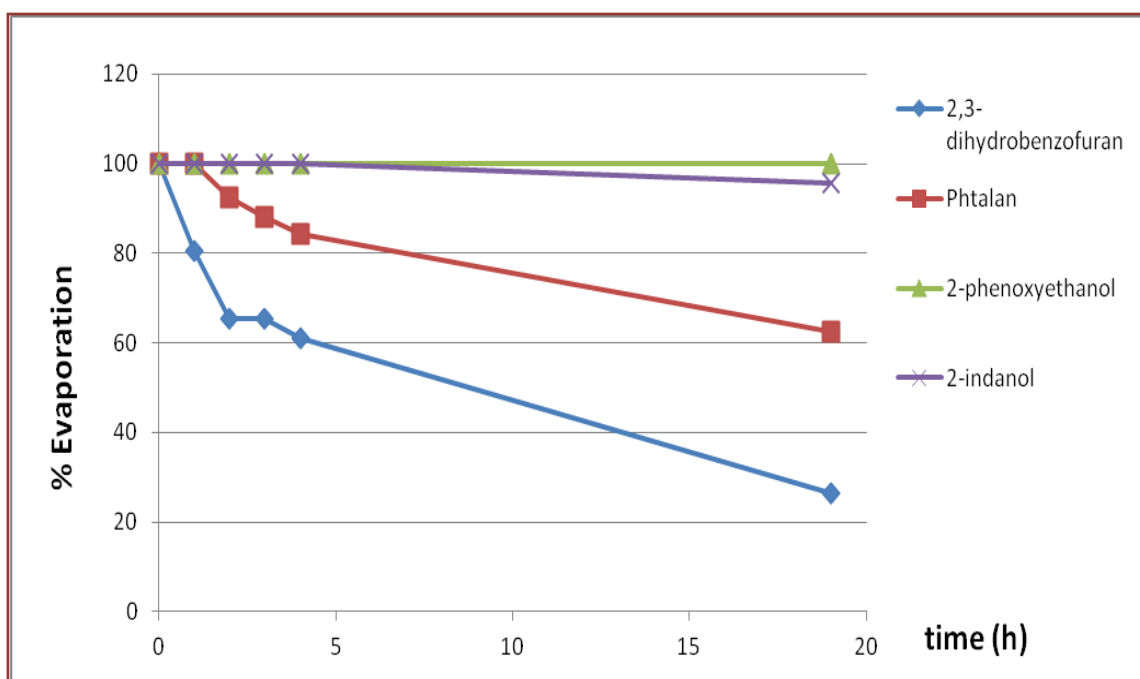


Figure 10: Evaporation curves of the aromatic substrates as a function of time.

	2,3-dihydrobenzofuran	Phtalan	2-phenoxyethanol	2-indanol
<i>time(h)</i>	<i>% of substrate</i>	<i>% of substrate</i>	<i>% of substrate</i>	<i>% of substrate</i>
0	100	100	100	100
1	80,5	100	100	100
2	65,48	92,3	100	100
3	65,4	88,1	100	100
4	60,9	84,2	100	100
19	26,4	62,4	100	95,6

Table 1 : In this table, for each compound, time and corresponding percentage of residual substrate are reported.

(from now on indicated as M9-G), and at a temperature of 28°C. The evaporation rate was evaluated spectrophotometrically, by recording the spectrum at different time intervals and comparing the corresponding ABS values at λ_{\max} . As evident from the analysis of the data presented in Table 1, 2,3-dihydrobenzofuran and phthalan are more volatile than 2-indanol and 2-phenoxyethanol. This is an important consideration to take into account, because, due to their volatility, it could be necessary to increase their concentration in the growth medium for a future optimization of the biotransformation assays and for a correct estimation of products yield. Even though 2-indanol and 2-phenoxyethanol are quite stable under the experimental conditions used, we decided to increase the initial concentration of all compounds used in the following biotransformation processes up to 2 mM.

Cells of *E. coli* strain JM109 transformed with plasmid pBZ1260, expressing the complete *wt tou* gene cluster, were grown in LB and ToMO expression was induced as described in Materials and Methods. After 1 hour of induction, cells were collected by centrifugation, resuspended in M9-G at a final concentration of 6 OD₆₀₀ and incubated with 2 mM of either 2-phenoxyethanol or phthalan or 2-indanol or 2,3-dihydrobenzofuran.

After incubation for different time intervals (0, 30 min, 1h, and 16 h) at 30°C under constant shaking (220 rpm), samples were withdrawn, cells were collected by centrifugation, and an aliquot of exhausted medium was loaded on HPLC to check for the presence of hydroxylated products. HPLC analysis of these samples was performed as described in section 2.2. As it is evident from Fig. 11, where only samples from the 16 h incubation have been reported for clarity, *wt* ToMO was able to hydroxylate 2-phenoxyethanol, phthalan, and 2,3-dihydrobenzofuran. Three different peaks eluting respectively at 10.38 min (λ_{\max} = 287.5 nm), at 12.6 min (λ_{\max} =273.5nm) and 15.16 min (λ_{\max} =275.3nm) were evident in the case of 2-phenoxyethanol (Fig.11A). When using phthalan as substrate a single peak was eluted at 14.3 min (λ_{\max} =279.2 nm) (Fig. 11B). For 2,3-dihydrobenzofuran one single peak of product was evident from the chromatogram (Fig.11C) eluting at 14 min (λ_{\max} =299nm).

No evident hydroxylation product was instead observed when the substrate used for the bioconversion was 2-indanol, thus confirming the results obtained from the manual docking of these aromatic substrates into the active site of ToMOA performed in collaboration with Dr. Eugenio Notomista at the Department of Biology (data not shown). For the bioconversion of 2-indanol the ToMO variant E103G/F176A was used whose expression and induction were performed as described above for *wt* ToMO system. HPLC chromatogram in Fig. 12 shows in this case the presence of two peaks of hydroxylated products eluting respectively at 13 min (λ_{\max} = 280.3 nm) and 10 min (λ_{\max} =288nm), thus indicating that in this mutant a wider cavity of the active site permits the entrance of 2-indanol and allows its hydroxylation.

Once checked for the presence of hydroxylation products in the reactions involving these aromatic compounds, the exhausted media obtained from each bioconversion were further purified through organic extraction, as described in Materials and Methods. Samples were then loaded on a preparative HPLC C-18 column, each peak was manually collected, lyophilized and analyzed by NMR and mass spectrometry by Dr. Alessandro Pezzella at the Department of Chemistry, University Federico II of Naples (see Materials and Methods). Results are presented in Table 2. All hydroxylated compounds were identified except for the product obtained from 2,3-dihydrobenzofuran; in this case the lyophilization

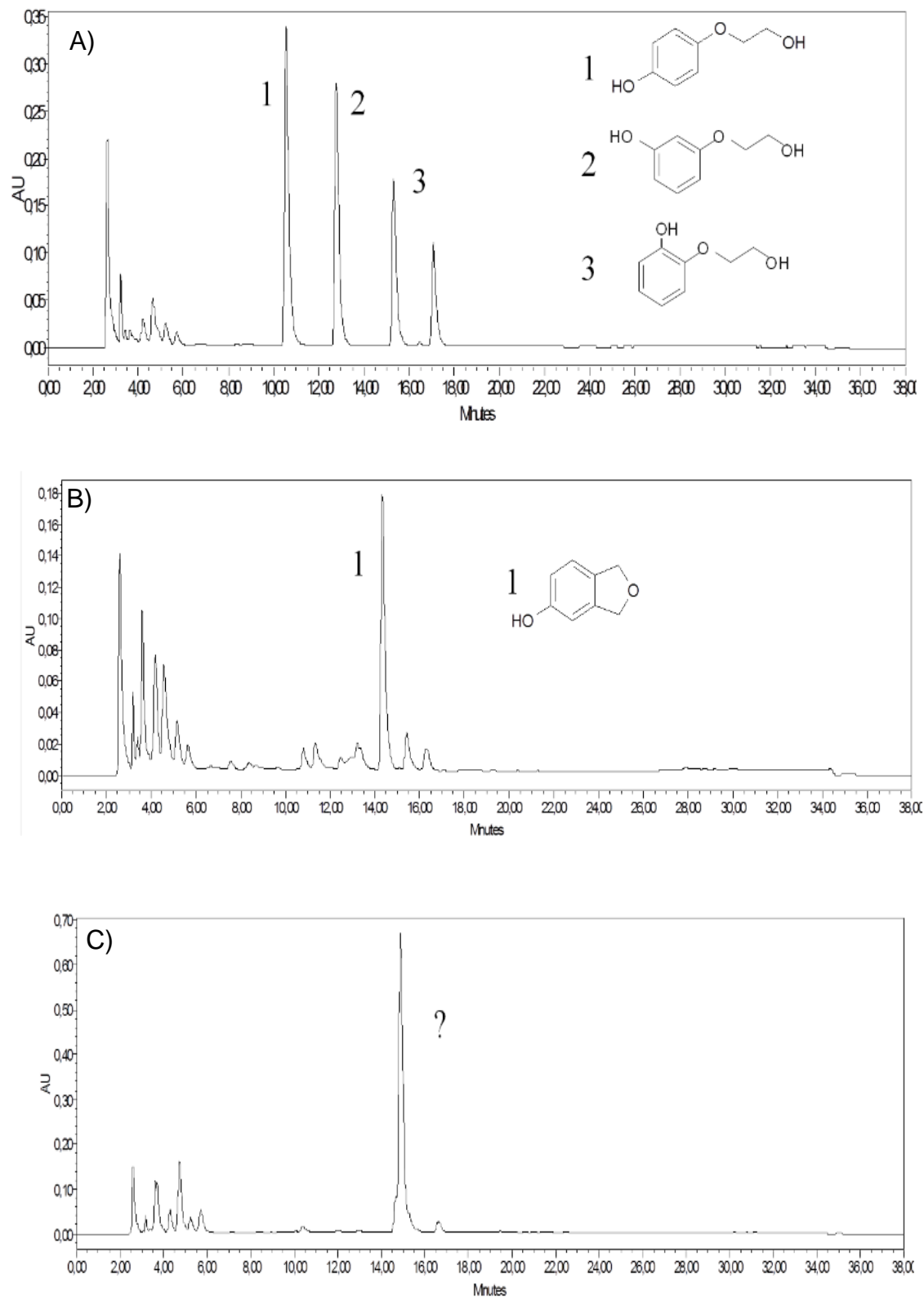


Figure11: HPLC chromatograms of aliquots of exhausted media obtained after 16 hours of wt ToMO-catalyzed bioconversion of A) **2-phenoxyethanol**, B) **phthalan**, C) **2,3-dihydrobenzofuran**.

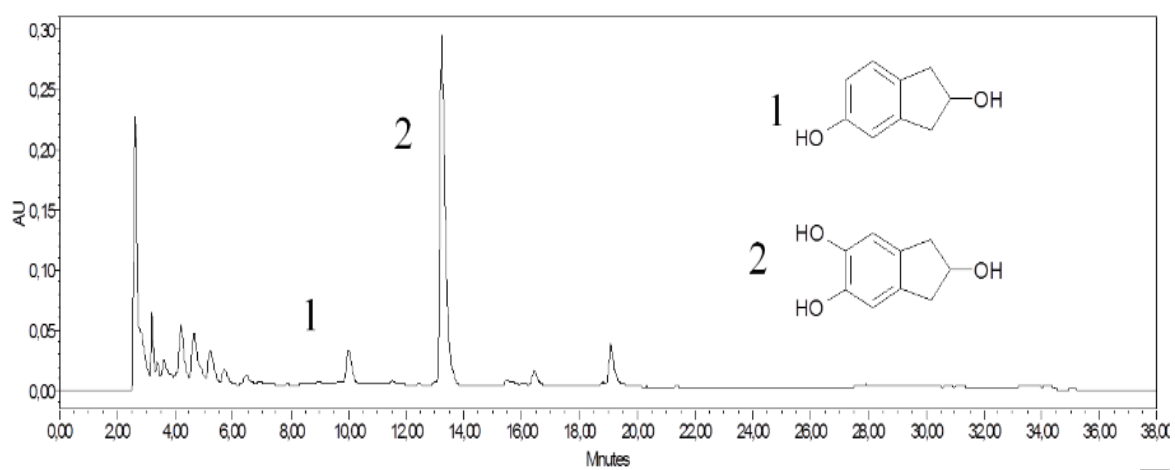


Figure 12: HPLC chromatogram of an aliquot of exhausted medium obtained after 16 hours of E103G/F176A ToMO variant-catalyzed bioconversion of **2-Indanol**.

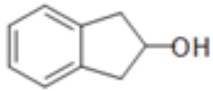
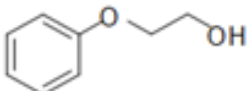
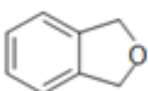
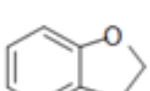
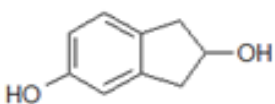
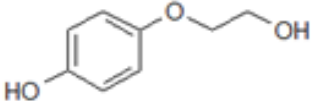
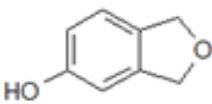
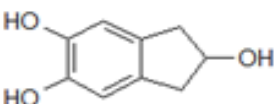
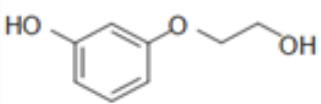
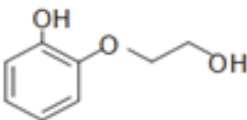
			 2,3- Dihydrobenzofuran
			
			
			

Table 2: Hydroxylation products obtained from ToMO-catalyzed reaction on each aromatic substrate. Hydroxyl group positions were deduced on the base of the spin-coupling pattern in the aromatic region of the ^1H NMR spectra (see Materials and Methods).

process lead to a mixture of oxidized compounds whose structure could not be univocally assigned. Preliminary data showed that this non-purified mixture had antioxidant activity both *in vitro* and *ex vivo* (data not shown). However, it was decided not to proceed any further on this mixture for the difficulty in determining both its exact composition and concentration.

To evaluate the concentration of the novel hydroxylated compounds obtained from ToMO-catalyzed reaction we selected, for each of them, a similar compound whose UV-vis spectrum and corresponding extinction coefficient is available in literature (Fig. 13). All the spectroscopic data used for calculations were obtained from "Organic Electronic Spectral Data" book series (Wiley eds.).

3.1.3 *In vitro* assessment of the antioxidant potential: the DPPH assay.

The capacity of the new hydroxylated compounds to scavenge the stable radical 2,2-diphenyl-1-picrylhydrazyl (DPPH) was determined spectrophotometrically by measuring the loss of absorbance of DPPH at $\lambda=515$ nm (see Materials and Methods for details). In a final volume of 1mL of methanol, 0.1 mM DPPH and different concentrations of each hydroxylated compound were added, and the loss of ABS_{515} was monitored for 30 minutes. At this time, once the ABS_{515} value is stable, residual DPPH ($DPPH_{res}$) is calculated as:

$$DPPH_{res} = [DPPH]_{res}/[DPPH]_{t=0}$$

The concentration of hydroxylated compound added in each experiment was plotted against the DPPH effectively reduced calculated as $[DPPH_{red}] = 1 - ([DPPH]_{res}/[DPPH]_{t=0})$ (Fig. 14A). The concentration that causes a decrease in initial DPPH concentration by 50% was defined as EC_{50} and was obtained by a non-linear regression of the experimental curves using the Graphpad Prism software. Each EC_{50} is the result of at least two independent experiments.

Once obtained the EC_{50} value for a specific compound we estimated also at that specific concentration the time needed to reach a stable value of the ABS at 515 nm (the plateau), thus introducing a parameter indicated in literature as T_{EC50} (Fig.14B) **(76,77)**. At this point we calculated what has been defined by Sanchez-Moreno and coworkers **(76)** as the "antiradical efficiency (AE)" a parameter that is expressed by the following formula: $AE = 1 / (EC_{50} \times T_{EC50})$.

In all experiments described in this and in the following paragraphs, known antioxidants as tyrosol and hydroxytyrosol (Fig. 5, Introduction) have been always tested, as reference molecules, in parallel with our novel hydroxylated compounds.

Results are shown in Table 3, where it is evident that some among the novel phenols and catechols produced by the ToMO-catalyzed reaction on non-natural aromatic substrates show an antiradical efficiency comparable to both the natural phenolic antioxidant hydroxytyrosol and to carotenoids (Table 4). Interestingly, compounds such as tyrosol, which has been reported to be antioxidant *in vivo* **(78)**, 2-(3'-hydroxyphenoxy)-ethanol, 5-hydroxy-2-indanol, and 3-hydroxyphtalan (Fig.13) were almost non responsive to the DPPH assay causing negligible losses of ABS_{515} even when used at mM concentrations.

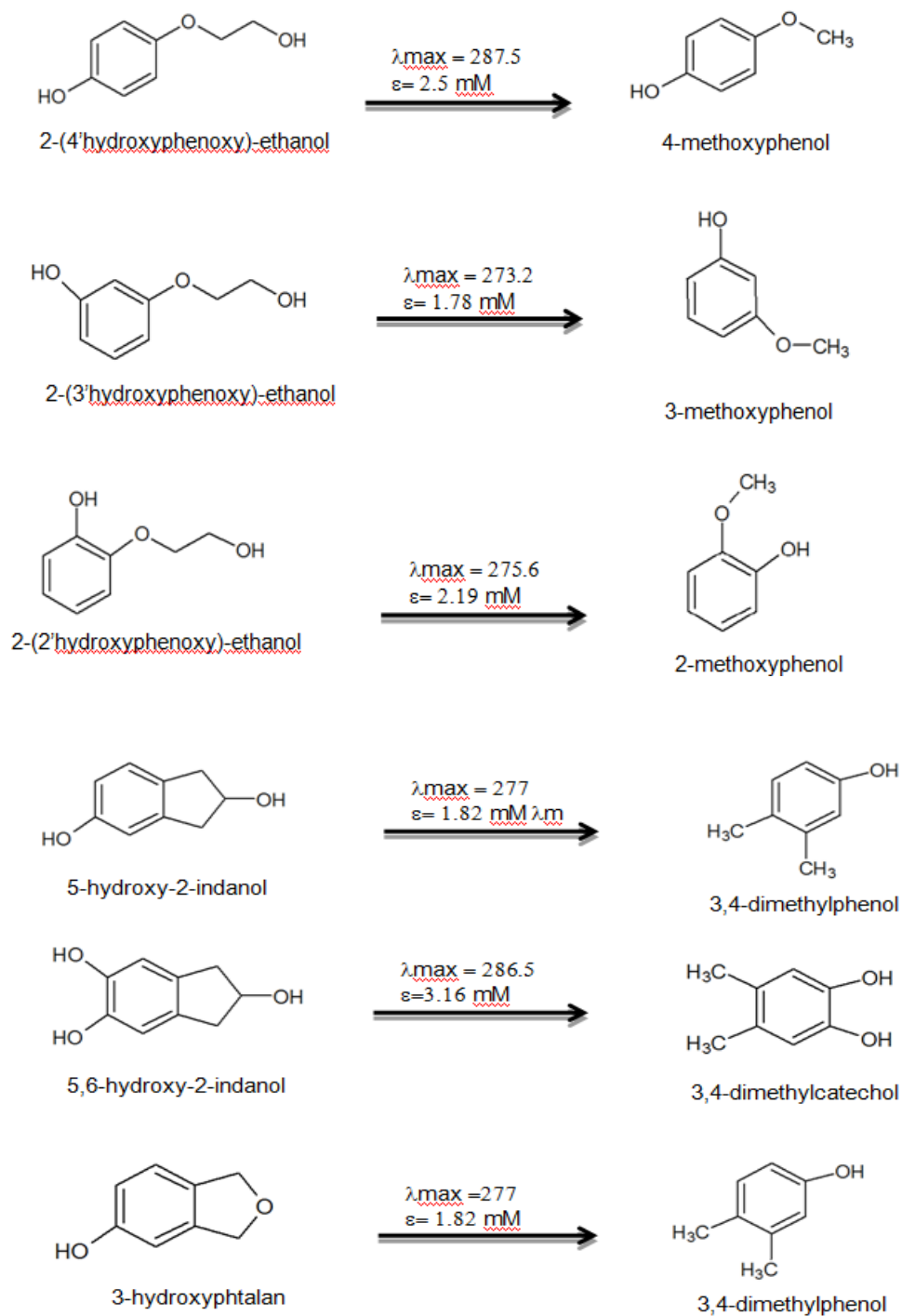


Figure 13: Hydroxylated products obtained from the ToMO-catalyzed reaction and similar compounds whose extinction coefficient is available in literature.

Compound	EC₅₀(μM) μM Antioxidant/ μM DPPH	T_{EC50}(min)	AE
Hydroxytyrosol	0,22	16	0,28
2-(2'-hydroxyphenoxy)- ethanol	1	24,5	0,04
2-(4'-hydroxyphenoxy)- ethanol	0,36	19,5	0,14
5,6-hydroxy-2-indanol	0,41	18	0,135

Table 3: Antioxidant efficiency (AE) for each hydroxylated compound tested.

Compound	AE
Lycopene	0,250
<i>α-Carotene</i>	0,047
<i>β-Carotene</i>	0,037
<i>β-Cryptoxanthin</i>	0,042
<i>Lutein</i>	0,011
<i>Zeaxanthin</i>	0,018

Table 4: Antioxidant efficiency (AE) of several carotenoids (**75**).

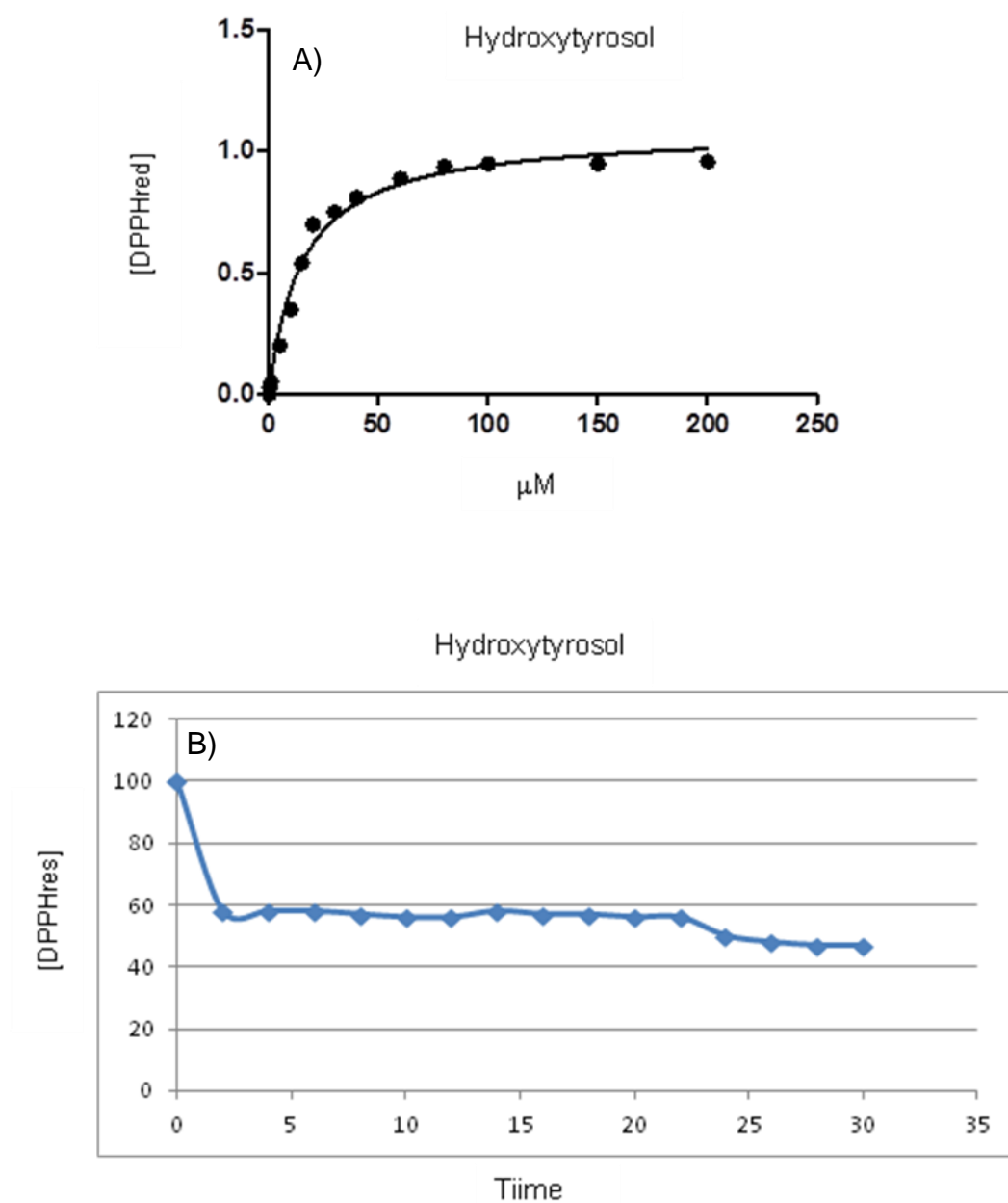


Figure 14:

A) A typical $[DPPH]_{red}$ vs. concentration curve when using hydroxytyrosol in the DPPH assay.

B) A $[DPPH]_{res}$ vs. time (min) curve when using hydroxytyrosol in the DPPH assay.

3.1.4 Antioxidant activity on H9c2 cells.

The antioxidant activity of the novel hydroxylated compounds was evaluated on a selected eukaryotic cell line, the embryonic rat cardiomyoblast cell line H9c2, subjected to a mild oxidative stress induced by sodium arsenite. H9c2 cells are currently used as a model system of non-malignant and cardiac-like cells, suitable to study cellular response to oxidative damage. The experiments performed on this cell line were performed in collaboration with Dr. Eliodoro Pizzo, Dr. Carlo Di Cristo and Dr. Carmen Sarcinelli (Department of Biology, University of Naples Federico II).

Prior to analyze the antioxidant potential of our novel compounds, we assessed their cytotoxicity by evaluating *i*) the influence on the MTT assay and *ii*) the apoptotic effect on treated cells.

MTT assay is a colorimetric assay that allows to analyze cell survival by measuring, after a specific treatment, the residual activity of mitochondrial enzymes which reduce the tetrazolium dye, MTT, to its insoluble form, formazan, thus giving a purple color.

Cells were plated on 96-well plates at a density of 2,500 cells in 100 μ L of medium containing either novel hydroxylated compound at an optimized concentration \geq EC₅₀ (5 to 10 μ M higher than the EC₅₀ value, see Materials and Methods for details). When this value was not available, as in the case of tyrosol, 2-(3'-hydroxyphenoxy)-ethanol, 5-hydroxy-2-indanol, and 3-hydroxyphthalan (Fig.13), two arbitrary concentrations of 40 and 80 μ M were tested.

After 72 h of incubation, 10 μ L of a MTT stock solution in 1X PBS were added to the cells to a final concentration of 0.5 mg/mL in Dulbecco's modified Eagle's medium (final volume 100 μ L). After a 4h incubation, the MTT solution was removed and MTT formazan salts were dissolved in 100 μ L of 0.1 N HCl in anhydrous isopropanol. Cell survival was expressed as the ABS of blue formazan measured at 570 nm with an automatic plate reader (Victor ³TM Multilabel Counter; Perkin Elmer, Shelton, CA, USA). (79). Standard deviations were always <5% for each experiment.

Data obtained showed that our compounds, as well as their non-hydroxylated precursors (data not shown), induce a minor reduction of cell viability (Fig. 15). Residual viability for any compound tested was never lower than 92% and in some cases cell viability appeared to be even improved (Fig.15).

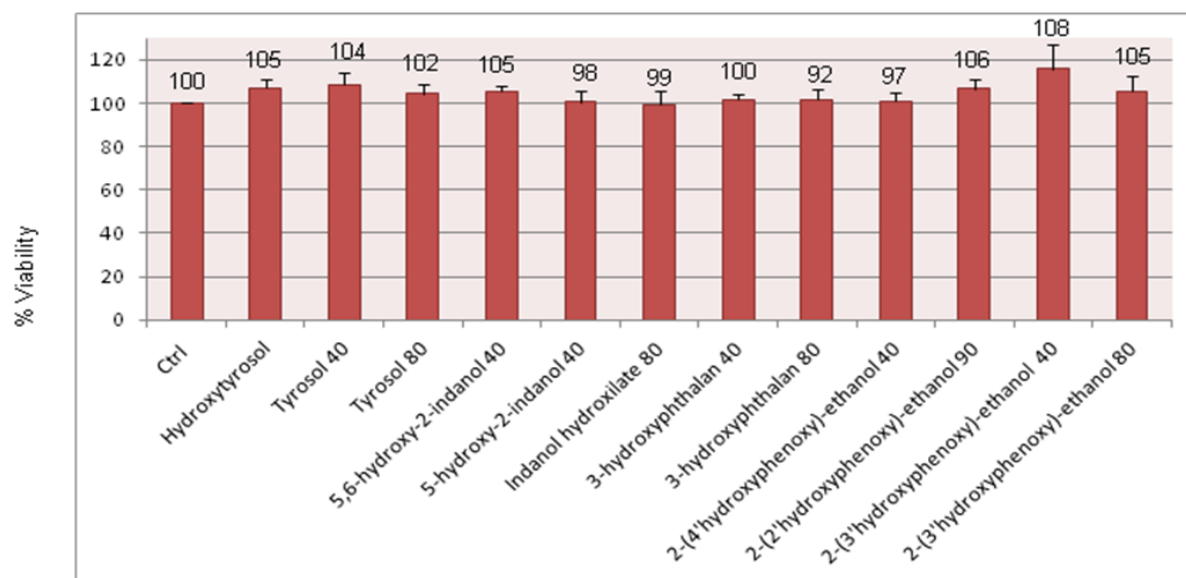


Figure 15: Cell survival is expressed as ABS_{570} of blue formazan. Standard deviations were always <5% for each experiment.

To examine the effect of our compounds on cell apoptosis, ethidium bromide and acridine orange staining was used to identify apoptotic nuclei (Fig. 16A). Acridine orange (AO) permeates intact cells and stains all nuclei green, while Ethidium bromide (EB) stains apoptotic nuclei with red fluorescence when cytoplasmic membrane integrity is compromised. Experiments were performed as described in Materials and Methods. Under our conditions a basal apoptotic frequency in non-treated cells was observed which corresponded to a value of $13 \pm 7\%$. Incubation with hydroxytyrosol reduced the percentage of apoptotic nuclei to a value of $11 \pm 4.1\%$. Hydroxylated compounds did not significantly alter the occurrence of apoptotic nuclei (blue bars, Fig.16B). Incubation with either 5-hydroxy-2-indanol or 5,6-hydroxy-2-indanol or 2-(4'-hydroxyphenoxy)-ethanol or 2-(3'-hydroxyphenoxy)-ethanol provided a percentage of apoptotic nuclei of $11 \pm 4.8\%$, $11 \pm 1.7\%$, $12 \pm 6.3\%$, $7 \pm 4.2\%$ respectively. However, when incubated with either 2-(2'-hydroxyphenoxy)-ethanol or 3-hydroxyphthalan the percentage of apoptotic nuclei were of $18 \pm 3.5\%$ and $18 \pm 3.8\%$ respectively.

Oxidative stress in this cell line was induced by adding $250 \mu\text{M}$ of sodium arsenite for 1.5 hours (Materials and Methods). Exposure of cells to arsenite results in numerous effects including apoptosis, malignant cell transformation, cell cycle arrest, induction of stress response, inhibition of cell proliferation and cytoskeletal injury **(80)**. The exact mechanism of arsenite's toxicity is currently unknown. Several possibilities have been proposed including alterations in DNA repair and methylation and the generation of ROS. Arsenite also has the ability to bind to protein thiol groups. It is believed that the binding of thiol groups, as well as ROS generation, can alter many protein functions. Thus, the distinct and diverse effects of arsenite may result from the activation and/or inactivation of a variety of signal transduction pathways in cells **(80)**. Following oxidative stress (red bars, Fig.16B), the percentage of apoptotic nuclei in non-treated cells showed a two-fold increase, giving a value of $31 \pm 2.9\%$. A 3h pre-treatment with our hydroxylated compounds (Materials and Methods) lead to different results: when cells were pre-treated with 5-hydroxy-2-indanol, 5,6-hydroxy-2-indanol, 2-(4'-hydroxyphenoxy)-ethanol and 2-(2'-hydroxyphenoxy)-ethanol, the occurrence of apoptotic nuclei decreased, thus indicating a protective effect of these compounds. On the other hand, the use of either tyrosol, hydroxytyrosol, 2-(3'-hydroxyphenoxy)-ethanol or 3-hydroxyphthalan led to a slight increase in cell apoptosis.

It is worth to note that even if a two-fold increase of cell apoptosis was observed in non-treated cells incubated with $250 \mu\text{M}$ of sodium arsenite, the value obtained is still compatible with a general viability of the cell population analyzed, thus allowing the use of this oxidant for the experiments of immunofluorescence described in the next paragraph.

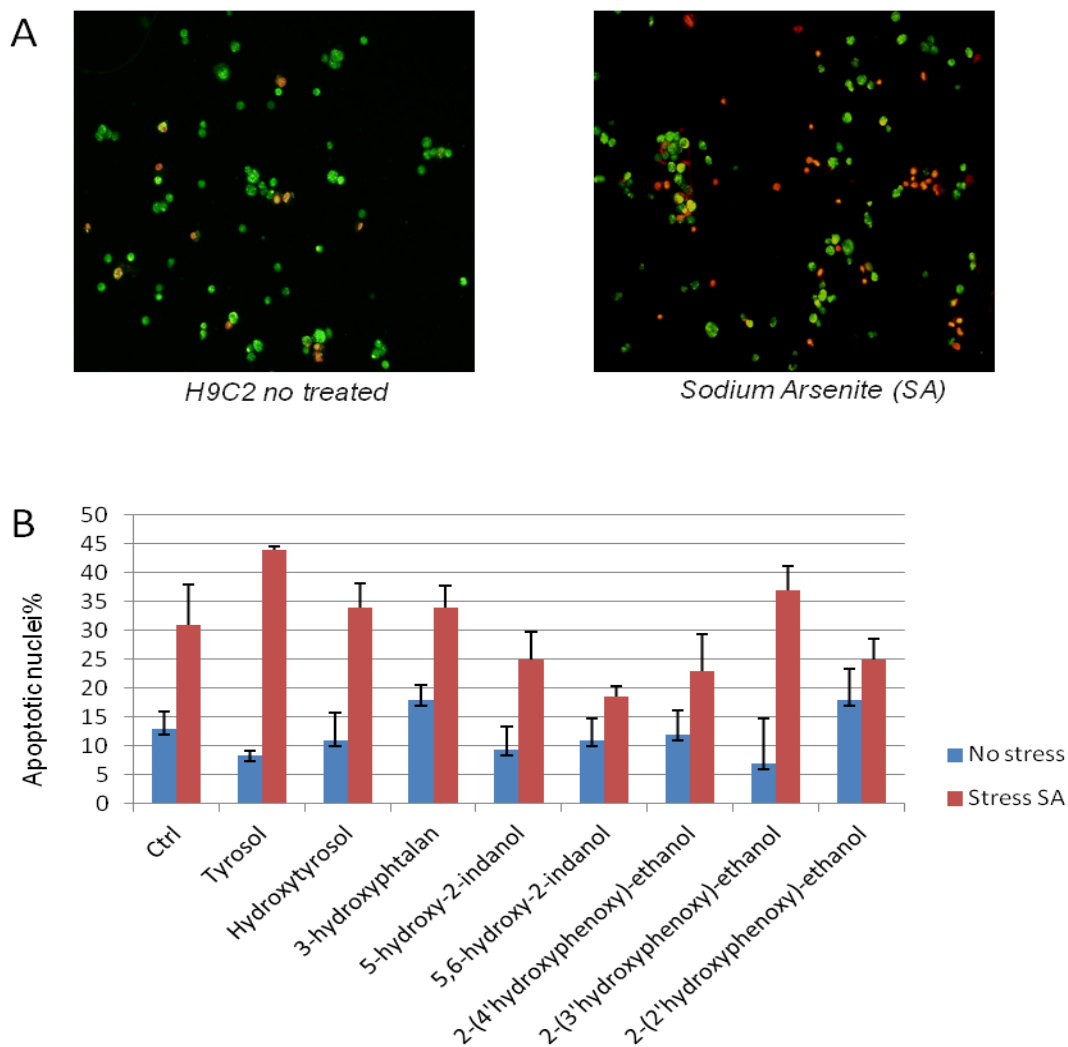


Figure 16:

A) Apoptotic cells under physiological (left panel) and oxidative stress conditions (right panel).

B) Cell survival was evaluated from ABS_{570} of blue formazan. Standard deviations were always <5% for each experiment.

As underlined before, exposure to sodium arsenite inhibits protein synthesis and activates multiple stress signaling pathways. When translation is initiated in the absence of a functional eIF2-GTP-tRNAⁱ Met complex, the 40S ribosome stalls on the mRNA to form a 48S pre-initiation complex. These complexes composed by 40S ribosomes, initiation factors, and their associated mRNA transcripts accumulate in the cell cytoplasm to form what is usually referred to as “stress granules” (SGs) (81).

To better investigate the antioxidant potential of our novel hydroxylated compounds we analyzed the occurrence and the number of stress granules (SGs) in H9c2 cells subjected to sodium arsenite-induced oxidative stress by using a specific antibody against PABP, a protein that binds to poly(A)tails of mRNA and regulates mRNA stability and protein translation. PABP is a prominent component of SGs (81).

Experiments were performed as described in Materials and Methods. SGs number was examined by using suitable plugins for imaging software and a statistical analysis was applied to microscope images acquired. For each experiment, at least 350-400 cells were analyzed.

Immunofluorescence and confocal microscopy analysis revealed a 3.59 fold increase in SGs number of cells incubated with sodium arsenite, when compared to non-treated cells (Fig. 17 A and B). Two-tailed Student's *t* student analysis confirmed this statistical difference ($p < 0.05$). No statistically significant difference was instead observed in SGs number in cells treated with our compounds, thus indicating that they do not increase the basal SGs number of non-treated cells.

When sodium arsenite-stimulated cells were pre-treated with each of our compounds, a strong and statistically significant decrease in SGs number was observed (Fig. 17B) with a maximum effect obtained when using 40 μ M of 5,6-hydroxy-2-indanol.

$p < 0.05$ for cells pretreated with:

- 40 μ M of 2-(4'-hydroxyphenoxy)-ethanol;
- 40 μ M of 3-hydroxyphthalan;
- 80 μ M of 5-hydroxy-2-indanol.

$p < 0.01$ for cells pretreated with:

- 90 μ M 2-(2'-hydroxyphenoxy)-ethanol;
- 2-(3'-hydroxyphenoxy)-ethanol;
- 80 μ M of 3-hydroxyphthalan;
- 25 μ M Hydroxytyrosol;
- 40 μ M of 5,6-hydroxy-2-indanol;
- 40 μ M of 5-hydroxy-2-indanol;
- Tyrosol.

In order to exclude a putative antioxidant role of the aromatic compounds used as substrates in the ToMO-catalyzed biosynthesis, their effect on SGs number in H9c2 treated cells was also evaluated (data not shown). In these experiments no significant decrease in SGs number was observed, when compared with the control, thus excluding any antioxidant effect of the non-hydroxylated precursor of our compounds.

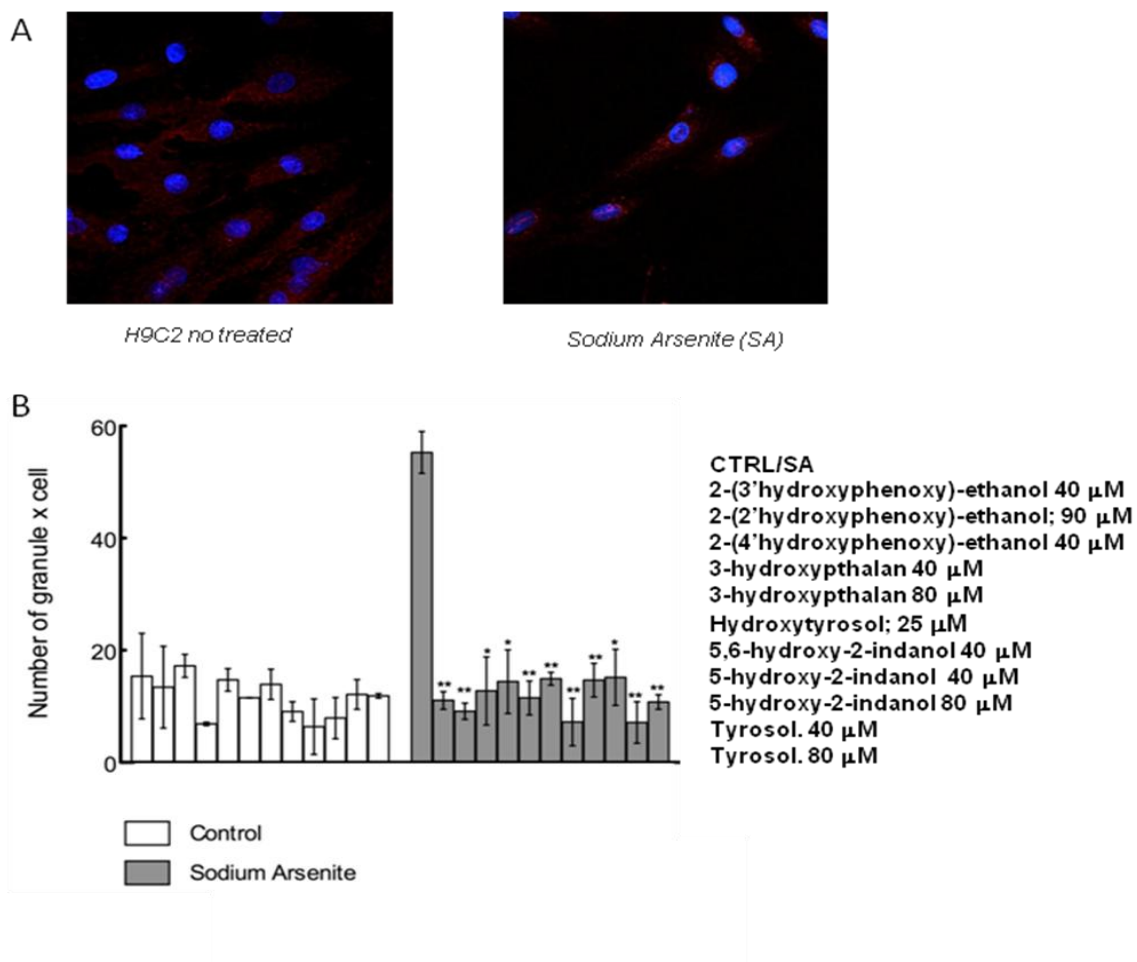


Figure 17:

A) Immunofluorescent representative images of stress granules in physiological (left panel) and stress condition (right panel).

B) Estimation of the number of stress granules in H9c2 cells in the presence and absence of the novel hydroxylated compounds.

3.2.1 The Industrial scale-up of ToMO-catalyzed hydroxylation: use of *Bacillus subtilis* as a GRAS host for the heterologous expression of oxygenase activities.

The first step for a future industrial scale-up of ToMO-catalyzed hydroxylation of aromatic substrates to produce high-added value compounds is the use of a GRAS (**G**enerally **R**ecognized **A**s **S**afe) host microorganism for the recombinant expression of this multicomponent monooxygenase.

The system currently used for the recombinant expression of ToMO is one of the most widely used expression hosts, *i.e.* *Escherichia coli*. The techniques for protein overexpression in *E. coli* are well developed; nevertheless, the use of this microorganism for the recombinant expression is often related to the formation of inclusion bodies due to the inefficacy of its folding machinery. Additional problems that strongly limit the use of this microbial host for the industrial scale-up of any bioprocess are related to the presence in its outer membrane of the lipopolysaccharide (LPS), an harmful endotoxin that complicates the purification process.

As outlined in the Introduction section, *Bacillus subtilis* is a good alternative to *E.coli*, and, most importantly, the microorganism has been defined as GRAS and non-pathogenic to humans (68).

Recently, the ToMO system was used for the production of tyrosol, a strong phenolic antioxidant commonly found in extra-virgin olive oil, starting from 2-phenylethanol, a cheap and commercially available compound (38). Tyrosol belongs to a class of molecules commonly referred to as “nutraceuticals”, whose role in the prevention of diseases such as cancer and cardiovascular diseases is rapidly emerging (13).

Due to the inability of *wt* ToMO to produce tyrosol as the sole isomer from the hydroxylation of 2-phenylethanol, a computational model was developed which provided a molecular explanation for this outcome. The bioinformatic analysis led to the identification of residue F176 as a major steric hindrance for the correct positioning of the reaction intermediate leading to tyrosol production. In fact, all the mutations at position 176 allowed ToMO to produce only tyrosol from 2-phenylethanol. Moreover, the combination of mutations at position F176 with mutation E103G increased the k_{cat} values on 2-phenylethanol. In conclusion, among the E103G/F176X variants prepared in the laboratory where this PhD project was developed, it was found that mutant E103G/F176T was one of the most efficient, allowing, in batch experiments, the conversion of about 50% of 2-phenylethanol into tyrosol in 2h (38.).

In this chapter, the use of *B. subtilis* as a host for the recombinant expression of ToMO variant E103G/F176T is described, with the aim of investigating the potential use of this microorganism for the industrial scale-up of the bioconversion of 2-phenylethanol into tyrosol, previously validated in the strain JM109 of *E.coli*.

The strategies used were *i*) to integrate the *tou* gene cluster in the genome of *B. subtilis* through single crossing over, and *ii*) to express the *tou* gene cluster in a *B. subtilis* compatible expression vector.

The direct integration of a gene of interest in the genome of *B. subtilis* is the preferable approach from a biotechnological point of view because it generates a stable mutant strain whose selection does not need the use of antibiotics. However, the expression level of the recombinant protein might be too low to allow the effective evaluation of the potential use of this novel host strain for the bioconversion of 2-phenylethanol into tyrosol. As a consequence, a more “classical” approach was also attempted which involved the cloning of the *tou* gene cluster in a non-integrative

IPTG-inducible vector suitable for the heterologous expression of proteins in *B. subtilis*.

3.2.2 Cloning of the *tou* gene cluster: integration into the genome of *B. subtilis*.

The integration was intended to occur through a single crossing over mediated by the presence, at the 5' of the *tou* gene cluster, of a specific constitutive promoter of *B. subtilis*. A constitutive promoter was selected because, generally, an inducible promoter leads to the use of expensive inducers for the fine-tuning of gene expression, a characteristic which can be considered prohibitive for an industrial scale-up of a biosynthetic process. In collaboration with Dr. Rachele Isticato (Department of Biology, University of Naples Federico II) we decided to use the *B. subtilis rrnO* promoter, which is a strong promoter for the rRNA transcription (82). The *rrnO* promoter is cloned in the pGEM–T Easy vector between the *SphI* and *PstI* sites (Fig.9A). *rrnO* promoter was excised from this vector and subcloned into a destination vector named Pr19. This latter consists of a 2,382 bp region of the pUC 19 vector and a 1,400 bp region of the pJM03 vector, a pUC18 derivative containing a chloramphenicol resistance that can be expressed in *B. subtilis* (83).

The *tou* E103G/F176T gene cluster is cloned into the *SmaI* site in pGEM-3Z vector (Fig. 18B) (38).

The cloning strategy (Fig.18C), developed after careful restriction analysis of the genetic constructs involved, consisted initially in the following steps:

- 1a) the pGEM3Z/*tou* vector was digested with restriction endonucleases *XbaI/KpnI* to excise the complete *tou* E103G/F176T gene cluster (6,432 bp);
- 2a) the pGEM T-easy/*rrnO* vector (Fig. 18A) was digested with the enzymes *SphI/XbaI* to excise the *rrnO* promoter (600 bp);
- 3a) the integration vector Pr19 was digested with the enzymes *SphI/KpnI* (3,800 bp).

As underlined before, the aim was to excise the *tou* gene cluster and the *rrnO* promoter from their original vectors and to insert these fragments into plasmid Pr19 which was intended to be used for the integration of both promoter and the *tou* gene cluster in *B. subtilis* genome. To this purpose, 2µg of each purified plasmidic DNA were incubated at 37°C for 2h with 20 U of each enzyme in the presence of the appropriate buffer. The products of digestion were run on a 1% agarose gel, and the bands of interest were excised and purified as described in the Materials and Methods section.

Afterwards, a two-step, three fragments-ligation was performed as follows:

- 1b) the *tou* gene cluster digested with *XbaI/KpnI* (1a) and the *rrnO* promoter digested with *SphI/XbaI* (2a) were ligated;
- 2b) the product derived from reaction 1b) was ligated with Pr19 vector digested with the enzymes *SphI/KpnI* (3a).

Ligation 1b) was performed by mixing 30 ng of purified *rrnO* promoter and 400 ng of *tou* gene cluster. 10 µL of 2x “fast ligation buffer” (Promega) and 1 µL of 10 mM ATP

were added and the reaction mix was brought to a final volume of 17 μ L with ddH₂O. The sample was incubated at 42°C for 10 minutes, at RT for additional 10 minutes and then 1 μ L of T4-ligase (3U/ μ l) was added.

The reaction was incubated for 30 minutes at RT and then 2 μ L of purified Pr19 vector (60 ng) were added to the reaction mixture together with 1 μ L of T4-ligase (reaction 2b). Final volume of the ligation mix was of 20 μ L.

This reaction mixture was used to transform *E. coli* strain Top 10. Cells were plated on LB/amp agar plates and incubated at 37°C for 16 hours. 12 colonies were picked and analyzed for the presence of the recombinant plasmid Pr19 containing both the *tou* gene cluster and the *rrnO* promoter. The analysis was performed using a colony PCR procedure. Among the positive clones, two were selected. Their plasmids purified and used for a restriction analysis which confirmed the presence in the isolated recombinant Pr19 vectors of both the *tou* E103G/F176T gene cluster and the *rrnO* promoter. This plasmid will be indicated from now on as **NIC11**.

In order to verify the expression of the ToMO complex from plasmid NIC11, analytical expression experiments were performed and analyzed by SDS-PAGE.

To this purpose, *E. coli* JM109 cells were transformed with either plasmid NIC11 or pGEM3Z-E103G/F176T. As already mentioned above, promoter *rrnO* is constitutive, therefore no inducer was added for the expression of the recombinant protein. Instead, 0.2 mM Fe(NH₄)₂(SO₄)₂ was added to the growing culture when it reached an optical density of 0.7 OD₆₀₀, to supply an additional exogenous source of iron for the correct assembly of the iron-containing catalytic center of recombinant ToMO. We decided to analyze the recombinant expression of plasmid NIC11 1.5 and 3 hours after the addition of Fe(NH₄)₂(SO₄)₂. For the positive control, *i.e* plasmid pGEM3Z-E103G/F176T, it was instead necessary to add both 0.1 mM IPTG and 0.2 mM Fe(NH₄)₂(SO₄)₂ when the cell culture reached an optical density of 0.7 OD₆₀₀ to induce the heterologous expression of the ToMO system.

After induction, cells were collected by centrifugation, resulting pellets were suspended in 50 mM MOPS pH 7.0 and disrupted by sonication (3 min effective: 30 sec ON, 30 sec OFF). Cell suspensions were centrifuged at 12,000 rpm for 10 min at 4°C; 0.126 OD of each cell extract were analyzed by SDS-PAGE (Fig.19).

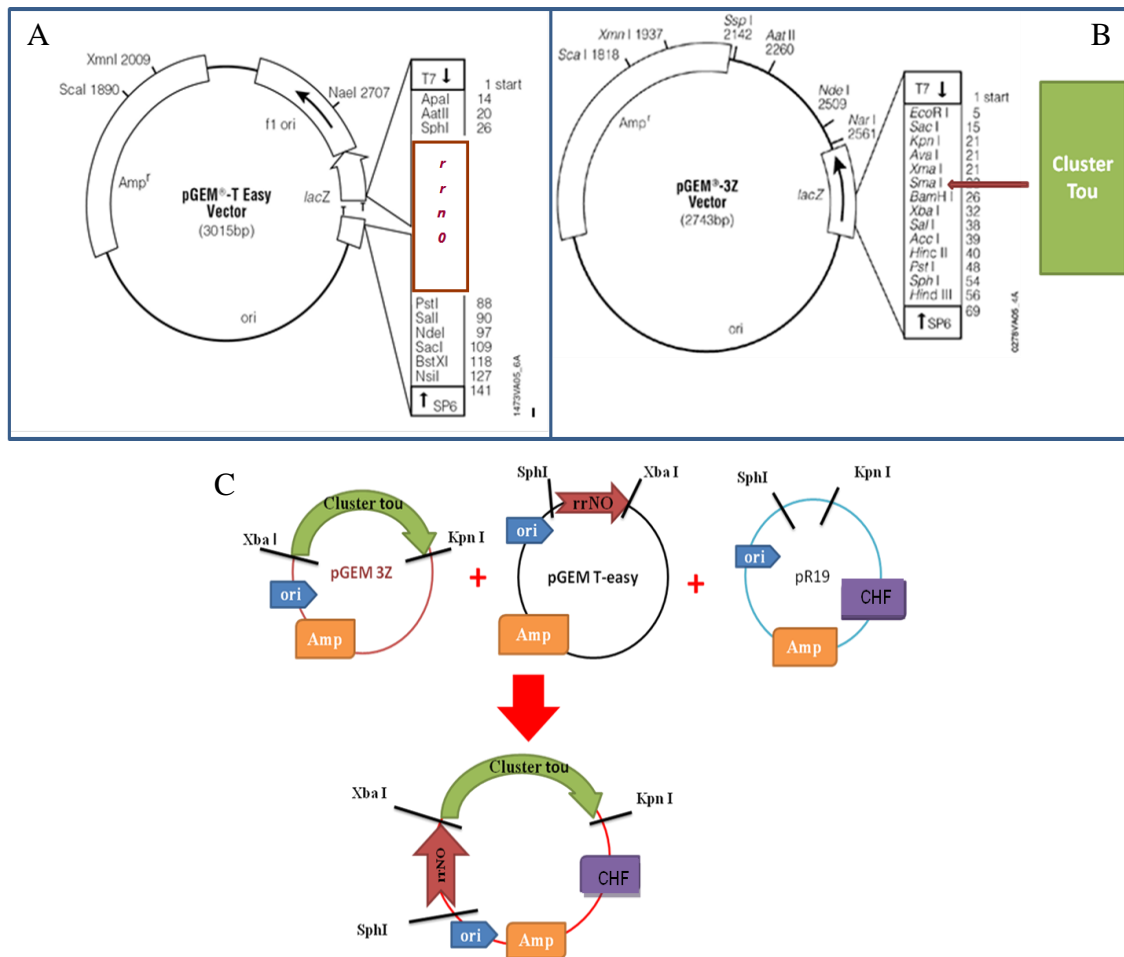


Figure 18: The *rrnO* promoter is cloned in the pGEM–T Easy vector (**A**). The *tou* E103G/F176T gene cluster is cloned into pGEM-3Z vector (**B**). The cloning strategy (**C**).

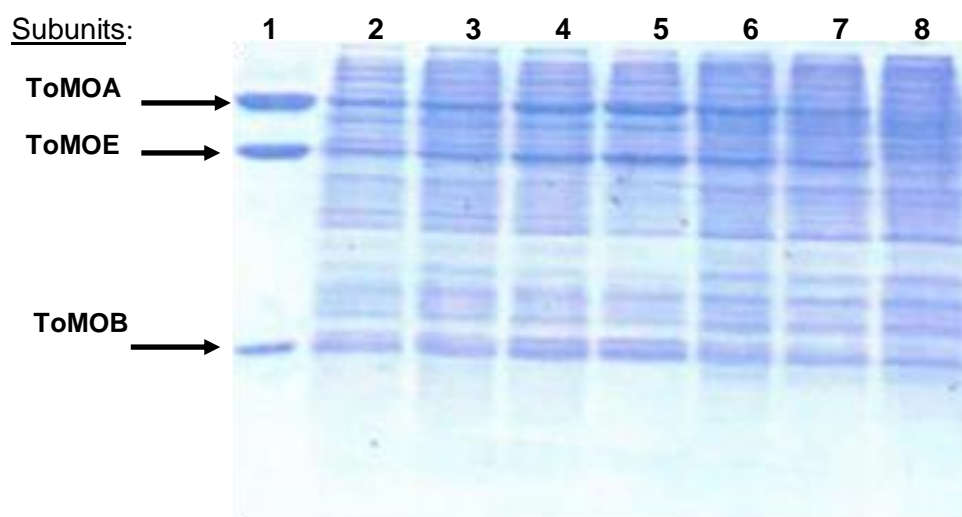


Figure 19: Lane 1: purified ToMO catalytic complex. Subunits **ToMOA** (57.6 kDa), **ToMOE** (38.2 kDa) and **ToMOB** (9.84 kDa) of the ToMO hydroxylase subcomplex ToMOH are indicated by the arrows.

Lane 2, 3 and 6: cell extracts of JM109 transformed with plasmid pGEM3Z-E103G/F176T after 45 minutes, 3h and O/N after the addition of $\text{Fe}(\text{NH}_4)_2(\text{SO}_4)_2$. Subunits **A**, **E** and **B** of the ToMO hydroxylase complex are evident.

Lane 4, 5 and 7 cell extracts of JM109 transformed with plasmid NIC11 after 45 minutes 3h and O/N after induction. Subunits **A**, **E** and **B** of the ToMO hydroxylase complex are more evident at 3h and O/N.

Lane 8: cell extracts of JM109 transformed with plasmid pGEM3Z after O/N induction. No bands relative to subunits A, E and B are evident.

As it is evident from the SDS-PAGE, the expression level of the ToMO complex in plasmid NIC11 is comparable to what obtained when using pGEM3Z-E103G/F176T. Moreover, *E.coli* cells expressing plasmid NIC11, both on solid and in liquid media, show the accumulation in the extracellular medium of a blue pigment, indigo, which is the result of the hydroxylation of cellular aromatic compounds by the active ToMO system.

Once verified that plasmid NIC11 actively expressed recombinant ToMO variant E103G/F176T in *E.coli*, the plasmid was used to transform *B. subtilis* as described in Material and Methods. Transformed cells of *B. subtilis* were plated on selective LB/agar plates containing chloramphenicol (5 µg/mL) and incubated at 37°C O/N. A few clones of transformed *B. subtilis* were separately inoculated in 4 mL of LB containing chloramphenicol (5 µg/mL), from now on indicated as LB/chf, and incubated O/N at 37°C. The cell pellet obtained from each clone was then subjected to genomic DNA extraction as described in Material and Methods.

To verify the integration of the *tou* gene cluster in the genome of *B. subtilis* different PCR reactions using not less than 1 µg of template genomic DNA were performed. Moreover, the oligonucleotides used, which amplify either a 1,000 or a 1,700 bp specific region of the *touA* gene, one of the six orfs of the *tou* gene cluster, were chosen for the high annealing temperature (60°C) that was intended to avoid non-specific amplifications.

The PCR program used was the following:

a) 2 min of initial denaturation at 94°C

b) 31 cycles of:

- 1 min of denaturation at 94°C;
- 1 min of annealing at 60°C;
- 1.5 min of synthesis at 72°C;

c) 10 min of synthesis at 72°C.

No amplification product was observed, thus indicating the absence of the integrated *tou* gene cluster in the genome of transformed *B. subtilis* clones.

The lack of integration of the *tou* gene cluster in *B. subtilis* genome was also confirmed by discontinuous coupled enzymatic assays performed on crude extracts of transformed cells of *B. subtilis*.

To this purpose, selected clones were separately inoculated in 12 mL of LB/chf and incubated O/N at 37°C. Cell cultures were then diluted to 0.1 OD₆₀₀ in 250 mL of LB/chf and grown under constant shaking at 37°C. 60 mL were withdrawn from each growing culture at 1.5h, 3h and 16h after the addition of 0.2 mM Fe(NH₄)₂(SO₄). Cell cultures were supplemented with iron at an optical density of 0.9 OD₆₀₀ (the promoter *rrnO* is constitutive, so no inducer was added for the expression of the recombinant protein). At the time intervals indicated above, cells were collected by centrifugation and the resulting pellets were suspended in 50 mM Tris HCl pH 7.5 at an optical density of 20 OD₆₀₀ and disrupted by sonication (10 min effective: 30 sec ON , 30 sec OFF).

Cell suspensions were centrifuged for 20 min at 4°C at 12,000 rpm and the supernatants filtered through a 0.45 µm filter. 500 µL of each sample were incubated for 30 minutes at RT in a final volume of 600 µL of 0.1 M Tris-HCL pH7.5 containing 1mM phenol and 500 µM NADH. It is important to underline that in the ToMO system the presence of the substrate phenol triggers the concomitant electron transfer chain that shuttles the electrons from NADH to the active site, in subunit ToMOA. When handling crude extracts most of the intracellular NADH might be oxidized, thus an

external addition of NADH is needed to support the enzymatic activity of the ToMO system.

Afterwards, 3U of catechol 2,3-dioxygenase (see Materials and Methods) were added in order to convert the catechol formed from the hydroxylation of phenol to 2-hydroxymuconic semialdehyde, a product whose formation can be monitored at 410 nm. Unfortunately, no product was observed even after longer times of incubation or increasing the concentration of the cell extract in the assay.

3.2.3 Cloning of *tou* gene cluster: the use of the non-integrative plasmid pHT01.

The destination vector pHT01 (Fig.20) was a kind gift of Dr. Isticato's research group. Vector pHT01 allows for high-level expression of recombinant proteins within the cytoplasm and is based on the strong σ A-dependent promoter preceding the *groE* operon of *B. subtilis* which has been converted into an efficiently controllable (IPTG-inducible) promoter by addition of the *lac* operator. Whereas the background level of expression in pHT01 is very low in the absence of inducer, a 1,300 fold increase in the level of recombinant expression was detected using the *bgaB* reporter gene (84). Our cloning strategy is summarized in Fig.21 and involved the following steps:

- A. The pHT01 vector was digested with restriction enzyme *KpnI*, followed by "fill-in" in order to eliminate this unique restriction site. The plasmid obtained was named pHT01/*KpnI*.
- B. The pGEM3Z plasmid was digested with restriction endonucleases *XbaI/AatII* to isolate a fragment that contained the unique restriction site *KpnI*.
- C. The fragment obtained at step 2) was cloned into plasmid pHT01/*KpnI* using restriction sites *XbaI/AatII*. The resulting plasmid was named PG5.
- D. The *tou* variant E103G/F176T was excised from its vector of origin *ptou* by digestion with enzymes *XbaI/KpnI* and cloned into plasmid PG5 using the same unique restriction sites.

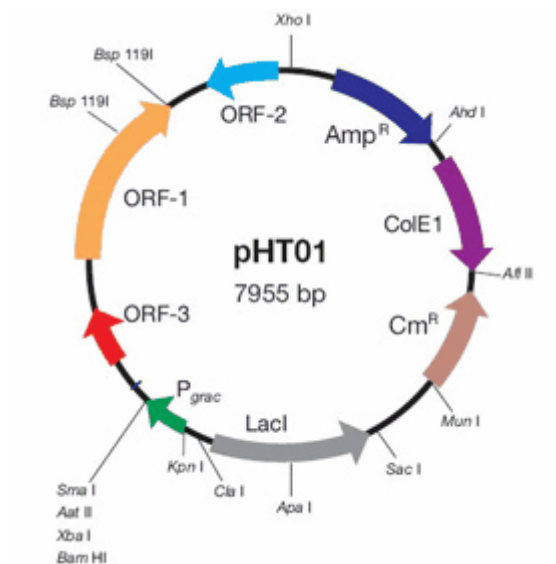


Figure 20: Map of the pHT01 plasmid.

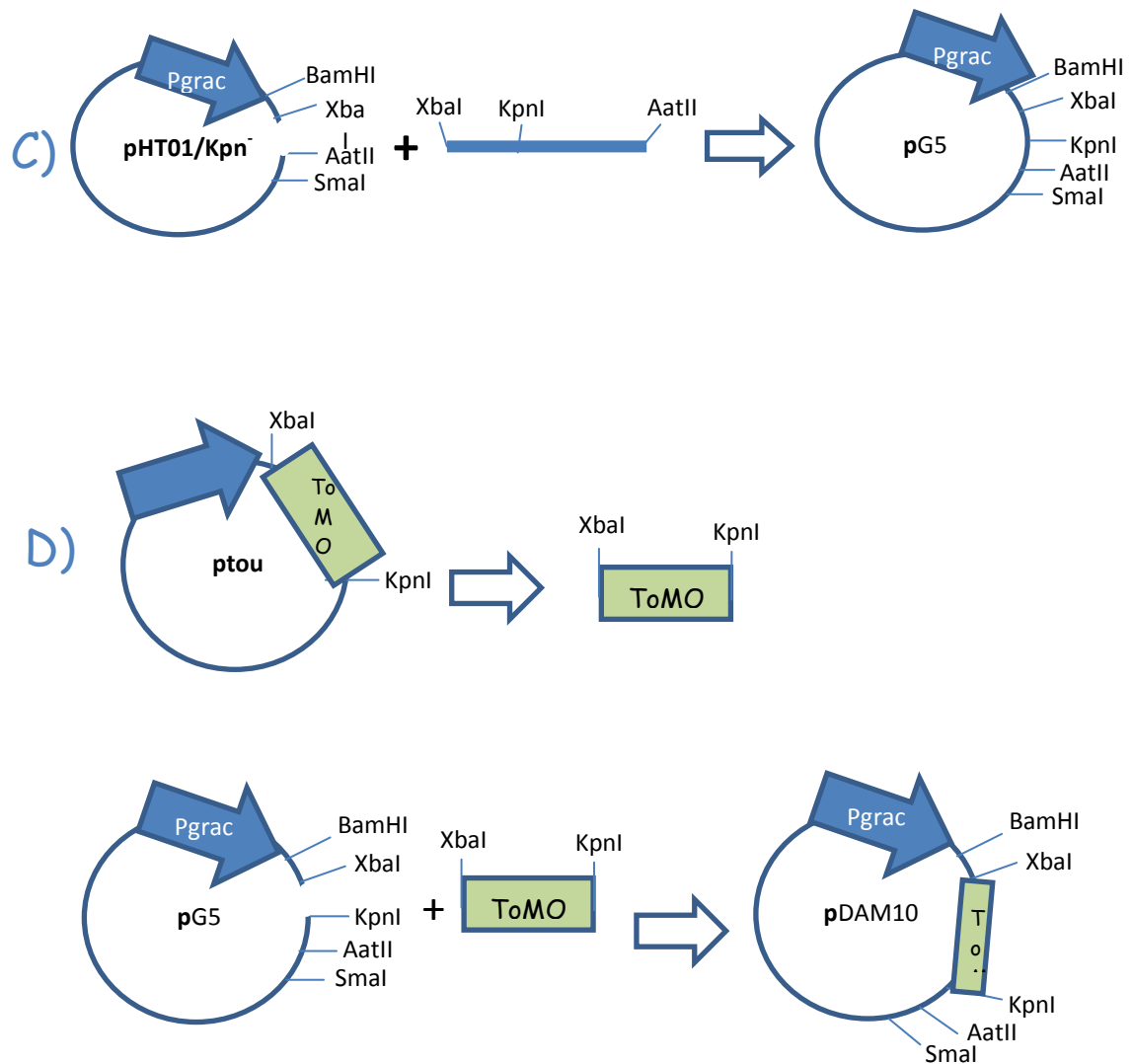


Figure 21: Schematic representation of steps C) and D) of the cloning strategy described in paragraph 2.3.

A. Digestion of plasmid pHT01 with the restriction enzyme *KpnI* and fill-in.

Approximately 3 μg of purified plasmid pHT01 were digested at 37° C for 4 h with 40 U of enzyme *KpnI* (NEB) according to the following scheme:

	Volume μL
Plasmid pHT01 (100 ng/ μL)	30
10X Buffer 1 NEB	4
BSA 100X	0.4
<i>KpnI</i> (10 U/ μL)	4
H ₂ O	1.6
Total Volume	40

The linearized vector was run on a 1% agarose gel, excised and purified as described in Materials and Methods. 2 μg of linearized plasmid were used for the fill-in procedure according to the following scheme.

	Volume μL
Linearized pHT01 (100 ng/ μL)	20
10X T4 DNA polymerase Buffer Promega	5
1.25 mM dNTP	8
T4 DNA polymerase Promega (10 U/ μL)	0.5
H ₂ O	16.5
Total Volume	50

The reaction was allowed to proceed for 5 min at 37°C.

The reaction catalyzed by T4 DNA polymerase was blocked by incubating the sample at 75° C for 10 min. The sample was purified and used in a ligation reaction according to the following scheme:

	Volume μL
Plasmid pHT01 linearized and fill-in (30 ng/ μL)	7
Buffer T4 DNA ligase 10X Promega	1
10 mM ATP	1
T4 DNA ligase Promega (3 U/ μL)	1
Total Volume	10

The reaction mixture was incubated at 14°C O/N.

The reaction mixture was used to transform *E. coli* strain Top 10. Cells were plated on LB/amp agar plates and incubated at 37°C for 16 hours. 6 clones were selected

from the transformation plates, their plasmids isolated and subjected to analytical digestion to verify the absence of the recognition site of the enzyme *KpnI* following the fill-in procedure. One of the positive clones, named pHT01/*KpnI*⁻, was selected and used in subsequent cloning procedures.

B. Extraction of a *XbaI/AatII* fragment, containing a unique *KpnI* restriction site, from pGEM3Z plasmid.

2.8 µg of plasmid pGEM3Z were digested with restriction enzymes *XbaI* and *AatII* to obtain a 515 bp fragment that contains a unique *KpnI* restriction site. The reaction scheme was as follows:

	Volume µL
Plasmid pGEM3Z (100 ng/µL)	28
10X Buffer 4 NEB	4
<i>XbaI</i> (20U/µL)	2
<i>AatII</i> (20U/µL)	2
10X BSA	4
Total Volume	40

The sample was loaded on 1% agarose preparative gel. The 515 bp fragment was excised from the gel and purified.

C. Insertion of the pGEM3Z-derived 515 bp fragment into pHT01/*KpnI*⁻

Approximately 3 µg of pHT01/*KpnI*⁻, prepared as described above (step A), were digested for 3 h at 37 ° C with restriction enzymes *XbaI* and *AatII* according to the following scheme:

	Volume µL
Plasmid pHT01/ <i>KpnI</i> ⁻ (100 ng/µL)	28
10X Buffer 4 NEB	4
<i>XbaI</i> (20U/µL)	2
<i>AatII</i> (20U/µL)	2
10X BSA	4
Total Volume	40

The sample was loaded on 1% agarose preparative gel. The linearized fragment (7,955 bp) was excised, purified and used in the ligation reaction summarized below. The ligation was incubated O/N at 4° C and the fragment:vector ratio used was of ca. 5:1.

	Volume μL
Plasmid pHT01/ <i>KpnI</i> ⁻ digested with <i>XbaI</i> / <i>AatII</i> (100 ng/ μL)	1
Frgment <i>XbaI</i> / <i>AatII</i> from pGEM3Z (10 ng/ μL)	3
10X Buffer T4 DNA ligase Promega	1
ATP 10 mM	1
T4 DNA ligase Promega (3 U/ μL)	1
H ₂ O	3
Total Volume	10

E. coli cells strain TOP10 were transformed with 1 and 9 μL of the ligation mix, plated on LB-agar/amp and incubated O/N at 37°C. 6 clones were selected, their plasmid isolated and analyzed by restriction analysis. Among the positive clones containing the *XbaI*/*AatII* fragment correctly inserted into plasmid pHT01/*KpnI*⁻, one was selected and indicated as PG5.

D. Cloning of *tou* gene cluster in plasmid PG5.

2 μg of pGEM3Z-E103G/F176T were digested with enzymes *XbaI* and *KpnI*, at 37°C for 3h to obtain a fragment containing the entire gene cluster encoding for the active ToMO complex.

	Volume μL
pGEM3Z-E103G/F176T (100 ng/ μL)	20
10X Buffer 2 NEB	4
<i>XbaI</i> (20U/ μL)	2
<i>KpnI</i> (10U/ μL)	2
10X BSA	4
H ₂ O	8
Volume Totale	40

The sample was loaded on a 1% agarose preparative gel and subjected to electrophoresis. The fragment (6,000 bp) was excised from the gel and purified. 2 μg of plasmid PG5 were digested at 37° C for 3 h with *XbaI* and *KpnI* according to the following scheme:

	Volume μL
Plasmid pG5 (100 ng/ μL)	20
10X Buffer 2 NEB	4
<i>Xba</i> I (20U/ μL)	2
<i>Kpn</i> I (10U/ μL)	2
10X BSA	4
H ₂ O	8
Total Volume	40

The sample was loaded on a 1% agarose preparative gel. The linearized vector (8,500 bp) was excised, purified and used in the ligation reaction. The ligation reaction was incubated O/N at 4° C and the fragment:vector ratio used was 2:1.

	Volume in μL
Plasmid pG5 digerito <i>Xba</i> I/ <i>Kpn</i> I (50 ng/ μL)	2
Fragment <i>Xba</i> I/ <i>Kpn</i> I contenente the gene cluster <i>tou</i> (25 ng/ μL)	5
10X Buffer T4 DNA ligasi Promega	1
ATP 10 mM	1
T4 DNA ligasi Promega (3 U/ μL)	1
Total Volume	10

E. coli cells strain TOP10 were transformed with 1 and 9 μL of the ligation mix, plated on LB-agar/amp and incubated O/N at 37°C. 6 clones were selected, their plasmid isolated and analyzed by PCR to identify clones bearing the *tou* mutated gene cluster correctly inserted in PG5 plasmid. This plasmid will be indicated from now on as **pDAM10**.

In order to verify the expression of the ToMO complex cloned in the new plasmid pDAM10, analytical expression experiments were performed and analyzed by SDS-PAGE. To this purpose, *E. coli* JM109 cells were transformed with either plasmid pDAM10, or PG5 or pGEM3Z-E103G/F176T. In all three cases, for the recombinant expression both 1 mM IPTG and 0.2 mM Fe(NH₄)₂(SO₄)₂ were added to the growing cultures when they reached an optical density of 0.7-0.8 OD₆₀₀. Induction time intervals analyzed were of 45 minutes, 3 hours and O/N.

Cell extracts were analyzed by SDS-PAGE (Fig. 22); the expression level of the ToMO complex cloned in plasmid pDAM10 was comparable to that obtained when using pGEM3Z-E103G/F176T vector. Moreover, continuous coupled enzymatic assays (see Materials and Methods) performed on whole recombinant JM109 cells expressing either one of the two different plasmids confirmed a comparable hydroxylating activity using phenol as substrate (data not shown).

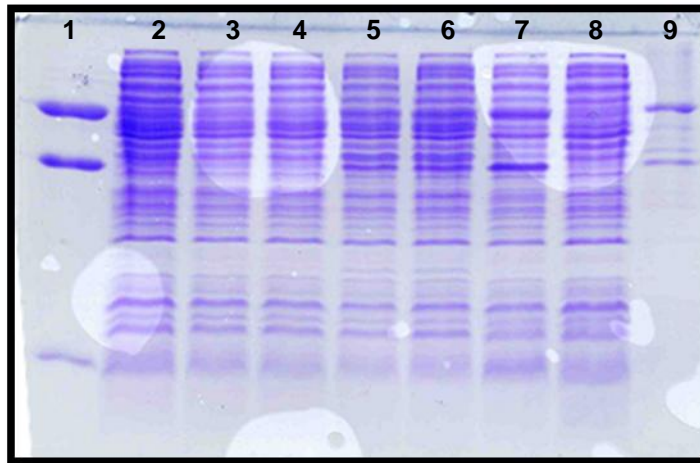


Figure 22: Lane 1 and 9: purified ToMO catalytic complex. Subunits **ToMOA** (57.6 kDa), **ToMOE** (38.2 kDa) and **ToMOB** (9.84 kDa) of the ToMO hydroxylase subcomplex are indicated with the arrows. Lane 2 and 8: cell extracts of JM109 transformed with plasmid pG5, Lane 3-7: cell extracts of JM109 transformed with plasmid pDAM10 after 45', 1,5 h and O/N after the addition of $\text{Fe}(\text{NH}_4)_2(\text{SO}_4)_2$ and IPTG. Subunits **A**, **E** and **B** of the ToMO hydroxylase complex are evident after O/N induction (lane 7).

Plasmid pDAM10 was then used to transform *B. subtilis*. Cells of *B. subtilis* were plated on selective LB/agar containing chloramphenicol (5 µg/ml) and incubated at 37°C for 14 h. To verify the presence of the plasmid in the chloramphenicol-resistant colonies of *B. subtilis* selected on the transformation plate, a PCR reaction was set-up in which total DNA obtained from the cell crude extract was used as template. Thus, selected colonies were picked from the LB agar plate, inoculated separately into 500 µL of LB/chf and incubated at 37°C up to saturation. Samples were centrifuged for 10 min at 4°C at 12,000 rpm. Pellets were resuspended in 50 µL of lysis buffer (1x *Taq* polymerase buffer, 3.25 mM MgCl₂, 2% Tween 20, 0.1 mg/mL Proteinase K). Cell suspensions were incubated at 60° C for 45 min and then at 90°C for 10 min. 0.5 µL of each cell lysate were used as the template for a PCR reaction performed in a final volume of 10 µL.

The PCR reaction mixture contained:

- 1x *Taq* polymerase buffer
- 3.25 mM MgCl₂
- 0.21 mM mix dNTP
- 1 µM Reverse Primer (touD down, specific for a region of the *tou* gene cluster)
- 1 µM Forward Primer (touF up, specific for a region of the *tou* gene cluster)
- 1 U *Taq* polymerase

The amplification conditions used were as follows:

- 1) 2 min at 94°C of initial denaturation
- 2) 30 cycles of:
 - 1 min at 94°C
 - 1 min at 46°C
 - 3 min at 72°C + 0.5 extension for each cycle
- 3) final synthesis step of 10 min at 72°C.

Among positive clones, two were selected, their plasmids purified and used for an additional restriction analysis (data not shown) which confirmed the presence of the pDAM10 plasmid in the isolated clone of *B. subtilis*.

After that, cell suspensions were diluted in 250 mL of LB/chf in the case of the recombinant clone or in 250 mL of LB without chloramphenicol for the *wt* microorganism.

In order to verify the effective expression in *B. subtilis* of the ToMO recombinant system encoded by plasmid pDAM10, a colony of the recombinant clone was inoculated in 12 mL of LB/chf and incubated O/N at 37°C. Afterwards, the saturated culture was diluted to 0.1 OD₆₀₀ in 250 mL (final volume) of LB/chf. The culture was supplemented with 1mM IPTG at an optical density of 0.7/0.8 OD₆₀₀. After 2h, 4h and 6h cells were collected by centrifugation and pellets were suspended in 0.1 M Tris HCl pH 7.5.

Both discontinuous assays on crude cell extracts (see paragraph 2.2) and continuous coupled assays were performed in the presence of purified catechol 2,3 dioxygenase and phenol as substrate, but no hydroxylating activity was observed (data not shown).

3.2.4 Total RNA purification and RT-PCR

The lack of hydroxylating activity in the recombinant clones of *B. subtilis* transformed with plasmid pDAM10 might be either due to a transcriptional or to a translational problem. In this latter case a different codon usage might have been responsible for the absence of the ToMO active complex in the cell extract of transformed *B. subtilis* cells.

Thus, we decided to verify the presence of the mRNA coding for the *tou* gene cluster by RT-PCR. To this purpose, cell pellets of 12 mL of O/N grown cultures of *B. subtilis*/pDAM10, *E. coli*/PG5 and *E. coli*/pGEM3Z-wt ToMO were collected.

Total RNA was extracted with the TRI-Reagent kit (Sigma) and RT-PCR reactions were performed using the "Access RT-PCR System" kit (Promega) as described in Material and Methods section 2.15.

Specific primers amplifying a 700 bp region in the *touA orf* were selected. As shown in Fig. 23, RT-PCR experiments yielded fragments of the expected length only when RNA was extracted from *E. coli*/pGEM3Z-wt ToMO. No amplification was detected in the case of *B. subtilis* transformed with PG5. Little amplification was observed in the case of *B. subtilis* transformed with pDAM10. However a band of the same intensity and apparent length was observed in the control reaction performed in the absence of reverse transcriptase. This indicates the residual presence in the sample of plasmidic DNA despite the DNaseI treatment that had been performed on all samples analyzed in this experiment (Materials and Methods).

In conclusion, this experiment would indicate that the ToMO system was not expressed in our transformed *B. subtilis* clones due to a transcriptional problem.

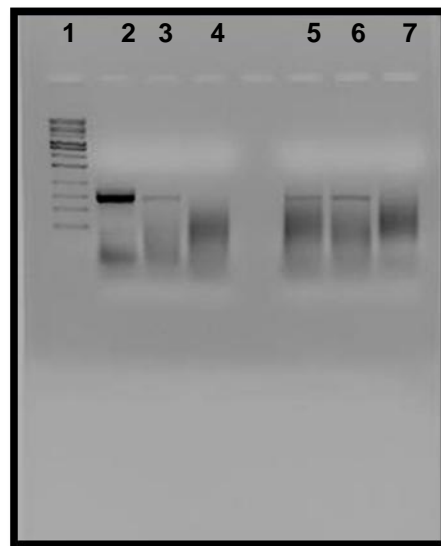


Figure 23: Analysis on 1% agarose gel of the RT-PCR amplification products obtained using oligonucleotides specific for a 700 bp region of the *touA* *orf*. **Lane 1:** 2-log ladder (New England Biolabs). **Lane 2:** amplification products obtained using as template total RNA extracted from *E.coli* transformed with pGEM3Z/wtToMO. **Lane 3:** amplification products obtained using as template total RNA extracted from *B. subtilis* transformed with pDAM10. **Lane 4:** amplification products obtained using as template total RNA extracted from *E.coli* transformed with plasmid PG5. **Lane 5, 6 and 7** are negative controls, namely RT-PCR reactions carried out in the absence of reverse transcriptase.

3.3.1. 3,6 diketocamphane 1,6-monooxygenase, a type II Baeyer-Villiger Monooxygenases from *Pseudomonas putida* NCIMB 10007.

BVMOs can be classified into two distinct groups (85). Type I BVMOs contain flavin adenine dinucleotide (FAD) as the co-factor and use NADPH as the source of electrons (86). These enzymes contain two Rossmann sequence motifs, GxGxxG, suggesting that they bind the two cofactors (FAD and NADPH) using separate dinucleotide binding domains. Type II BVMOs use FMN as flavin cofactor and NADH as electron donor and are composed of two different subunits that occur in a quaternary structure of the type $\alpha_2\beta$ (86,87).

Since their discovery, much research has been performed to explore the biocatalytic properties of BVMOs, either using whole-cells or isolated enzymes. However, whereas most of the enzymes characterized so far refer to type I BVMOs (88), only a few examples for FMN/NADH-containing type II BVMOs have been investigated. A reason might be the challenging overexpression of these enzymes in a heterologous host since, in contrast to type I BVMOs, the oxygenating and dehydrogenase subunits are distinct proteins. Type II BVMOs are of special interest for industrial applications because -among others- of the lower costs of NADH compared to NADPH, but hold more challenges regarding the structural feature because the oxygenase and FMN reductase subunits are distinct polypeptide chains forming only a loose complex.

Pseudomonas putida NCIMB 10007 is able to grow on camphor as unique carbon and energy source. Camphor exists in two enantiomeric forms; the (+)- isomer occurs primarily in the wood of *Cinnanocum camphora* and, although the (-)-isomer is less widely distributed, it occurs in a number of plant essential oils. Three different Baeyer-Villiger monooxygenases (BVMOs) were reported to be involved in the camphor metabolism of *Pseudomonas putida* NCIMB 10007. After initial hydroxylation of (+)-camphor by a P450 monooxygenase and oxidation by a dehydrogenase, the resulting 2,5-diketocamphane is degraded by 2,5-diketocamphane monooxygenase (2,5-DKCMO). The corresponding enzyme for the decomposition of the (-)-isomer, namely 3,6-diketocamphane 1,6-monooxygenase (3,6-DKCMO), was first reported in 1965 (Conrad et al. 1965) (Fig. 24).

The aim of this part of my PhD project, carried out in the laboratory of Prof. Littlechild at the University of Exeter, was to *i*) optimize the heterologous expression and the purification of 3,6 DKCMO in *E.coli*, and crystallize the protein, *ii*) clone and express the flavin reductase component of 3,6 DKCMO, and *iii*) co-crystallize the oxygenase and the reductase components of the 3,6 DKCMO.

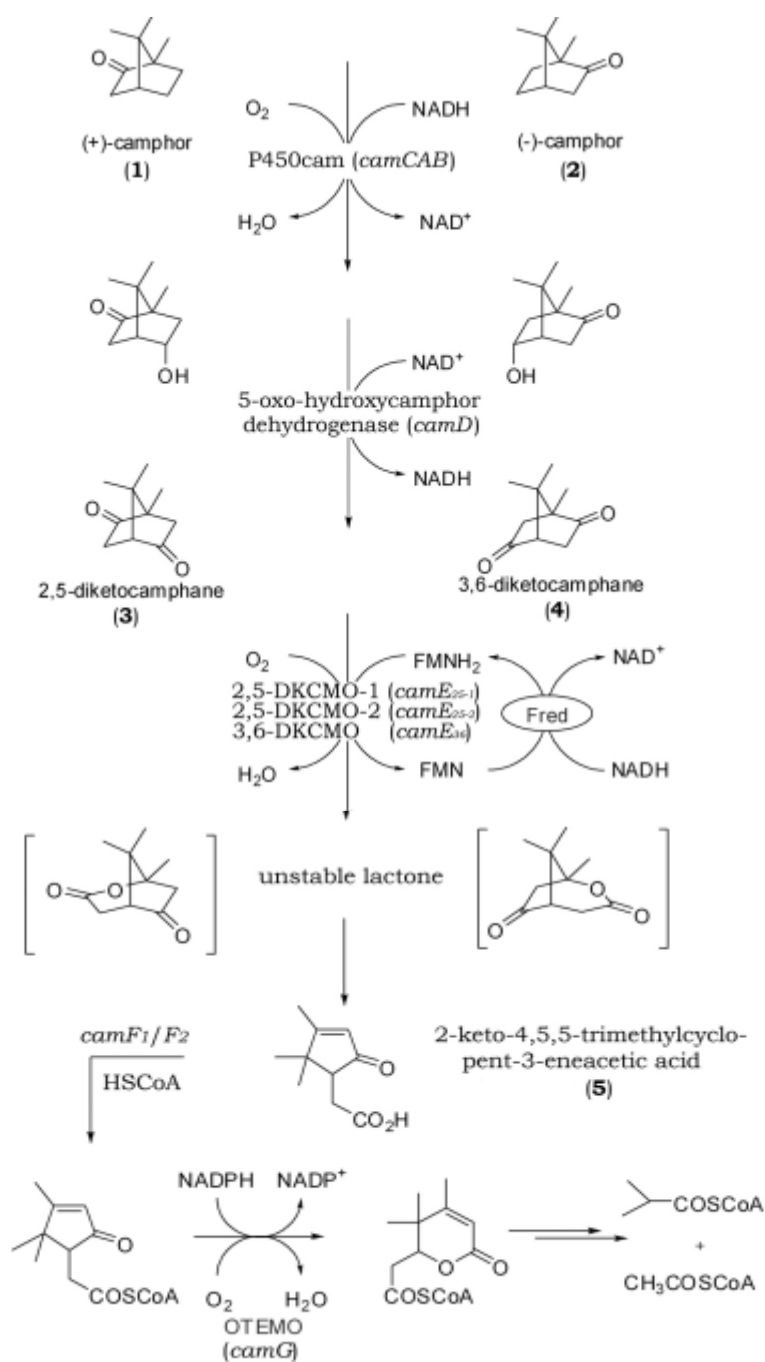


Figure 24: Degradation of (+)- and (-)- camphor isomers by *Pseudomonas putida* NCIMB 10007. “Fred” is the acronym for the flavin reductase.

3.3.2. Expression and purification of 3,6-diketocamphane 1,6 monooxygenase (3,6 DKCMO).

Transformation of *E. coli* strain BL21(DE3) with pET-28_3,6-DKCMO, a plasmid bearing the gene encoding for the oxygenase component of 3,6-DKCMO and a N-terminal His-tag, was carried out as described in the Material and Methods section. The construction of this plasmid has been reported elsewhere (89).

For soluble expression of recombinant 3,6-DKCMO, co-expression of chaperones GroES and GroEL was necessary (89). To this purpose, BL21(DE3) cells were co-transformed with both the pET-28_3,6-DKCMO plasmid and Pgro7(TaKara Chaperone Plasmid Set), an arabinose-inducible plasmid designed to express groES and groEL proteins that function together as a "chaperone team" to enable optimal protein expression and folding in heterologous hosts.

An O/N preinoculum of fresh transformed BL21(DE3) cells was grown at 37°C, under constant shaking, in 5 mL of sterile TB containing kanamycin (50 µg/mL, for the selection of pET-28_3,6-DKCMO) and chloramphenicol (50 µg/mL, for the selection of Pgro7). From now on the presence of both antibiotics in the growth medium at these concentrations will be referred to as "kan/chf". After 14 hours, the saturated preinoculum was diluted in 250 mL of fresh sterile TB (kan/chf) in a 1L-Erlenmeyer flask and was allowed to grow under constant shaking at 37°C up to 0.6 OD₆₀₀. Afterwards, 10 mL of this cell culture were diluted 100 fold in 1L of fresh sterile TB (kan/chf) in a 2L-Erlenmeyer flask and allowed to grow at 37°C at 200 rpm.

Expression of the recombinant GroES-GroEL system was induced by adding to the growing culture 2 mg/mL of l-arabinose at an optical density of 0.5 OD₆₀₀. After 30 minutes the recombinant expression of 3,6-DKCMO was induced by adding IPTG to a final concentration of 0.1 mM. To improve protein solubility, the growth temperature was shifted from 37°C to 20°C. The induced cell culture was allowed to grow under these conditions for 16 hours.

Cells were harvested by centrifugation and resuspended in a buffer containing 20 mM K₂HPO₄, 0.1 mM EDTA, 6 mM β-mercaptoethanol, 0.01 mM PMSF, at pH 7.5. Cell disruption was performed by a single passage through a French press.

After centrifugation of the cell suspension for 45 min at 10,000×g, the soluble fraction was purified by affinity chromatography via the N-terminal His-tag on an automated Äkta purifier system. To this purpose, 1 mL of HisTrap FF resin with bound Ni²⁺ was equilibrated with buffer A (100 mM K₂HPO₄, 300 mM NaCl, pH 7.5) supplemented with 30 mM imidazole. After loading, the column was washed with three volumes of buffer A (100 mM, 300 mM NaCl, pH 7.5) supplemented with 30 mM imidazole followed by two volumes of buffer A supplemented with 60 mM imidazole to remove unspecific bound proteins. Elution was performed by adding three volumes of buffer A supplemented with 1 M imidazole. Protein fractions were analyzed via online absorption measurement at λ=280 nm; aliquots of peak fractions were loaded on a SDS-PAGE (Fig.25-A). SDS-PAGE analysis confirmed the presence of a major band at approximately 40 kDa, which corresponds to the theoretical estimated molecular weight of 44.5 kDa of the His-tagged protein. 3,6-DKCMO-containing fractions were yellowish, and their UV-vis spectrum suggested the presence of a bound FMN cofactor (data not shown).

Most relevant fractions were pooled and, in order to remove imidazole from the sample, were loaded into a 60 mL size exclusion desalting column (Sephadex G25 matrix), equilibrated with 50 mM Tris-HCl pH 7.5/100 mM NaCl. Protein fractions were again analyzed via online absorption measurement at 280 nm, loaded on a SDS-PAGE (Fig.25-B) and pooled. SDS-PAGE analysis showed that the purity of the

protein sample obtained was suitable for crystallization experiments. In this case, however, 3,6-DKCMO-containing fractions were colorless, which confirmed previous studies in which FMN was reported not to be covalently bound to the enzyme and easily lost during purification procedures.

Determination of protein concentration of all samples described so far (cell extract, purified sample, desalted sample) was carried out with the BCA kit and a standard curve of BSA in the same buffer in a range of 2–0.005 mg/ml was used. Samples were measured in triplicates in three different dilutions.

The purified protein sample was then concentrated using Vivaspin Centrifugal concentrator tubes to obtain a final concentration of 10 mg/ml for crystallization studies.

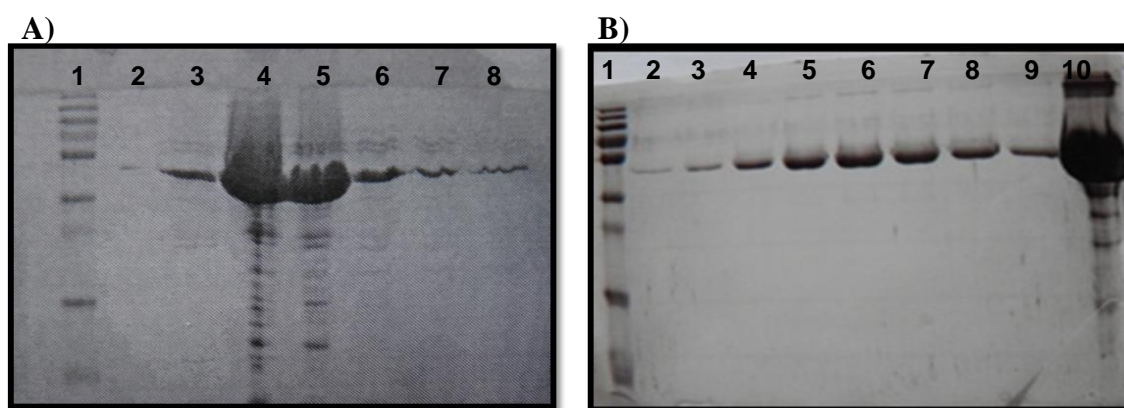


Figure 25:

A) lane 1: Pageruler prestained molecular weight standard 10-170 kDa (Pierce);
lanes 2-8: aliquots of peak fractions eluting from the affinity chromatography.

B) lane 1: Pageruler prestained molecular weight standard 10-170 kDa (Pierce);
lanes 2-9: aliquots of peak fractions eluting from the Sephadex G25;
lane 10: Molecular weight standard (40 kDa).

3.3.3 Crystallization of 3,6-diketocamphane 1,6 monooxygenase (3,6 DKCMO).

The main aim of any enzyme study is the resolution of the protein structure. Structural information helps understanding the conformational and functional details of the biocatalytic mechanism. Successful purification and crystallization of protein is essential to extract appropriate X-ray diffraction data which can lead to resolution of the protein structure.

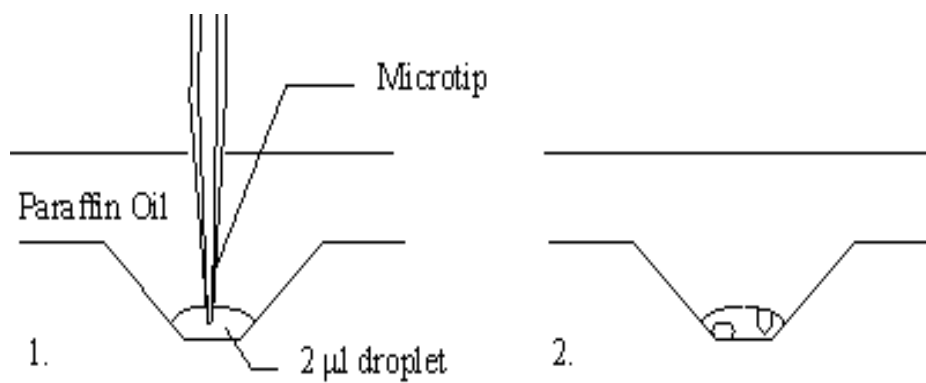
Crystallization studies were carried out with purified 3,6-DKCMO prepared as described in paragraph 3.2. A protein concentration in the range 7-10 mg/mL was used in all experiments of crystallization. The protein solution used for crystallization contained also 5 mM FMN, 0.2 mM NADH, 0.2 μ M (-)- Camphor, which are, respectively, the cofactors and the substrate used by 3,6-DKCMO. This addition was performed to try to obtain crystals of 3,6-DKCMO with these molecules bound, which might give more details on the catalytic mechanism of this enzyme. Samples were always incubated 3h at RT before starting the crystallization experiments. Crystal screenings were set up in micro-batch trials in JCSG-plusTM HT-96 wells plate using Oryx 6 robot (Douglas Instruments, Fig.26-A). JCSG-plus HT-96 is a 96 reagent deep-well block, optimized sparse-matrix screen of classic and modern conditions, devised at the Joint Centre for Structural Genomics and developed further by Newman and Perrakis at the Netherlands Cancer Institute. The robot was set up to dispense 1:1 mixture of Protein:Screen condition in each well (Fig.26-B). The volume of the dispensed droplet was 1 μ L. The resultant plates were covered with Al's oil (a 50:50 mixture of silicon oil:paraffin oil) and stored at 20°C. Appearance and growth of crystals was monitored over every three days.

The best crystals were obtained in the presence of PEG as precipitant and were distinctly needle-like or fibrous in shape. The largest and the best-looking crystals were thin-rod needles (Fig. 27).

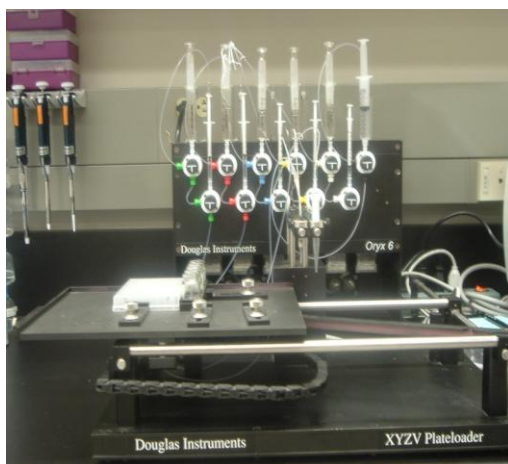
A selection of 3,6-DKCMO crystals were flash-frozen. The crystals were frozen in a vial immersed in liquid nitrogen until they were analyzed at the Diamond Light Source UK national synchrotron. Prior to freezing, a cryoprotectant (PEG 400 or 30% glycerol) was added to the crystal. The cryoprotectant solution consisted, in addition to the cryoprotectant itself, in an adjusted mixture of the original crystallization reagents with an additional precipitant when required. A total of 30 crystals were frozen.

These crystals diffracted to beyond 2 Å resolution, allowing a complete data set to be collected to 2.5 Å resolution at 100 K. The space group was identified as $P2_12_12_1$, with unit-cell dimensions $a = 54.6$, $b = 93.2$ and $c = 154.1$ Å.

The crystals of 3,6-DKCMO obtained under the conditions reported above diffracted but FMN was mainly found in solution in the droplet. Moreover the crystal diffraction pattern clearly showed that residual FMN present in the crystal was external to the protein structure (data not shown). As a consequence, the crystallization experiment was repeated by increasing the concentration of FMN up to 20 mM and in the presence of all other components (substrate and NADH), whose concentration was kept identical compared to the previous experiment. Also in this case it was not possible to recover any FMN correctly inserted in the binding site.



A



B

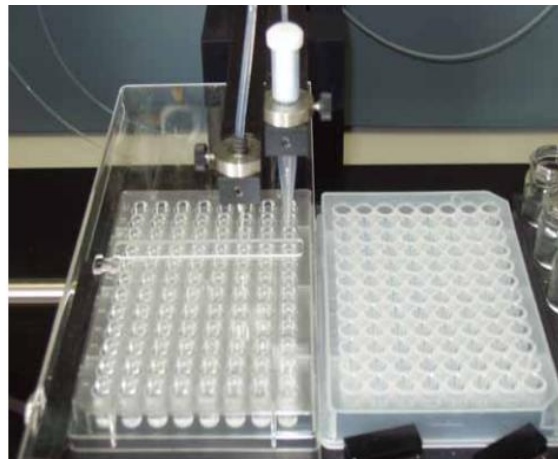


Figure 26:

A) An image of Oryx 6 robot (Douglas Instruments);

B) A close-up of the robotic arm of the Oryx 6 robot (Douglas Instruments).

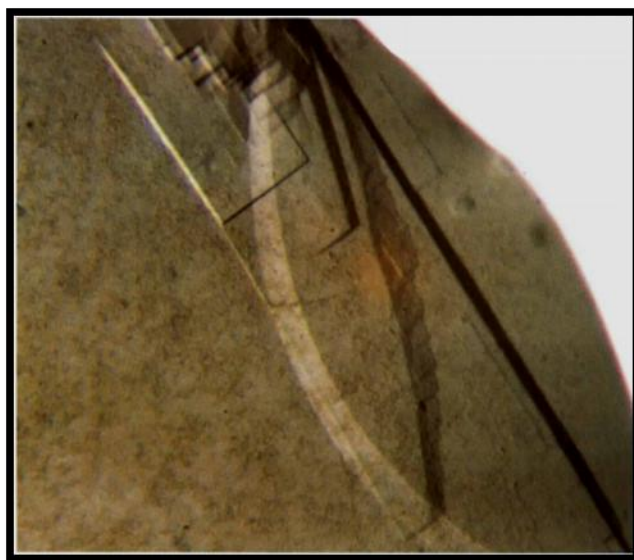


Figure 27: Crystals of the oxygenase component of 3,6-diketocamphane monooxygenase.

Data are currently under investigation. However, the lack of FMN in the crystal structure of 3,6-DKCMO undoubtedly limits the detailed understanding of the catalytic mechanism and needs further investigation.

However, it could be hypothesized that the His-tag could interfere with crystal growth and X-ray diffraction studies. Therefore, with the aim of improving the incorporation of FMN inside the 3,6-DKCMO, to improve the quality of crystals and obtain better structure refinement, the His-tag could be cleaved off before undertaking crystallisation work, or the protein could be purified using a different purification methodology using a non-His tagged protein.

3.3.4 ThermoFluor Assay on 3,6-DKCMO.

ThermoFluor assay is a miniaturized high-throughput protein stability assay that can be used to analyze the relationship between protein thermal stability and ligand binding. Binding ligands generally increase protein thermal stability by an amount that is proportional to the concentration and affinity of the ligand. Binding constants (K_b) are measured by examining the systematic effect of ligand concentration on protein stability. The effects of ligand binding depend on the thermodynamics of protein stability and in particular on the unfolding enthalpy. It is important to underline that an extension of current theoretical treatments has been recently developed for tight binding inhibitors, where ligand effect on T_m can also reveal binding stoichiometry. In the typical experimental set-up, a fluorescent dye such as SYPRO orange is used. This latter is a solvatochromic dye used as an indicator of protein unfolding that has a low-fluorescence quantum yield in water. Partitioning of the dye into melted protein results in a significant increase in fluorescence (Fig.28)

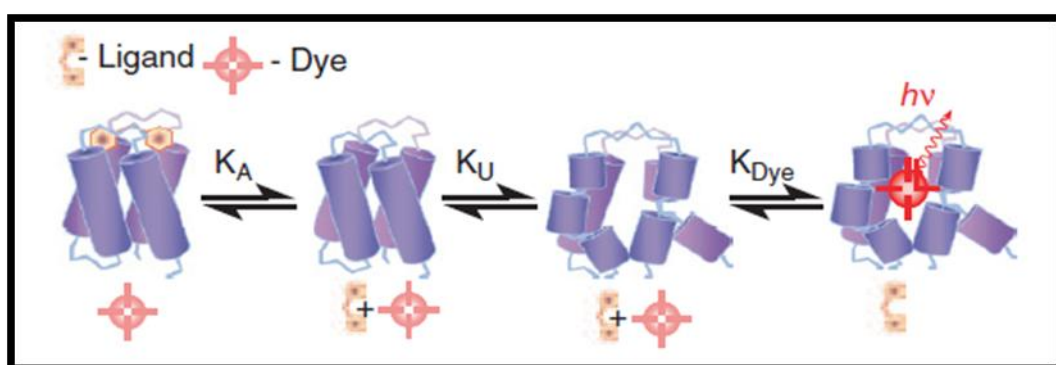


Figure 28: Schematic representation of the ThermoFluor binding assay.

The samples used for the ThermoFluor binding assay contained, in a final volume of (Fig. 28):

- 7 mg of 3,6 DKCMO (blue trace);
- 30 mM FMN (red trace);
- 7 mg of 3,6 DKCMO, 20 mM FMN, 0.2 mM NADH, 0.2 μ M (-)- camphor (yellow trace);
- 7 mg of 3,6 DKCMO, 30 mM FMN, 0.2 mM NADH, 0.2 μ M (-)- camphor (green trace).

Preliminary results showed that an increase of T_m was obtained in the samples containing the cofactors and the substrate (trace yellow and green). Moreover, this temperature shift (ΔT_m) was proportional to the FMN concentration in the sample.

Data are still under investigation, and further experiments are needed in order to investigate the possible role of NADH and camphor on the ΔT_m .

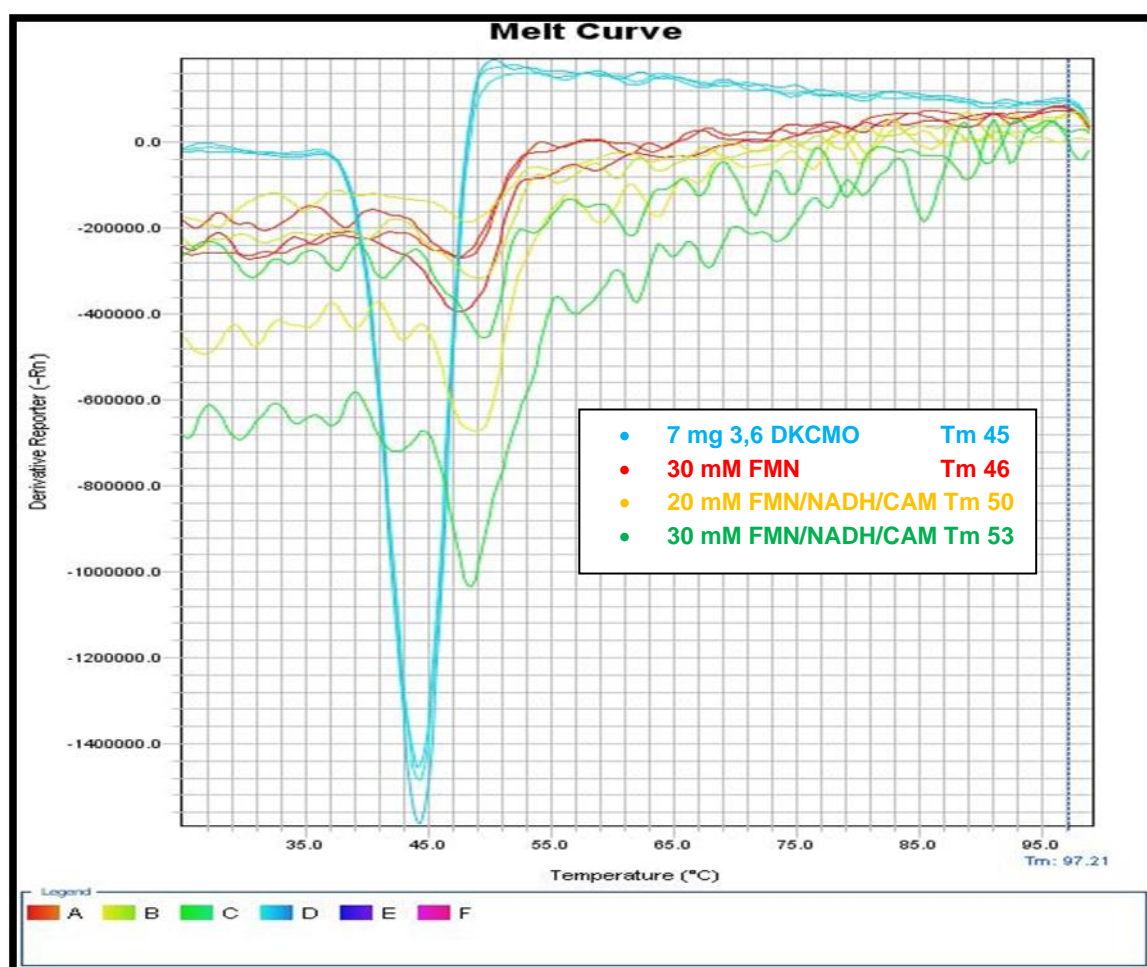


Figure 28: ThermoFluor binding assay.

3.3.5 Cloning, expression and purification of the flavin reductase component of 3,6-DKCMO.

As already underlined in paragraph 3.1, 3,6-DKCMO consists of a homodimeric FMN-containing oxygenase and a second component that has been referred to as a NADH dehydrogenase or NADH oxidase. This latter has not been expressed as a recombinant protein and characterized yet, thus leading to a fundamental lack of information on the catalytic relationship between the oxygenase and the reductase components present in the $\alpha_2\beta$ quaternary complex of 3,6-DKCMO.

Amplification of the Flavin Reductase encoding gene (from now on referred to as FRED, Fig. 29) was performed by using the CAM-plasmid as template (88).

Flavin reductase (CAM PLASMID) Pseudomonas putida

```
ATGACTAAAGTCGCCGCAGAGATAGTACGAAGCGCTATCGACCCACAATGGTTCAGAGCTGTTCTGGGTC
AGTATCCCACTGGCGTATGCGCCGTTACCGCGATGGATCCGGACGGCAAGATGTCGGGTATGGCGGTAGG
TTCTTTCACCTCGGTTTCGCTGAATCCGCCGTTGGTGGCCTTTCTGCCGGATCGCAGCTCAACGAGTTGG
CCGAAAATCGAGCGCGCCGGCAAGTTCTGCGTCAACGTGTTGAGTGATCAGCAACTGGGAGTTTGTAAAGC
GTTTTGCCTCCAAGGACGAAGACAAGTTTTCCGGGCTGGTATATCGCCTCTCCGACAACGGTTCACCGAT
CATCGAGGGCGTCGTAGCCTGGATCGATTGTGACCTGCATTGCGTTTCAGGAGGCGGGGGATCACTATATC
GTCATTGGCTCTGTACGTGAATTGCAGGTCGAGTCCGAGGATTCCGCACTGCTTTTCTATCGGGGTGGTT
ATGGTGGCTTTGCCGCTATCTGA
```

Figure 29: Flavin Reductase sequence

After initial denaturation for 30's at 98 °C, the primers annealing was performed for 30 s at 60 °C; the elongation step was performed at 72 °C for 1 min. This sequence was repeated for 34 cycles. The final elongation step was allowed to proceed for 10 min at 72 °C.

The degenerate primers used for amplification were designed to insert restriction sites for *EcoRI* at the N-terminus and *NotI* at the C-terminus (*EcoRI*_G1_fw: 5'-GAATTCATGACTAAAGTCGCCGCAGA-3'; *NotI*_G2_rv: 5'-GCGGCCGCTCAGATAGCGGCAAAGCC-3').

The resulting amplified 550 bp fragment was directly ligated into plasmid pJET1.2/blunt. This latter is a linearized cloning vector, which accepts inserts from 6 bp to 10 kb. The 5'-ends of the vector cloning site contain phosphoryl groups, therefore, phosphorylation of the PCR primers was not required. Recircularized pJET1.2/blunt vector expresses a lethal restriction enzyme after transformation and is not propagated. As a result, only recombinant clones containing the insert appear on culture plates.

The ligation reaction was performed by using a fragment:vector molar ratio of 3:1 and was incubated at room temperature for 5 min. The ligation mixture was used to transform competent cells of *E. coli* strain BL21(DE3). Cells were then plated on LB/amp agar plates and incubated at 37°C for 16 hours.

11 colonies were picked and analyzed for the presence of the recombinant plasmid pJET 1.2/blunt containing the FRED gene. The presence of the gene correctly cloned in this vector was verified by restriction analysis with *NotI* and *EcoRI* endonucleases. The FRED gene was excised from pJET1.2/blunt vector by digesting with *NotI* and *EcoRI* endonucleases and ligated into vector pET-28b digested with the same enzymes. Ligation was performed under the same conditions described above.

This reaction mixture was used to transform *E. coli* strain BL21(DE3). Cells were plated on LB/amp agar plates and incubated at 37°C for 16 hours. 3 colonies were picked, their plasmids purified and used for a restriction analysis which confirmed the presence in the isolated clones of the recombinant pET-28b vector with the FRED gene correctly inserted. The resulting plasmid was called pET-28_FRED.

For the recombinant expression of the protein encoded by the FRED gene, a O/N preinoculum of transformed BL21(DE3) cells was grown at 37°C, under constant shaking, in 5 mL of sterile TB containing kanamycin (50 µg/mL). After 14 hours, the saturated preinoculum was diluted in 250 mL of fresh sterile TB (kan) in a 1L-Erlenmeyer flask and was allowed to grow under constant shaking at 37°C up to 0.6 OD₆₀₀. Afterwards, 10 mL of this cell culture were diluted 100 fold in 1L of fresh sterile TB (kan) in a 2L-Erlenmeyer flask and allowed to grow at 37°C at 200 rpm.

At an optical density of 0.7/0.8 OD₆₀₀ recombinant expression of FRED was induced by adding IPTG to a final concentration of 0.1 mM. To improve protein solubility, the growth temperature was shifted from 37°C to 20°C. The induced cell culture was allowed to grow under these conditions for additional 16 hours.

Cells were harvested by centrifugation and resuspended in a buffer containing 20 mM K₂HPO₄, 0.1 mM EDTA, 6 mM β-mercaptoethanol, 0.01 mM PMSF, at pH 7.5. Cell disruption was performed by a single passage through a French press.

After centrifugation of the cell suspension for 45 min at 10,000×g, the soluble fraction was purified by affinity chromatography via N-terminal His-tag on an automated Äkta purifier system. The optimized experimental conditions found for the elution of the protein are the same as those reported in paragraph 3.2 for the oxygenase component of 3,6-DKCMO.

Protein fractions were analyzed via online absorption measurement at λ=280 nm; aliquots of peak fractions were loaded on a SDS-PAGE (Fig.30).

As it is evident from the SDS-PAGE analysis a protein band with an apparent molecular weight of 18 kDa is present in the peak fractions. However, the protein was heavily contaminated with other proteins. Therefore the affinity chromatography was repeated by using an imidazole gradient consisting of the following steps: 5%; 10%; 15%; 20%; 30% and 50% imidazole. The protein eluted at a concentration of imidazole in the range 10%-15% and the SDS-PAGE analysis showed a sample whose purity was undoubtedly higher than the previous attempt.

Most relevant fractions were pooled and, in order to remove imidazole from the sample, were loaded onto a 60 mL size exclusion desalting column (Sephadex G25 matrix), which was equilibrated with 50 mM Tris-HCl pH 7.5/100 mM NaCl. Protein fractions were again analyzed via online absorption measurement at 280 nm, loaded on a SDS-PAGE and pooled. SDS-PAGE analysis showed that the purity of the protein sample obtained is very high and suitable for crystallization experiments and activity assays (data not shown).

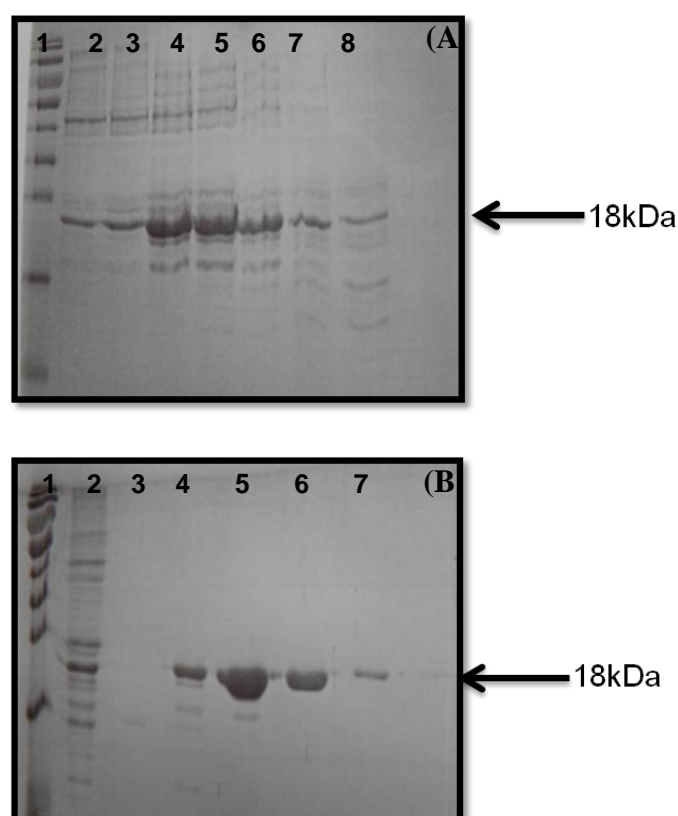


Figure 30:

A) lane 1: Pageruler prestained molecular weight standard 10-170 kDa (Pierce); **lanes 2-7:** aliquots of peak fractions eluting from the affinity chromatography.

B) lane 1: Pageruler prestained molecular weight standard 10-170 kDa (Pierce); **lanes 2-7:** aliquots of peak fractions eluting from affinity chromatography with a concentration of imidazole in the range 10%-15%.

In conclusion, the expression and purification of recombinant FRED have been optimized and the availability of the purified protein will allow to carry out in the near future activity studies with the two protein both individually (3,6 DKMCO and FRED) and as a complex. Moreover, co-crystallization attempts will be performed to gain further insight into their conformational dynamics and their ability to distinguish enantiomerically specific camphor molecules. With a detailed account of the structure, substrate specificity and mechanism, the purified enzymes can be modulated to aid large scale production of useful drug intermediates.

Conclusions

In this PhD thesis the use of oxygenase activities for the biosynthesis of novel aromatic antioxidants has been investigated, in the more general framework of the “oxyfunctionalization” of aromatic compounds and its effective use for industrial processes. Main aims were *i)* to validate the use of the ToMO system for the production of novel antioxidants starting from non-natural substrates; *ii)* to verify the possibility of expressing recombinant ToMO in a GRAS microorganism such as *B. subtilis*; *iii)* to express and purify the oxygenase and the flavin reductase components of the 3,6 diketocamphane 1,6 monooxygenase (3,6 DKCMO) from *Pseudomonas putida* NCIMB 10007.

During this PhD project six novel hydroxylated compounds were obtained through the bioconversion of non-natural substrates using the ToMO multicomponent monooxygenase from *P. sp.* OX1, thus confirming the versatility of this enzyme in catalyzing hydroxylation reactions on a wide array of monocyclic aromatic molecules. Interestingly, we found that not all these novel hydroxylated compounds were able to reduce the DPPH stable radical, a common test system for determining the scavenging properties of putative antioxidants. In fact, phenols such as those produced from the hydroxylation of 2-phenoxyethanol characterized by the fact that an oxygen atom, different from the one derived from the hydroxyl group added by the enzyme, is directly bound to the aromatic ring (Fig.8 of the Introduction section), were “responsive” to this assay. On the other hand, phenols derived from both phthalan and 2-indanol, molecules in which no other oxygen atom is directly bound to the aromatic ring (Fig.8 of the Introduction section), and from 2-phenylethanol (Fig.5), were not able to reduce the DPPH radical. Otherwise, only catechols, such as hydroxytyrosol – always used in our experiments as a reference compound- and the dihydroxylated derivative of 2-indanol gave a positive response in this experiment. Noteworthy, all the compounds share a common, although differential, antioxidant effect on eukaryotic cells of the H9c2 cell line subjected to a mild oxidative stress induced by sodium arsenite. The discrepancy between the *in vitro* and the *ex vivo* assays showed from one side a possible limitation in the use of the DPPH assay as the unique methodology to assess the *in vitro* antioxidant potential of novel compounds, and on the other hand might suggest that the antioxidant effect observed in cells might not be due to a simple scavenge of ROS based on the chemical mechanisms briefly described in the Introduction (paragraph 1.2), but it might be dependent on other molecular events that have not been elucidated yet.

In the near future, the antioxidant potential of our novel hydroxylated compounds has to be analyzed more in detail using for example other eukaryotic cell lines and inducing the oxidative stress also with other agents, such as H₂O₂, that might be considered the more common physiological source of ROS. Moreover, the availability of the molecules produced under the present study opens new possibilities for obtaining new antioxidant molecules. In fact, they can be now functionalized, to modify their biological activity, by using different approaches such as (*i*) the use of the hypervalent iodine reagents *IBX* (2-Iodoxybenzoic acid) to obtain thiolic and selenolic derivatives that might show improved antioxidant properties both *in vitro* and *in vivo*; and/or the use of glycosylases to produce glycosidic derivatives. Indeed, it has been frequently reported that glycosylation strongly affects both the stability and the hydrophilicity of target molecules thus modifying their bioavailability and their *in vivo* effect.

All the data collected will also have important implications for the rational design of multipotent antioxidants based on aromatic nuclei that, for their chemical versatility,

are ideal candidates to create molecules with multiple pharmacological effects. Phenols and catechols are in fact promising starting points to merge with other pharmacophores thus obtaining multipotent agents with antioxidant effects and beyond.

The effective biotechnological use of the ToMO system and its variants is strongly dependent on the stable integration of the gene encoding this enzyme either in the genome or in plasmids whose selection is not dependent on the presence of antibiotics, of a GRAS microorganism. The expression of ToMO in a heterologous host different from *E.coli* and compatible with a future scale-up of bioprocesses based on the use of this enzymatic activity was only partially successful. We were able to clone the *tou* gene cluster into a suitable shuttle vector and to express the functional multicomponent system in strain JM109 of *E.coli*. The presence of the novel plasmid was assessed in *B. subtilis* after transformation of competent cells. However, no recombinant expression was detected. RT-PCR experiments suggested that this was due to the lack of the corresponding mRNA. This result prompts our interest in trying to insert the recombinant pDAM10 plasmid in different strains of *B. subtilis*, as the lack of transcription could be related to a scarce recognition from endogenous RNA polymerases of the promoter region present in our genetic construct, that was instead correctly transcribed in *E. coli*. In a parallel approach other shuttle vectors for *B.subtilis* will also be used for the cloning of the complete *tou* gene cluster as our experiments cannot exclude that the lack of mRNA might be due to an intrinsic incompatibility between our plasmid and the host strain used. Moreover, the use in the near future of other GRAS microorganisms for the scale-up of ToMO-catalyzed biosynthesis such as *Kluyveromyces lactis*, or *Lactobacillus casei* will be attempted.

Bacterial Multicomponent Monooxygenases such as the ToMO system are not the only enzymatic tool which have a great biotechnological potential for the functionalization of aromatic compounds to produce high-added value molecules. Great attention, in fact, has been devoted in the last decades to the Baeyer–Villiger Monooxygenases (BVMOs). During my experience at the Laboratory of Prof. Jennifer Littlechild at the Exeter Biocatalysis Centre (College of Life and Environmental Sciences at the University of Exeter, UK) the recombinant expression and purification of the oxygenase and flavin reductase component of 3,6 DKCMO from *Ps. putida* NCIMB 10007 were optimized. This allowed obtaining suitable amounts of both these proteins to set-up several successful experiments of crystallization. The data collected from crystal analysis are still under investigation. The determination of the three-dimensional structure of these proteins, both individually and in complex with their substrate, will give important clues for the future site-directed mutagenesis of this BVMO, a mandatory step to effectively evaluate the versatility of this enzymatic complex in catalyzing the conversion of non-natural substrates of industrial interest.

References

1. *Reactive oxygen species: metabolism, oxidative stress, and signal transduction.* Apel K., Hirt H.. *Annu. Rev. Plant. Biol.* 2004; 55:373-399.
2. *Transmitting biological information using oxygen: Reactive oxygenspecies as signaling molecules in cardiovascular pathophysiology.* Shah M.A., Sauer H. *Cardiovascular Research* 2006; 71:191–194.
3. *Role of oxidative stress in female reproduction.* Agarwal A., Gupta S., Sharma R.K. . *Reproductive Biology and Endocrinology.* 2005; 3:28.
4. *Strategies of antioxidant defense.* Sies H. *Eur. J. Biochem.* 1993; 215: 213-219.).
5. *Role of oxidative stress in development of complications in diabetes.* Baynes J.W. 1991;40(4):405-12.
6. *Antioxidants in health and disease.* Young I.S., Woodside J.V. . *J Clin. Pathol.* 2001;54(3):176-86.
7. *Antioxidant relevance to human health.* Wahlqvist M.L. . *Asia Pac. J. Clin. Nutr.* 2013;22(2):171-6.
8. *The antioxidative protecting role of the Mediterranean diet.* Hadziabdić M.O., Bozikov V., Pavić E., Romić Z. . *Coll. Antropol.* 2012;36(4):1427-34.
9. *Oxidative stress: damage to intact cells and organs.* Sies H., Cadenas E. . *Philos Trans R Soc Lond B Biol Sci.* 1985; 311(1152):617-31.
10. *Role of reactive oxygen species in biological processes.* Sies H. *Klin Wochenschr.* 1991;69(21-23):965-8.
11. *Fruit, vegetables, and cancer prevention: a review of the epidemiological evidence.* Block G., Patterson B., Subar A.. *Nutr Cancer.* 1992; 18(1):1-29.
12. *Vegetables, fruit, and cancer. I. Epidemiology.* Steinmetz K.A., Potter J.D.. *Cancer Causes Control.* 1991; 2(5):325-57.
13. *New insights into controversies on the antioxidant potential of the olive oil antioxidant hydroxytyrosol.* Rietjens, S.J., Bast A., Haenen G.R. *J Agric Food Chem.* 2007 Sep 5;55(18):7609-14.
14. *Inhibition of the autoxidation of organic substances in the liquid phase.* Ingold K. U. *Chem. Rev.* 1961; 61: 563–589).
15. *Is vitamin E the only lipid-soluble, chain-breaking antioxidant in human blood plasma and erythrocyte membranes?* Burton G. W., Joyce A., Ingold K. U.. *Arch. Biochem. Biophys.* 1983; 221: 281–290.
16. *Antioxidant activity of food constituents: an overview.* Gülçin I. *Arch. Toxicol.* 2012; 86:345-391.
17. *Biochemical basis of 4-hydroxyanisole induced cell toxicity towards B16-F0 melanoma cells.* Moridani M.Y. *Cancer Letters* 2006;243:235–245.
18. *How many drugs are catechols.* Da-Peng Yang et al. *Molecules* 2007;12 p.878-884.
19. *Structure-activity relationships and rational design strategies for radical-scavenging dihydroxyflavone.* Zhang,H.-Y. *Curr. Comput-Aided Drug Des.*2005;1,257-273.


20. *Theoretical Investigation on Free Radical Scavenging Activity of 6,7-Dihydroxyflavone*. Hong-Yu Zhang. Quant.Struct.-Act.Relat.2000;19,50-53.
21. *Substituent Effects on O-H Bond Dissociation Enthalpies and Ionization Potentials of Catechols: A DFT Study and Its Implications in the Rational Design of Phenolic Antioxidants and Elucidation of Structure–Activity Relationships for Flavonoid Antioxidants*. Hong-Yu Zhang Prof., You-Min Sun Dr.,Xiu-Li Wang.Chem. Eur. J.2003; 9,502-508.
22. *Chemical properties of catechols and their molecular modes of toxic action in cells, from microorganism to mammals*. Schweigert N. et al.. Environmental Microbiology 2001;3(2), 81-91.
23. *A Comparative Study of the Synthesis of 3-Substituted Catechols using an Enzymatic and a Chemoenzymatic Method*; Advanced Synthesis & Catalysis. Berberian et al 2007.349 4-5 p: 727-739.
24. *Biotransformations in organic synthesis*. Loughlin, W.A.. Biores. Technol.2000. 74: p. 49-62.
25. *Monooxygenases as biocatalysts: Classification, mechanistic aspects and biotechnological applications*. Torres Pazmino, D.E., et al.. J Biotechnol, 2010. 146(1-2): p. 9-24.
26. *Ortho-Formylation of phenols; preparation of 3-bromosalicylaldehyde*.Trond V. H. et al. 2005. Vol. 82, p. 64-68.
27. *Synthesis of catechols from Phenols via Pd-Catalyzed Silanol-Directed C-H Oxygenation*. Chunhui H., Nugzar G., Buddhadeb C., Gevorgyan V. . J. Am. Chem. Soc. 2011,133, p:17630-17633.
28. *Whole organism biocatalysis*. Ishige, T., Honda K., and Shimizu S.. Curr. Opin. Chem. Biol., 2005. 9(2): p. 174-80.
29. *Advances in the enzymatic reduction of ketones* Moore J. C. et al., Acc. Chem. Res. 40, 1412–1419, 2007.
30. *Arene cis-dihydrodiol formation: from biology to application*. Boyd, D.R. and T.D. Bugg Org. Biomol. Chem., 2006. 4(2): p. 181-92.
31. *Aromatic dioxygenases: molecular biocatalysis and applications*. Boyd, D.R., Sharma N.D., and Allen C.C., Curr. Opin. Biotechnol., 2001. 12(6): p. 564-73.
32. *The evolution of biotransformation technologies*. Dordick, J.S., Y.L. Khmelnitsky, and M.V. Sergeeva, Curr. Opin. Microbiol., 1998. 1(3): p. 311-8.
33. *Evolution of bacterial and archaeal multicomponent monooxygenases*. Notomista E., et al.. J Mol Evol, 2003. 56(4): p. 435-45
34. *Biodegradation, biotransformation, and biocatalysis (b3)*. Parales, R.E., et al.. Appl. Environ. Microbiol., 2002. 68(10): p. 4699-709.
35. *Regiospecificity of two multicomponent monooxygenases from Pseudomonas stutzeri OX1: molecular basis for catabolic adaptation of this microorganism to methylated aromatic compounds*. Cafaro, V., et al.. Appl. Environ. Microbiol. 2005. 71(8): p. 4736-43.
36. *Mutation of glutamic acid 103 of toluene o-xylene monooxygenase as a means to control the catabolic efficiency of a recombinant upper pathway for*

- degradation of methylated aromatic compounds*. Cafaro, V., et al.. Appl. Environ. Microbiol., 2005. 71(8): p. 4744-50.
37. *Molecular determinants of the regioselectivity of toluene/o-xylene monooxygenase from Pseudomonas sp. strain OX1*. Notomista, E., et al.. Appl. Environ. Microbiol., 2009. 75(3): p. 823-36.
 38. *Tuning the specificity of the recombinant multicomponent toluene o-xylene monooxygenase from Pseudomonas sp. strain OX1 for the biosynthesis of tyrosol from 2-phenylethanol*. Notomista E., et al.. Appl. Environ. Microbiol., 2011. 77(15): p. 5428-37.
 39. *Bioavailability of tyrosol, an antioxidant phenolic compound present in wine and olive oil, in humans*. Covas M.I., et al.. Drugs Exp. Clin. Res., 2003. 29(5-6): p. 203-6.
 40. *Nutraceutical antioxidants as novel neuroprotective agents*. Kelsey, N.A., H.M. Wilkins, and D.A. Linseman. Molecules, 2010. 15(11): p. 7792-814.
 41. *Antibacterial polyphenols from olive oil mill waste waters*. Capasso, R., et al.,. J. Appl. Bacteriol., 1995. 79(4): p. 393-8.
 42. *Inhibition of leukocyte 5-lipoxygenase by phenolics from virgin olive oil*. de la Puerta, R., V. Ruiz Gutierrez, and J.R. Hoult. Biochem. Pharmacol., 1999. 57(4): p. 445-9.
 43. *Inhibition of peroxynitrite dependent DNA base modification and tyrosine nitration by the extra virgin olive oil-derived antioxidant hydroxytyrosol*. Deiana, M., et al.. Free Radic. Biol. Med., 1999. 26(5-6): p. 762-9.
 44. *Active components and clinical applications of olive oil*. Waterman, E. and B. Lockwood Altern Med. Rev, 2007. 12(4): p. 331-42.
 45. *Antioxidant and other biological activities of phenols from olives and olive oil*. Visioli, F., A. Poli, and C. Gall, Med Res Rev, 2002. 22(1): p. 65-75.)
 46. *Protective effects of synthetic hydroxytyrosol acetyl derivatives against oxidative stress in human cells*. Manna, C., et al J Agric Food Chem, 2005. 53(24): p. 9602-7.
 47. *Olive-oil consumption and health: the possible role of antioxidants*. Owen R.W., et al Lancet Oncol., 2000. 1: p. 107-12.
 48. *Inhibition of platelet aggregation and eicosanoid production by phenolic components of olive oil*. Petroni, A., et al., Thromb Res, 1995. 78(2): p. 151-60.
 49. *New insights into controversies on the antioxidant potential of the olive oil antioxidant hydroxytyrosol* Rietjens, S.J., A. Bast, and G.R. Haenen. J Agric Food Chem, 2007. 55(18): p. 7609-14.
 50. *The effect of Caro's reagent on ketones* A. Baeyer, V. Villiger, Ber. Dtsch. Chem. 1899, 32, 3625-3633.
 51. *Baeyer-Villiger Monooxygenases, an Emerging Family of Flavin-Dependent Biocatalysts* Nanne M. Kamerbeek, Dick B. Janssen, Willem J. H. van Berkel, Marco W. Fraaije Advanced Synthesis & Catalysis 2003 p. 667-678.
 52. *Baeyer-Villiger monooxygenases, an emerging family of flavin-dependent biocatalysts*. KamerbeekNM, JanssenDB, van BerkelWJ, FraaijeMW. Adv. Synth. Catal. 2003; 345:667-678

53. *Relative effectiveness of worker safety and health training methods.* Burke, M. J., Sarpy, S. A., Smith-Crowe, American Journal of Public Health, 2006 96, 315–324.
54. *Towards large-scale synthetic application of Baeyer-Villiger monooxygenase* Veronique Alphanh Giacomo Carrea Roland Wohlgemuth Roland Furstoss and John M. Woodley Trends in Biotechnology, July 2003 Volume 21, Issue 7, 318-323.
55. *A novel ketone monooxygenase from Pseudomonas cepacia. Purification and properties* Britton LN, Markovetz AJ. J Biol Chem. 1977 Dec 10;252(23):851-6.
56. *An enzyme system for aliphatic methyl ketone oxidation.* Forney FW, Markovetz AJ. Biochem Biophys Res Commun. 1969 Sep 24;37(1):31-8.
57. *The metabolism of cyclohexanol by Acinetobacter NCIB 9871.* Donoghue NA, Trudgill PW. Eur J Biochem. 1975 Dec 1;60(1):1-7.
58. *Microbial degradation of chlorinated acetophenones.* Havel J, Reineke W. Appl Environ Microbiol. 1993 Aug;59(8):2706-12.
59. *Recent developments in the application of Baeyer-Villiger monooxygenases as biocatalysts.* de Gonzalo G, Mihovilovic MD, Fraaije MW Chembiochem. 2010; 11(16):2208-31.
60. *4-Hydroxyacetophenone monooxygenase from Pseudomonas fluorescens ACB. A novel flavoprotein catalyzing Baeyer-Villiger oxidation of aromatic compounds.* Kamerbeek N.M. , Moonen M.J., Van Der Ven JG, Van Berkel WJ, Fraaije MW, Janssen DB. Eur J Biochem. 2001;268(9):2547-57.
61. *Baeyer-Villiger monooxygenases, an emerging family of flavin-dependent biocatalysts.* Kamerbeek NM, Janssen D.B., van Berkel W.J., Fraaije M.W. Adv. Synth. Catal. 2003; 345:667–678.
62. *Snapshots of enzymatic Baeyer-Villiger catalysis. Oxygen activation and intermediate stabilization.* Orru R., Dudek H.M., Martinoli C., Torres Pazmiño D. E., Royant A., Weik M., Fraaije M. W., Mattevi A. J. Biol. Chem. 2011; 286, 29284–29291.
63. *Baeyer–Villiger monooxygenases: recent advances and future challenges.* Daniel E., Torres Pazmiño D.E., Dudek H.M., Fraaije M.W.. Current Opinion in Chem Biology 2010; 14(2): 138–144.
64. *Designing new Baeyer-Villiger monooxygenases using restricted CASTing.* Clouthier C.M., Kayser M.M., Reetz M.T.. J Org Chem. 2006; 71(22):8431-7.
65. *Blending Baeyer-Villiger monooxygenases: using a robust BVMO as a scaffold for creating chimeric enzymes with novel catalytic properties.* Van Beek H.L., de Gonzalo G., Fraaije M.W.. Chem. Commun. (Camb). 2012; 48(27):3288-90.
66. *Single chain antibody fragment production and metabolic engineering of hyaluronic acid in Bacillus and Escherichia coli .* Cavallarin, N. 2011 PhD thesis, University of Padua, Italy..
67. *Developments in the use of Bacillus species for industrial production.* Schallmeyer M., Singh A., Ward O.P.. Can J Microbiol. 2004 Jan;50(1):1-17.

68. *Production of recombinant proteins in Bacillus subtilis*. Schumann, W., Adv. Appl. Microbiol, 2007. 62: p. 137-89.
69. *Molecular Cloning. A Laboratory Manual*. Sambrook, J., E. Fritsch, and T. Maniatis, 1989 New York: Cold Spring Harbor Laboratory Press.
70. *The role of the conserved residues His-246, His-199, and Tyr-255 in the catalysis of catechol 2,3-dioxygenase from Pseudomonas stutzeri OX1*. Viggiani, A., et al., J Biol Chem, 2004. 279(47): p. 48630-9.
71. Cleavage of Structural Proteins during the Assembly of the Head of Bacteriophage T4. U.K. Laemmli *Nature* 15 August 1970 227, 680-685
72. *Genesis and development of DPPH method of antioxidant assay*. Sagar B. Kedare et al., Journal of Food Science and Technology 2011 48; p.412-422.
73. *A simple technique for quantifying apoptosis in 96-well plates*. Ribble D, Goldstein NB, Norris DA, Shellman YG. BMC Biotechnol. 2005 May 10;5:12.
74. *Oxidative stress: damage to intact cells and organs*. Sies H, Cadenas E. Philos Trans R Soc Lond B Biol Sci. 1985; 311(1152):617-31.
75. *Role of reactive oxygen species in biological processes*. Sies H. Klin Wochenschr. 1991;69(21-23):965-8.
76. *Evaluation of free radical scavenging of dietary carotenoids by the stable radical 2,2-diphenyl-1-picrylhydrazyl*. Sánchez-Moreno et al. J.Sci Food Agric. 2000;80, p:1686-1690.
77. *The Chemistry behind antioxidant capacity assay*. Dejian Huang, et al. J.Agric.Food Chem 2005, 53, p:1841-1856.
78. *Screening of Antioxidants from Medicinal Plants for Cardioprotective Effect against Doxorubicin Toxicity*. Suvara K., Wattanapitayakul L., Chularojmontri, Angkana Herunsalee, Suphan Charuchongkolwongse, Somchit Niumsukul, John A. Bauer, 2003;78(1):57–64.
79. *Essential stations in the intracellular pathway of cytotoxic bovine seminal ribonuclease*. Bracale, D. Spalletti-Cernia, M. Mastronicola, F. Castaldi, R. Mannucci, L. Nitsch, G. D'Alessio, Biochem. J. 362 (2002) 553e560.
80. Sodium Arsenite Exposure Alters Cell Migration, Focal Adhesion Localization and Decreases Tyrosine Phosphorylation of Focal Adhesion Kinase in H9C2 Shannon L. Yancy, Eric A. Shelden, Robert R. Gilmont, and Michael J. Welsh§, Toxilogical sciences 200584, 278-286.
81. *RNA granules: post-transcriptional and epigenetic modulators of gene expression* Paul Anderson & Nancy Kedersha *Nature Reviews Molecular Cell Biology* June 2009 10, 430-436.
82. *Differential responses of Bacillus subtilis rRNA promoters to nutritional stress*. Samarra, W., et al., J. Bacteriol. 193(3): p. 723-33.
83. *Amino acid replacements at binding sites of monoclonal antibody in the F1-ATPase beta subunit from Escherichia coli caused altered subunit interactions*. Miki, J., et al., J Biol Chem, 1994. 269(6): p. 4227-32.
84. *Novel plasmid-based expression vectors for intra- and extracellular production of recombinant proteins in Bacillus subtilis*. Phan, T.T.P., Nguyen, H.D. and Schumann, W. Protein Expr. Purif.; 2006 Apr; 46(2): 189-95.

85. *Investigating the coenzyme specificity of phenylacetone monooxygenase from *Thermobifida fusca**. Dudek HM, Torres Pazmiño DE, Rodríguez C, de Gonzalo G, Gotor V, Fraaije MW. Appl Microbiol Biotechnol. 2010 Nov;88(5):1135-43. doi: 10.1007/s00253-010-2769-y. Epub 2010 Aug 12
86. *Altering the Substrate Specificity and Enantioselectivity of Phenylacetone Monooxygenase by Structure-Inspired Enzyme Redesign* Daniel E. Torres Pazmiño, Radka Snajdrova, Daniela V. Rial, Marko D. Mihovilovic, Marco W. Fraaije¹Advanced Synthesis & Catalysis Volume 2007 349, Issue 8-9, pages 1361–1368, June 4.
87. *Cloning, expression and characterisation of a Baeyer–Villiger monooxygenase from *Pseudomonas putida* KT2440*. Rehdorf, J., Kirschner, A., and Bornscheuer, U.T. Biotechnol. Lett. 2007.29, 1393–1398.
88. *Functional expression, purification, and characterisation of the recombinant Baeyer–Villiger monooxygenase MekA from *Pseudomonas veronii* MEK700*. Völker, A., Kirschner, A., Bornscheuer, U.T., and Altenbuchner, J. Microbiol. Biotechnol. 2008.77, 1251–1260.
89. *Completing the series of BVMOs involved in camphor metabolism of *Pseudomonas putida* NCIMB 10007 by identification of the two missing genes, their functional expression in *E. coli*, and biochemical characterization*. Kadow M., Loschinski K., Sass S., Schmidt M., Bornscheuer U.T.. Appl. Microbiol. Biotechnol. 2012, 96:419-429.



Appendices

List of publications

- 1) Notomista E., Scognamiglio R., Troncone L., **Donadio G.**, Pezzella A., Di Donato A., Izzo V. *Tuning the specificity of recombinant multicomponent monooxygenase ToMO from Pseudomonas sp. OX1 for the biosynthesis of tyrosol from 2-phenylethanol*. Appl Environ Microbiol (2011) 77(15):5428-37.

List of communications

- 1) Cafaro V., Notomista E., Izzo V., Troncone L., **Donadio G.**, Tedesco P., Di Donato A. *Bioaugmentation of Novosphingobium sp. PP1Y in natural and artificial soils contaminated by PAHs and heavy metals*. Environmental Microbiology and Biotechnology in the frame of the Knowledge-Based Bio and Green Economy Bologna, April 10-12, 2012.
- 2) **Donadio G.**, Notomista E., Serpico A., Pezzella A., Di Donato A., Izzo V. *Bacterial multicomponent Monooxygenases for the biosynthesis of antioxidants of industrial interest*. Environmental Microbiology and Biotechnology in the frame of the Knowledge-Based Bio and Green Economy Bologna, April 10-12, 2012.
- 3) Izzo V., Notomista E., Pezzella A., **Donadio G.**, Di Donato A. *Rational site-directed mutagenesis: a computational approach for the design of mutants of the toluene o-xylene monooxygenase*. XI National Congress of Biotechnology. Varese, Università dell'Insubria, 27th-29th June, 2012.
- 4) Izzo V., Russomanno G., Notomista E., Pizzo E., Conti V., **Donadio G.**, Di Cristo C., Pezzella A., Di Donato A., Filippelli A. *Novel antioxidant catechols: biosynthesis, characterization and biological activity*. XXXVI National Congress of the Italian Society of Pharmacology, Torino, 23th-26th October, 2013.

Experience in foreign laboratories

Stage at Exeter Biocatalysis Centre, Biosciences, College of Life and Environmental Sciences at the University of Exeter, UK. (April-June 2013). The work was supervised by Jennifer Littlechild, Prof of Biological Chemistry, Director of Biocatalysis Centre

Ringraziamenti

Caro Prof., semplicemente grazie perchè è sempre stato un esempio di onestà ed autorità, pronto ad ascoltarmi e riprendermi come un buon padre. E' stato un piacere lavorare nel suo gruppo e sono sicura che potrò sempre contare su di lei e i suoi preziosi e saggi consigli. Con immenso affetto Prof!

Un ringraziamento particolare vorrei farlo al mio capo, alla mia Vivvy. Infinitamente grazie, tu sei stata più di un' insegnante, tu hai avuto fiducia in me, nelle mie capacità e hai saputo farmi credere che quel "diesel" , come dici tu, poteva arrivare lontano. Regala a tutti quello che hai dato a me, non stancarti mai di trasmettere la tua passione e le tue conoscenze per chi li riceverà sarà un onore e una fortuna. In bocca al lupo per tutto e....non perdiamoci mai. Ti voglio bene.

Alle mie ragazze Aurora, Fabiana e Ornella. I vostri consigli, ma soprattutto i vostri sorrisi hanno reso questi 4 anni meravigliosi. Poi in questi anni siete diventate tecnologiche, con whatsapp staremo sempre in contatto!!! Non vi dimenticherò mai!

E poi tu...Roberta...Con te ho iniziato a fare i miei primi passi, tu mi hai accompagnata e poi lasciata andare con fiducia ma sempre guardandomi da lontano. Mi hai "cresciuta" e abbracciata quando sapevi che ne avevo bisogno. Grazie Rò...Ti voglio bene

A tutti i miei figlioletti Annabel, Pietro, Nicola, Vincenzo, Francesca. A voi spero di aver trasmesso tutta la passione che questo lavoro merita e qualche insegnamento; vi ringrazio perché m'avete arricchito insegnandomi ogni giorno qualche cosa. Andate avanti con umiltà e grinta e sono sicura che sentirò parlare di voi. Un in bocca al lupo al mio Vincy e a Nik per quello che verrà, voi avete reso questo ultimo periodo speciale.

Un ringraziamento particolare a Fekerika che in questi ultimi mesi mi ha supportata moralmente e lavorativamente. Mi commuove e onora il rispetto e la stima che mi dimostri. Non perdere il tuo sorriso e l'amore per quello che fai, ascolta sempre e ricordati di me quando ritirerai il nobel...

A Ennio e Valeria, i due saggi. Grazie per i vostri insegnamenti per avere sempre una risposta quando penso non ci sia, per la disponibilità. Continuate ad insegnare perché siete un patrimonio!

Alla mia Maura, la mia compagna di università, di vita. Siamo cresciute insieme in questi anni universitari e insieme ci siamo affacciate al mondo del lavoro e insieme proseguiamo sempre, per sempre.

Alla mia dolce Ly. Ormai lo sai già, sei sempre stata un esempio da seguire. La tua passione nel lavoro e nella vita è contagiosa e ti ringrazio per avermela trasmessa. Non perderla mai e noi...non perdiamoci mai.

A Luca, grazie per tutto quello che mi hai insegnato ma soprattutto per la fiducia che sei riuscito a trasmettermi. Tu in me hai sempre creduto. Sapevo che avresti conquistato il mondo, ricordati di me quando sarai ricco e famoso.

Un grazie a tutti i ragazzi che ho incontrato in questo cammino Lorenzo, la nuova dolcissima dottoranda Maria Luisa, Rita e il suo pancione, Rituzza, Carmen la mia fedele collaboratrice e non solo.... Un pensiero particolare a Katia. Il tuo sorriso non lo dimenticherò mai, la tua forza mi ha sempre aiutata a non perdere mai di vista le cose più importanti della vita. Meriti tanta felicità...ti voglio bene.

Grazie alla mia cugi Ilaria. Per me un punto di riferimento, una donna che ha lottato con forza ammirevole e ha vinto una dura battaglia. Il tuo esempio per me è prezioso.

A voi, la mia meravigliosa famiglia. Papà e Mamma, amici, voi siete l'esempio più importante che ho. Grazie a voi sono arrivata fino a qui. La vostra onestà, umiltà, sacrificio, allegria, fanno parte di me e a voi devo tutto. Al mio fratellone Cristiano sempre presente anche se lontano. Sei la mia ispirazione più grande, il tuo esempio è stato sempre uno sprono a fare meglio, la certezza di poter sempre contare su di te, su di noi, è la cosa più bella che ho. E a te, piccola Martina. Sei arrivata nella mia vita e l'hai cambiata. Sei l'amore più grande che ho, la persona per la quale farei tutto, credi sempre in te stessa e nelle tue capacità e arriverai lontano perché la tua dolcezza e la tua intelligenza sono caratteristiche rare da trovare. Vi amo.

Thank you to Jennifer Littlechild and her wonderful team! Exeter was a great experience that changed my mind and my heart. Mirelli...you are the best!

E alla fine arrivi tu.....la mia scoperta più bella, più importante. Mi hai sempre sostenuta, ascoltata, sopportata. Per te, per noi ho ritrovato la volontà per costruire un futuro migliore, un futuro che grazie a te oggi non mi fa più paura perché è il nostro futuro. Grazie Mario...con amore.

E a me.....dopo tutto me lo merito!

Tuning the Specificity of the Recombinant Multicomponent Toluene *o*-Xylene Monooxygenase from *Pseudomonas* sp. Strain OX1 for the Biosynthesis of Tyrosol from 2-Phenylethanol^{∇†}

Eugenio Notomista,¹ Roberta Scognamiglio,¹ Luca Troncone,¹ Giuliana Donadio,¹
Alessandro Pezzella,² Alberto Di Donato,¹ and Viviana Izzo^{1*}

Dipartimento di Biologia Strutturale e Funzionale, Università di Napoli Federico II, Via Cinthia, I-80126 Naples, and
CEINGE-Biotecnologie Avanzate s.c.ar.l., Naples, Italy,¹ and Dipartimento di Chimica Organica e Biochimica,
Università di Napoli Federico II, Via Cinthia, 80126 Naples, Italy²

Received 1 March 2011/Accepted 1 June 2011

Biocatalysis is today a standard technology for the industrial production of several chemicals, and the number of biotransformation processes running on a commercial scale is constantly increasing. Among biocatalysts, bacterial multicomponent monooxygenases (BMMs), a diverse group of nonheme diiron enzymes that activate dioxygen, are of primary interest due to their ability to catalyze a variety of complex oxidations, including reactions of mono- and dihydroxylation of phenolic compounds. In recent years, both directed evolution and rational design have been successfully used to identify the molecular determinants responsible for BMM regioselectivity and to improve their activity toward natural and nonnatural substrates. Toluene *o*-xylene monooxygenase (ToMO) is a BMM isolated from *Pseudomonas* sp. strain OX1 which hydroxylates a wide spectrum of aromatic compounds. In this work we investigate the use of recombinant ToMO for the biosynthesis in recombinant cells of *Escherichia coli* strain JM109 of 4-hydroxyphenylethanol (tyrosol), an antioxidant present in olive oil, from 2-phenylethanol, a cheap and commercially available substrate. We initially found that wild-type ToMO is unable to convert 2-phenylethanol to tyrosol. This was explained by using a computational model which analyzed the interactions between ToMO active-site residues and the substrate. We found that residue F176 is the major steric hindrance for the correct positioning of the reaction intermediate leading to tyrosol production into the active site of the enzyme. Several mutants were designed and prepared, and we found that the combination of different mutations at position F176 with mutation E103G allows ToMO to convert up to 50% of 2-phenylethanol into tyrosol in 2 h.

Reactions in which organic compounds are oxygenated or hydroxylated are of great value for organic synthesis (33). However, selective oxyfunctionalization of organic substrates can be a significant problem in organic synthesis, as these reactions are often carried out with strong oxidizing agents and occur with little chemo-, regio-, and enantioselectivity (33, 50). Therefore, growing attention has been dedicated in the last years to the development of biotransformations which make use of the metabolic versatility of either purified enzymes or whole microorganisms to perform oxyfunctionalization of organic substrates of industrial interest (1, 7, 10, 21, 50). These methodologies, compared with established chemical processes, are appealing alternatives as means to obtain active aromatic compounds under mild experimental conditions and without employing toxic reagents (20, 26, 48).

Bacterial multicomponent monooxygenases (BMMs) allow the preparation of several aromatic active compounds with high regioselectivity and stereoselectivity (23, 41, 50). BMMs

form a diverse group of nonheme diiron enzymes that activate dioxygen, thus facilitating oxygen atom transfer to specific organic substrates (32, 46), and perform a key metabolic function in promoting catabolic and detoxification reactions (55). These enzymes catalyze a variety of complex oxidations, including mono- and dihydroxylation of aromatic compounds (40, 55). BMMs usually consist of a 200- to 250-kDa dimeric hydroxylase component organized in a ($\alpha\beta\gamma$)₂ quaternary arrangement, a 10- to 16-kDa regulatory protein that enhances the catalytic turnover (3), and a FAD- and (2Fe-2S)-containing reductase that mediates the electron transfer from NADH to the active site of the hydroxylase (31, 38). An additional Rieske protein may be present to assist the electron transfer between the reductase and hydroxylase components. The hydroxylation chemistry takes place at a nonheme carboxylate-bridged diiron center, harbored in the active site of the hydroxylase moiety, coordinated by four glutamate and two histidine residues from a four-helix bundle (32, 35, 36, 38).

Oxygenase biocatalysts are already used in the chemical industry to obtain additives for agriculture, synthones, drugs, and plastics (7), and due to their catalytic properties, these multicomponent enzymes, either wild type (wt) or engineered, are a versatile biosynthetic tool for the preparation of different active aromatic compounds (8, 10, 11, 50).

Toluene *o*-xylene monooxygenase (ToMO) from *Pseudomo-*

* Corresponding author. Mailing address: Dipartimento di Biologia Strutturale e Funzionale, Università di Napoli Federico II, Via Cinthia, I-80126 Naples, Italy. Phone: 39-081-679207. Fax: 39-081-679313. E-mail: vizzo@unina.it.

† Supplemental material for this article may be found at <http://aem.asm.org/>.

[∇] Published ahead of print on 10 June 2011.

nas sp. strain OX1 (4, 5, 15, 45) is a BMM that belongs to the subfamily of four-component aromatic/alkene monooxygenases (group 2 BMMs) (38). ToMO is endowed with a broad spectrum of substrate specificity and, among others, is able to oxidize *o*-, *m*-, and *p*-xylene, 2,3- and 3,4-dimethylphenol, toluene, cresols, benzene, naphthalene, and styrene (4).

The ToMO complex, encoded by the *tou* gene cluster (GenBank accession number AJ005663), is composed of six polypeptides which are organized as four components (15). ToMOF is the NADH oxidoreductase responsible for supplying electrons to the diiron cluster housed into the active site of the hydroxylase moiety. The electron transfer is mediated by the Rieske protein ToMOC. The hydroxylase, named ToMOH, consists of three polypeptides (B, E, A) organized in a quaternary structure of the type (BEA)₂; the active site is housed in the subunit ToMOA (45). Finally, ToMOD has been shown to be a regulatory protein, essential for efficient catalysis and devoid of any metal or cofactor (15). The ToMO multi-component system has been thoroughly investigated to identify the molecular determinants responsible for its regioselective hydroxylation of aromatic compounds (12–14, 51, 52). Moreover, a computational model was recently developed that quantitatively predicts the effects of mutations into the active-site pocket of ToMOA, thus allowing the rational design of variants of the enzyme endowed with the desired regioselectivity (37).

The main aim of the present work has been to investigate the use of recombinant ToMO for the bioconversion of 2-phenylethanol, a cheap and commercially available substrate (22, 25), to the high-added-value compound tyrosol.

Tyrosol (17) belongs to a class of natural phenolic antioxidants commonly referred to as “nutraceuticals” (27) whose role in the prevention of diseases such as cancer and cardiovascular diseases is emerging (16, 18, 19, 56). Moreover, tyrosol is an excellent starting material for the microbial conversion to hydroxytyrosol (1, 2, 6, 21), an *ortho*-diphenol abundant in olive fruits and virgin olive oil, characterized by several attractive properties such as antibacterial activity, scavenging of free radicals, protection against oxidative DNA damage and low-density lipoprotein oxidation, prevention of platelet aggregation, and inhibition of 5- and 12-lipoxygenases (34, 39, 42, 43, 54).

Due to the inability of wt ToMO to produce tyrosol as the sole isomer from the hydroxylation of 2-phenylethanol, we developed a computational model to provide a molecular explanation for this outcome. To validate our computational model, several ToMO variants were designed and tested for their ability to transform 2-phenylethanol into tyrosol. Our results led to identification of residue F176 as a major steric hindrance for the correct positioning of the reaction intermediate leading to tyrosol production. In fact, all the mutations at position 176 allow ToMO to produce only tyrosol from 2-phenylethanol. Moreover, we found that the combination of mutations at position F176 with mutation E103G increases the k_{cat} values on 2-phenylethanol. Finally, among the E103G/F176X variants, we found that mutants E103G/F176I and E103G/F176T were the most efficient, allowing conversion of about 50% of 2-phenylethanol into tyrosol in 2 h.

The results presented in this paper confirm that a fine-tuning of ToMO regioselectivity can be achieved through a careful

alteration of the shape of the active-site pocket. Moreover, our data indicate that this strategy can also help in designing ToMO mutants that efficiently hydroxylate, with high regioselectivity, any desired substituted benzene ring.

MATERIALS AND METHODS

Materials. Bacterial cultures, plasmid purifications, and transformations were performed according to Sambrook et al (44). *Escherichia coli* strain JM109 was from Novagen. Plasmid pTou was kindly supplied by Valeria Cafaro (Department of Structural and Functional Biology, University Federico II, Naples, Italy). The pGEM3Z expression vector, Wizard SV gel, and the PCR cleanup system for the elution of DNA fragments from agarose gels were obtained from Promega. Enzymes and other reagents for DNA manipulation were from New England BioLabs. The oligonucleotides were synthesized at MWG-Biotech (Ebersberg, Germany). All other chemicals were from Sigma. Tyrosol was purchased from Fluka. The expression and purification of recombinant catechol 2,3-dioxygenase (C2,3O) from *Pseudomonas* sp. OX1 are described elsewhere (53).

ToMOA mutagenesis and construction of expression vectors. Plasmids for the expression of ToMO complexes with mutated ToMOA subunits were obtained by site-directed mutagenesis of plasmid pTou, coding for the complete *tou* gene cluster, and prepared as previously described (13). Plasmid pTou was digested with restriction enzymes MluI and SalI to extract a 1,200-bp internal fragment from the *touA* open reading frame. This fragment lacked the first 36 bp and the last 138 bp of the coding sequence and coded for amino acids 14 to 451 of the ToMOA subunit. The MluI/SalI fragment was cloned into the pET22b(+) commercial vector, and the resulting plasmid was designated pET22b(+)/*touA*. This plasmid was used to obtain single mutants (F176I)-, (F176L)- (previously constructed as reported in reference 37), and (F176T)-ToMOA and double mutants (E103G/F176A)-, (E103G/F176I)-, (E103G/F176L)-, (E103G/F176T)-, (E103G/F176S)-, and (E103G/F176V)-ToMOA.

Mutations were introduced by a PCR-based methodology performed on the parent pET-22b(+)/*touA* plasmid using a QuikChange site-directed mutagenesis kit provided by Stratagene (La Jolla, CA), according to the manufacturer's protocol, and an MJ Research MiniCycler apparatus. PCR products were used to transform by heat shock *E. coli* XL1-Blue competent cells (Stratagene, La Jolla, CA), and cells were grown overnight on LB agar plates containing ampicillin (100 µg/ml). Three clones were picked from each plate, and their plasmids were isolated with a Qiaprep Spin Miniprep kit (Qiagen) and used for sequencing. The MluI/SalI fragments of the nine mutants were completely sequenced (MWG-Biotech), digested with MluI and SalI, and cloned back into the pTou plasmid previously digested with the same enzymes.

Identification of reaction products of ToMO-catalyzed hydroxylation of 2-phenylethanol. Reaction products were identified by high-pressure liquid chromatography (HPLC) and nuclear magnetic resonance (NMR). All the regioselectivity studies were performed using substrate concentrations higher than the K_m values. Under these conditions, absolute yields of products were proportional to k_{cat} values. Reaction products were identified with an HPLC system equipped with a Waters 1525 binary pump coupled to a Waters 2996 photodiode array detector. Products were separated using an Ultrasphere C₁₈ reverse-phase column (4.6 by 250 mm; pore size, 80 Å), and the absorbance of the eluate was monitored at 254 nm for 2-phenylethanol and 276 nm for tyrosol. Separation was carried out at a flow rate of 1 ml/min by using a two-solvent system consisting of a 0.1% formic acid solution in water (solvent A) and a 0.1% formic acid solution in methanol (solvent B). Compounds were separated using a 3-min isocratic elution with 10% solvent B, followed by a 20-min linear gradient from 10 to 75% solvent B and an isocratic 5-min step at 98% solvent B. The retention times of 2-phenylethanol and tyrosol under these conditions were 24.2 and 16.4 min, respectively. The products were identified by comparing their HPLC retention times and UV-visible spectra with those of standard solutions. The amount of each product was determined by comparing the area of the peak with the areas obtained using known concentrations of standards.

For a more detailed identification of the reaction products, cell-free supernatants obtained after transformation of 2-phenylethanol were extracted twice with ethyl acetate added in a 1:2 ratio compared to the aqueous phase. The organic phase was recovered and dried with a Savant apparatus, and the pellet was dissolved in a solution of 10% methanol containing 0.1% formic acid. The sample was further purified on a high-pressure liquid chromatograph under the conditions described above; each peak was individually collected, concentrated, and used in the NMR analysis.

NMR analysis. Aliquots of the reaction mixture were withdrawn and fractionated by HPLC (see above). Fractions collected at elution times of 16.4, 17.7, and 19.6 min were then extracted with ethyl acetate (3 ml, three times). The combined organic layers were dried over sodium sulfate. The residues obtained were directly used for NMR analysis in deuterated methanol.

^1H NMR spectra were recorded at 600, 400, or 300 MHz, and ^{13}C NMR spectra were recorded at 75 MHz. ^1H and ^{13}C distortionless enhancement by polarization transfer heteronuclear single-quantum correlation and ^1H and ^{13}C heteronuclear multiple-quantum correlation (HMBC) experiments were run at 600 and 400 MHz, respectively, on instruments equipped with a 5 mm ^1H /broadband gradient probe with inverse geometry using standard pulse programs. The HMBC experiments used a 100-ms long-range coupling delay. Chemical shifts are reported in δ values (ppm) downfield from tetramethylsilane.

Regioisomers were distinguished on the base of the spin-coupling pattern in the aromatic region of the ^1H NMR spectra (see Fig. S1 in the supplemental material). Compound 1 showed only two signals featuring a doublet shape as a consequence of the *ortho*-type coupling. On this basis, the direct attribution of the symmetric *para*-substituted structure to compound 1, recognized as the 4-hydroxyphenylethanol, was allowed (see Fig. S1 in the supplemental material).

In the case of compounds 2 and 3 a more complex pattern in the aromatic region of the ^1H NMR spectra was present, suggesting a *meta* and an *ortho* substitution of the aromatic rings (see Fig. S2 and S3 in the supplemental material). The characterization of compounds 2 and 3 as 3-hydroxyphenylethanol and 2-hydroxyphenylethanol, respectively, resulted from the ratios of shielded and unshielded signals. Indeed, the ratio for compound 2 is 3 and is accounted with the two H atoms in *ortho* and the one H atom in *para* to the OH group (see Fig. S2 in the supplemental material). For compound 3, the ratio is 1, which is coherent with the presence of only two shielded H atoms, with only one in *ortho* and one in *para* to the OH group (see Fig. S3 in the supplemental material).

Whole-cell assays. The whole-cell assays were performed as previously described (12) using *E. coli* JM109 cells transformed with the plasmid of interest. Recombinant strains were routinely grown in Luria-Bertani medium (44) supplemented with 100 $\mu\text{g}/\text{ml}$ ampicillin at 37°C to an optical density at 600 nm (OD_{600}) of ~ 0.6 . Expression of the recombinant protein was induced with 0.1 mM isopropyl- β -D-thiogalactopyranoside at 37°C in the presence of 0.2 mM $\text{Fe}(\text{NH}_4)_2(\text{SO}_4)_2$. One hour after induction, cells were collected by centrifugation and suspended in M9 minimal medium containing 0.4% glucose, from here on indicated as M9-G (12). The hydroxylase activity of cells was measured using phenol as the substrate and monitoring the production of catechol in a continuous coupled assay with recombinant C2,3O from *Pseudomonas* sp. OX1, which cleaves the catechol ring and produces 2-hydroxymuconic semialdehyde. This can be monitored spectrophotometrically at 375 nm. The specific activity of cells on phenol was determined by their incubation at an OD_{600} of 0.1 to 0.5 in a quartz cuvette in a final volume of 600 μl of M9-G, 1 mM phenol, and saturating amounts of C2,3O (3 U). The rate of formation of catechol ($\epsilon_{375} = 29,100 \text{ M}^{-1} \text{ cm}^{-1}$) was measured at 25°C.

Specific activity was expressed as the number of mU/ OD_{600} , with one milliunit being defined as the amount of catalyst that oxidized 1 nmol of phenol per min at 25°C.

The determination of apparent kinetic parameters using 2-phenylethanol as a substrate was carried out by discontinuous assays with cells suspended in M9-G in a final volume of 3.5 ml at an OD_{600} of 0.5. Reactions were started by the addition to cell suspensions of various amounts of 2-phenylethanol dissolved in methanol. The final methanol concentration in cell suspensions was always kept below 5%.

At different times, a 1-ml aliquot was withdrawn and the reaction was stopped by the addition of 100 μl of 1 M HCl. Samples were centrifuged at 12,000 rpm for 30 min at 4°C. Soluble fractions were stored at -20°C until analysis. The amount of tyrosol produced from hydroxylation of 2-phenylethanol was estimated by the Folin-Ciocalteu reagent (47). The Folin-Ciocalteu reagent was used under the following conditions: 700 μl of soluble cell extract was added to 100 μl of M9-G and 50 μl of Folin-Ciocalteu reagent (Sigma). Samples were incubated for 10 min at 25°C. One hundred fifty microliters of saturated NaHCO_3 was added to each sample, which was then incubated for 2 h at 25°C. The A_{750} of each sample was recorded. To calculate the rate of formation of tyrosol, an extinction coefficient (ϵ_{750}) of $26,000 \text{ M}^{-1} \text{ cm}^{-1}$ was used.

Determination of kinetic parameters. Kinetic parameters were calculated with the program Prism (GraphPad Software). All the kinetic parameters were determined using whole cells as previously described (12–14, 37).

Maximum rate of hydroxylation (V_{max}) values for all mutants, using 2-phenylethanol as a substrate, were always normalized to the maximum rate measured on phenol in a parallel assay. This was done for each sample of induced cells, and for each mutant the experiment was repeated at least two or three times.

For each sample of induced cells, the level of expression of ToMO was measured as described below and used to calculate the apparent k_{cat} for phenol.

The amounts of ToMO complex were determined by densitometric scanning of Coomassie blue-stained sodium dodecyl sulfate-polyacrylamide gels containing cell extracts. Different amounts of samples of lysed cells were run on a single gel together with four different amounts of purified monooxygenases used as standards.

All ToMO mutants showed expression levels comparable to the level for the wild-type enzyme.

Modeling of substrates and intermediates into the active site of ToMOA.

Reaction intermediates were docked into the active site of ToMO by using the Monte Carlo energy minimization strategy essentially as described previously (37) but with a few modifications: (i) conformational energy calculations included a hydration component calculated as described previously (29, 30) (the hydration energy of Zn^{2+} was arbitrarily assigned to iron ions), (ii) the inner shell included 30 ToMO residues surrounding the active-site cavity, and (iii) complexes with total energies of up to 4 kcal/mol higher than that of the lowest-energy complex were stored for the analysis of energy contributions. 2-Phenylethanol was docked as described above for reaction intermediates but with the following modifications: (i) no hydration component was assigned to the iron ions, and (ii) the inner shell and the outer shell were enlarged to 51 and 181 ToMO residues, respectively. The docking of phenylethanol was performed in three steps: (i) the ToMO-phenylethanol complexes were minimized with phenylethanol locked to an orientation similar to that of the reaction intermediate for the hydroxylation at the *para* position using the atom-atom distance constraints; (ii) the centroid and grid functions were used to generate eight orientations of phenylethanol inside the active-site cavity; and (iii) the eight ToMO-phenylethanol complexes were minimized without constraining the orientation of phenylethanol, except that the oxygen-iron distances were constrained to values higher than 4 Å to avoid the accumulation of complexes with the oxygen atom of phenylethanol at a bridging position between the iron ions.

The Protein Data Bank files for the initial manually generated complexes and the ZMM instruction files containing the lists of mobile residues, constraints, and parameters used during calculations are available upon request.

Other methods. Polyacrylamide gel electrophoresis was carried out using standard techniques (28, 44). Tris-glycine gels were run as 18% gels under denaturing conditions. Protein concentrations were determined colorimetrically with the Bradford reagent (9) from Sigma, using 1 to 10 μg bovine serum albumin as a standard.

RESULTS AND DISCUSSION

ToMO-catalyzed hydroxylation of 2-phenylethanol. On the basis of the similarity between 2-phenylethanol and the natural aromatic substrates of ToMO, we investigated the possibility of using this multicomponent enzyme to hydroxylate 2-phenylethanol to form tyrosol.

Cells of *E. coli* strain JM109 transformed with plasmid pBZ1260 expressing the ToMO gene cluster were grown in LB medium, and the expression of the recombinant multicomponent system was induced as described in Materials and Methods. After 1 h of induction, cells were collected by centrifugation, resuspended in M9-G at a final concentration of 6 OD_{600} units, and incubated with 5 mM 2-phenylethanol. After incubation for different times (0.5, 2, 4, and 14 h) under constant shaking, 1-ml samples were withdrawn, cells were collected by centrifugation, and the supernatants were analyzed by HPLC as described in Materials and Methods. HPLC chromatograms showed that ToMO was able to hydroxylate 2-phenylethanol. Three different peaks were evident from the chromatogram (Fig. 1); the peaks were manually collected and identified by NMR (see Materials and Methods and Fig. S1 to S3 in the supplemental material). The analysis showed that the compound eluting in peak 1 (at 16.4 min) was 4-hydroxyphenylethanol (tyrosol; from here on indicated *p*-tyrosol [10]), the compound eluting in peak 2 (at 17.7 min) was 3-hydroxyphenylethanol (from here on indicated *m*-tyrosol [10]), and the

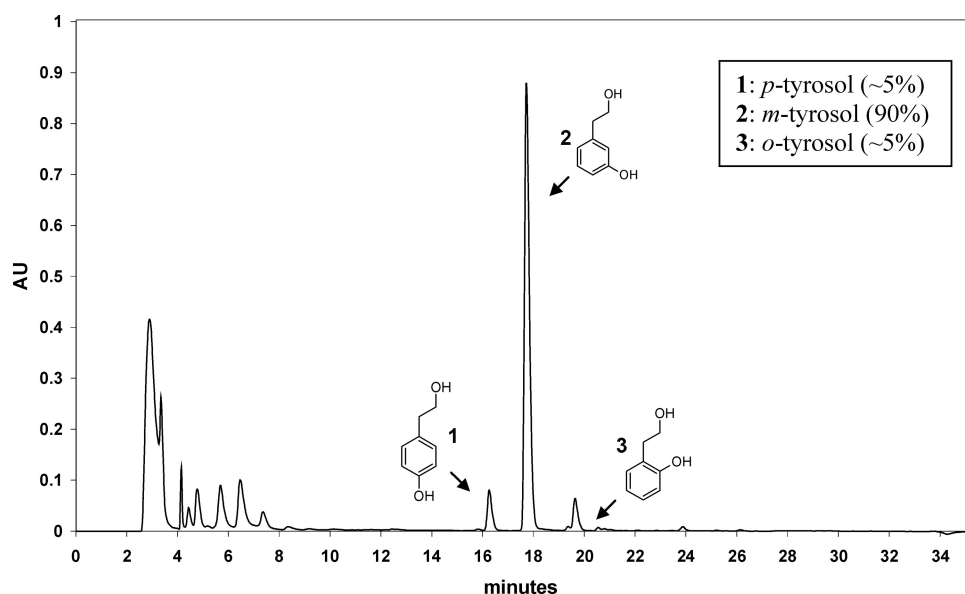


FIG. 1. Regioselectivity of the ToMO-catalyzed reaction using 2-phenylethanol as a substrate. An HPLC chromatogram was monitored at a λ of 276 nm and showed the presence of three products (compounds 1, 2, and 3) corresponding to *p*-tyrosol, *m*-tyrosol, and *o*-tyrosol, respectively. AU, absorbance units. (Inset) Relative percentages of each product.

compound eluting in peak 3 (at 19.6 min) was 2-hydroxyphenylethanol (from here on indicated *o*-tyrosol [10]). *m*-Tyrosol accounted for ca. 90% of the total yield of product, whereas *p*-tyrosol and *o*-tyrosol accounted only for ca. 5% each. It should be noted that the preferential regioselectivity of the ToMO-catalyzed reaction toward the *meta* position of 2-phenylethanol has recently been reported (10). Hence, it was evident that 2-phenylethanol can be hydroxylated by ToMO mainly to *m*-tyrosol, whereas the desired product, *p*-tyrosol, was produced in very low yields. Kinetic parameters of the hydroxylation reaction using 2-phenylethanol as a substrate were calculated in discontinuous assays using whole recombinant cells of *E. coli* strain JM109, as described in the Materials and Methods section. The K_m using this substrate is $211 \pm 22 \mu\text{M}$, and the k_{cat} value is $0.054 \pm 0.016 \text{ s}^{-1}$.

Docking of 2-phenylethanol into active site of ToMOA. A computational strategy, based on a Monte Carlo approach, was recently developed that quantitatively predicts the effects of mutations in the active-site pocket of the hydroxylase moiety of ToMO on the regioselectivity shown by this enzyme on physiological substrates (37). Our aim has been to broaden this computational strategy and to use its predictions to tune ToMO regioselectivity and catalytic efficiency also on non-physiological substrates.

Briefly, the computational strategy is based on a simple kinetic model which predicts the regioselectivity on aromatic substrates of ToMO and its mutants by calculating the relative stability of the orientations of different transition states generated by different enzyme-substrate complexes (37) (Fig. 2A and B). In this model the substrate binds to the active site in different orientations, generating productive and unproductive enzyme-substrate complexes (Fig. 2B). The three possible productive complexes are in equilibrium both with the unproductive complexes and with the three transition states, leading to the *o*-, *m*-, and *p*-substituted phenols (*oC*, *mC*, and *pC*, respec-

tively, in Fig. 2B). According to this kinetic model, the regioselectivity of the enzyme depends only on the relative stability of the three different transition states. This assumption allows us to predict the relative abundance of the products by docking the putative high-energy intermediates (arenium ions in Fig. 2A) into the active site (37).

However, the kinetic model shown in Fig. 2B also suggests that the catalytic efficiency and, in particular, the apparent k_{cat} value of a ToMO mutant should depend both on the absolute stability of the transition state(s) and on the relative abundance of the productive and unproductive enzyme-substrate complexes (Fig. 2B). Thus, the model will predict an efficient ToMO-catalyzed hydroxylation of a substituted benzene like 2-phenylethanol to a desired substituted phenol, e.g., *p*-tyrosol, (i) if the high-energy intermediate corresponding to the desired phenol product fits the active site well and fits better than any other possible high-energy intermediate and (ii) if the ToMO-substrate complex in which the substrate is productively oriented for catalysis is the most abundant one.

We have previously suggested (37) that the stability of the transition state is the sum of two contributions: (i) a noncovalent contribution (noncovalent binding energy [ncBE]) depending on noncovalent interactions between the high-energy intermediate and the active-site pocket, which can be calculated by molecular mechanics techniques like Monte Carlo docking (37), and (ii) a covalent contribution depending on the bonds between the oxygen atom of the high-energy intermediate and the iron ions of the cluster, i.e., on the geometrical parameters of the diiron clusters-arenium ion complex (Fig. 2A and C), which can be calculated only by a complex quantum-mechanical treatment of the transition state. However, the Monte Carlo docking of benzene, toluene, and *o*-xylene arenium intermediates showed that the arenium ring of all the intermediates deriving from these physiological substrates adopts very similar orientations within the active-site pocket of

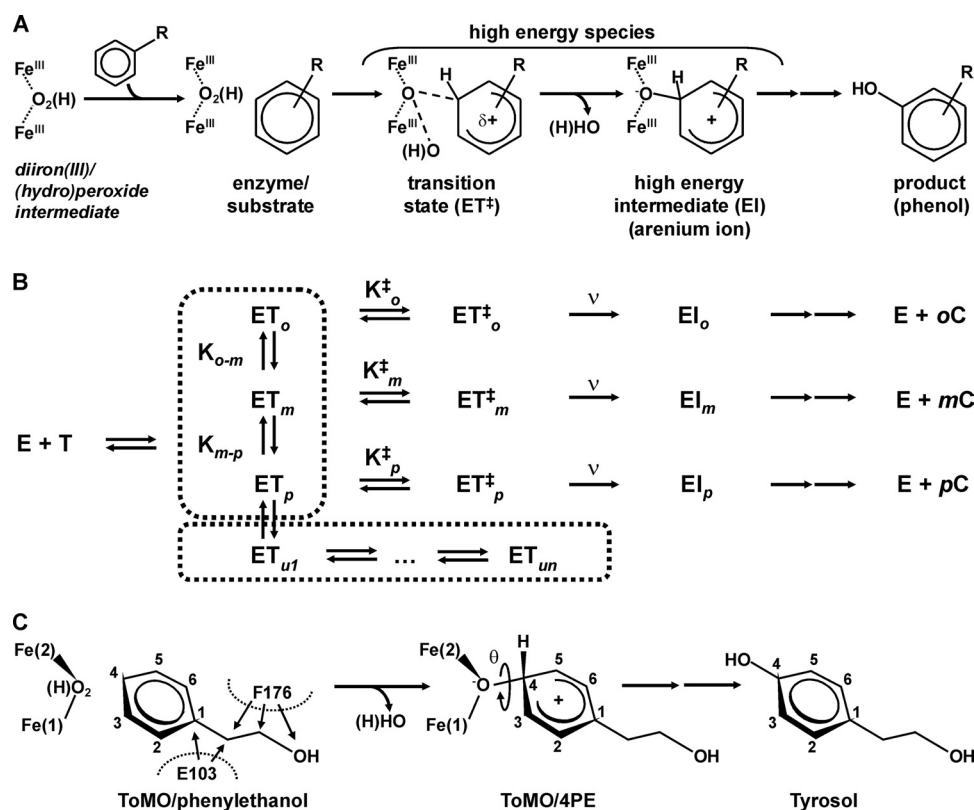


FIG. 2. Kinetic model depicting the regioselectivity of ToMO-catalyzed reactions. (A) Hypothetical enzyme-substrate intermediates during the hydroxylation of an aromatic substrate in the active site of ToMOA; (B) distribution and kinetic constants of productive and nonproductive enzyme-transition state complexes; (C) modeling of the 4-hydroxyphenylethanol intermediate in the active site of ToMOA.

wild-type ToMO (37). Therefore, these Monte Carlo energy-minimized complexes can be considered a reliable model of the optimal transition state for the aromatic hydroxylation reaction and can be used as a reference structure to analyze interactions between the ToMO active site and the high-energy intermediates deriving from nonnatural substrates of this enzyme (37).

In this study we used as a reference structure the Monte Carlo energy-minimized complex between wild-type ToMO and the high-energy intermediate for the conversion of toluene to *p*-cresol, since this reaction is similar to the desired hydroxylation of 2-phenylethanol to *p*-tyrosol.

Table 1 shows that a correlation exists between the k_{cat} values on toluene of some ToMO mutants (37) and the predicted orientation of the arenium intermediates for the toluene/*p*-cresol reaction with respect to that of our reference structure. Two geometrical parameters defining the orientation of the arenium ring with respect to the diiron cluster were used for the comparison: (i) the distance between the C-4 atom of the mutant-generated complex and the C-4 atom of the reference complex, and (ii) $\Delta\theta$, a parameter that measures the angle deviation of the plane of the arenium ring in a ToMO mutant-intermediate complex with respect to the plane of the arenium ring in the reference structure. θ , whose value in the reference structure is 103.6°, is the torsion angle Fe-2-O-C-4-C-3 (Fig. 2C). It should be noted that the choice of the C-4 atom was made on the basis of the critical importance of this

position of the substrate, which is responsible for accepting the oxygen atom from the diiron cluster during the hydroxylation reaction (Fig. 2A).

It is evident from the data in Table 1 and Fig. S4 in the supplemental material that ToMO mutants characterized by C-4-C-4 distances less than 0.15 Å and $\Delta\theta$ values of about -10° to +5° show high k_{cat} values (similar to or greater than

TABLE 1. Geometric parameters of the complexes between ToMO and ToMO mutants and the arenium intermediate for the toluene/*p*-cresol reaction

Complex	C-4-C-4 (Å)	$\Delta\theta$ (°)	k_{cat} (s ⁻¹) ^a
(L100, G103)/S4M ^b	0.05	-9.0	0.67
L100/S4M	0.06	-1.2	0.56
wt/S4M	0	0	0.43
G103/S4M	0.04	-6.8	0.42
(I180, G103)/S4M	0.04	-6.5	0.34
L176/S4M	0.11	-2.1	0.32
I176/S4M	0.07	+2.0	0.28
I103/S4M	0.15	+3.8	0.22
(V103, V100)/S4M	0.2	+2.5	0.097
A100/S4M	0.05	+12.0	0.03
I103/S4M	0.23	+15.0	0.030
V107/S4M	0.40	-7.1	0.024
I107/S4M	0.49	-9.2	0.0009

^a k_{cat} values are from reference 37.

^b S4M, toluene/*p*-cresol.

TABLE 2. Geometric parameters and ncBEs of the complexes between ToMO and ToMO mutants and the arenium intermediates for the 4PE, 3PE, and 2PE reactions

Amino acid		Arenium ion								
Position 103	Position 176	4PE			3PE			2PE		
		C-4-C-4 (Å)	$\Delta\theta$ (°)	ncBE (kcal mol ⁻¹)	C-4-C-4 (Å)	$\Delta\theta$ (°)	ncBE (kcal mol ⁻¹)	C-4-C-4 (Å)	$\Delta\theta$ (°)	ncBE (kcal mol ⁻¹)
Glu ^a	Phe ^a	0.30	+41	-7.8	0.23	+22	-5.7	0.37	+44	-5.0
Gly ^b	Phe ^b	0.28	+41	-7.5	0.23	+24	-5.6	— ^c	—	—
Glu	Ala	0.20	-10	-11.0	0.20	+17	-9.5	—	—	—
Glu	Ile	0.13	-4	-11.0	0.31	+35	-8.9	—	—	—
Glu	Leu	0.17	-6	-11.1	0.35	+37	-7.5	—	—	—
Glu	Ser	0.15	+9	-10.9	0.22	+20	-9.3	—	—	—
Glu	Thr	0.20	-10	-11.0	0.22	+17	-9.4	—	—	—
Glu	Val	0.14	-6	-11.0	0.21	+15	-9.5	—	—	—
Gly	Ala	0.08	-14	-11.8	0.22	+22	-9.0	—	—	—
Gly	Ile	0.08	-10	-11.7	0.20	+16	-8.5	—	—	—
Gly	Leu	0.14	-5	-10.8	0.30	+38	-6.3	—	—	—
Gly	Ser	0.06	-11	-11.5	0.22	+18	-8.9	—	—	—
Gly	Thr	0.05	-11	-11.5	0.20	+30	-8.9	—	—	—
Gly	Val	0.05	-7	-11.5	0.18	+29	-8.8	—	—	—

^a Wild-type ToMOA.^b (E103G)-ToMOA.^c —, not determined.

those for wild-type ToMO), whereas ToMO mutants characterized by C-4-C-4 distances higher than 0.2 Å and/or $\Delta\theta$ values $>+5^\circ$ show k_{cat} values significantly lower than those measured for the wild-type enzyme.

Hence, we docked into the active site of wild-type ToMO the three high-energy intermediates for the hydroxylation of 2-phenylethanol to *o*-, *m*-, and *p*-tyrosol (these intermediates are indicated 2PE, 3PE, and 4PE, respectively, from here on). As shown in Table 2, the geometries of all the high-energy intermediates showed considerable deviations from the ideal geometry, in agreement with the fact that wild-type ToMO is a bad catalyst for the 2-phenylethanol hydroxylation (k_{cat} value, $0.054 \pm 0.016 \text{ s}^{-1}$) compared to the natural substrate toluene (k_{cat} value, 0.43 s^{-1}). The highest deviations from the ideal orientation were observed in the case of the intermediates 2PE and 4PE, and the lowest was observed for the intermediate 3PE, in agreement with the observation that wild-type ToMO produces ca. 90% *m*-tyrosol.

A close inspection of the model of the ToMO-4PE complex (Fig. 3A), i.e., the analog of the intermediate leading from 2-phenylethanol to the desired substituted phenol, e.g., *p*-tyrosol, showed that van der Waals contacts between the side chain of Phe-176 and the hydroxyethyl moiety of 4PE that are too close prevent the positioning of the arenium ring of this intermediate in an orientation similar to that of the reference structure, thus providing a geometrical explanation for the low production of *p*-tyrosol by wild-type ToMO (Fig. 3A and B). We repeated the same analysis on six ToMO mutants with smaller residues at position 176 (Ile, Leu, Val, Thr, Ser, and Ala). In this case, the docking procedure was carried out only with the high-energy intermediates 3PE and 4PE, because a preliminary analysis revealed that mutations at position 176 did not significantly change the C-4-C-4, $\Delta\theta$, and ncBE values for 2PE with respect to that measured for wt ToMO (data not shown).

The data in Table 2 indicate that the geometrical parameters

of most of these mutants show a better similarity of their complexes with the reference structure only in the case of the arenium ring of 4PE, the intermediate leading to *p*-tyrosol. The data show that for all mutations at position 176, the orientation of the 4PE intermediate is more similar to that of the reference model than that of wt ToMO: the C-4-C-4 distances are between 0.13 and 0.20 Å and the $\Delta\theta$ values are between -9° and $+10^\circ$. However, these values are out of the limits defined from the data in Table 1. Moreover, a careful inspection of these complexes revealed that the side chain of Glu-103, which, in wt ToMO, is closely packed to the Phe-176 side chain, could limit the conformational freedom of the side chain of residues modeled at position 176. Therefore, we also modeled six double mutants in which all the mutations at position 176 were coupled with mutation E103G, which could, in principle, remove the hindrance of the bulky side chain at position 103. Data in Table 2 show that for all the double mutants, with the exception of ToMO mutant (E103G, F176L), the C-4-C-4 distances are less than 0.1 Å and $\Delta\theta$ values are less than 0° , i.e., within the limits defined from the data in Table 1 for high- k_{cat} mutants, only when docking the arenium ring of 4PE. It is also worth noting that as the orientation of the intermediate 4PE becomes more similar to that of the reference model complex, the ncBE of the intermediate becomes more negative, thus indicating a better fit between the 4PE intermediate and the active-site pocket.

Thus, on the basis of our assumption, i.e., that a correlation exists between the k_{cat} values and the predicted orientation of the arenium rings compared to that of the reference structure, we can hypothesize that all mutations at position 176, both alone and in combination with mutation E103G, selectively improve the binding of the intermediate 4PE. As a consequence, these mutants should exclusively produce *p*-tyrosol.

However, according to our kinetic model, a good positioning of the arenium intermediate, although essential, is not a sufficient condition for an efficient catalysis, given that mutations

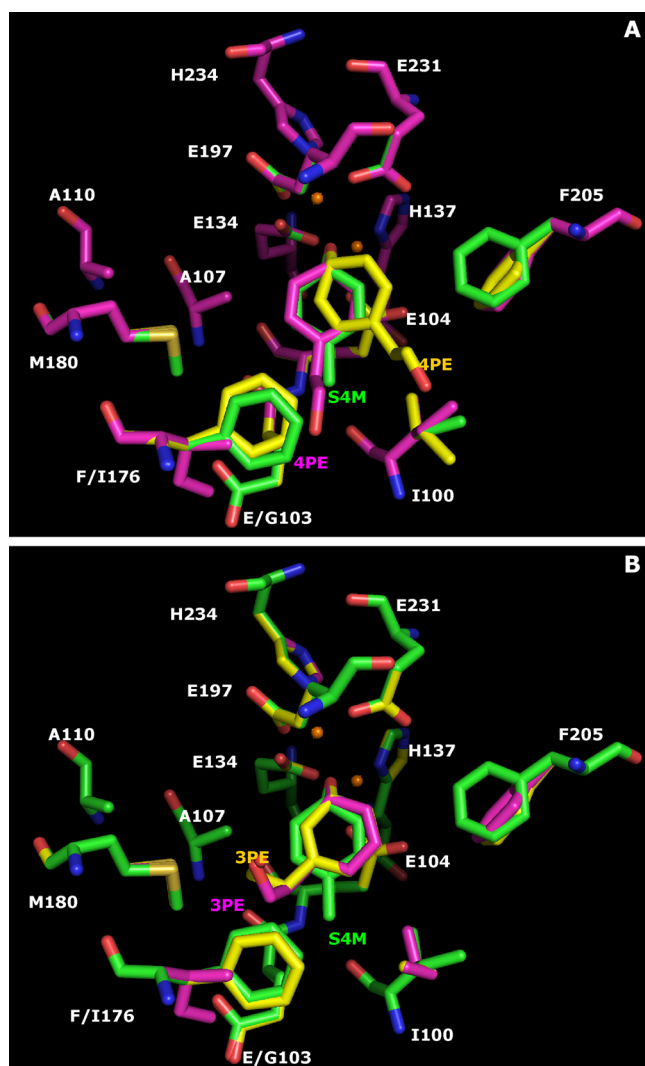


FIG. 3. Structures of the complexes between wt ToMO or ToMO mutants and the arenium intermediates for the reactions 4PE (A), 3PE (B), and toluene/*p*-cresol (S4M) (A and B). Carbon atoms are shown in green (S4M/ToMO), yellow (4PE/ToMO and 3PE/ToMO), and magenta [4PE/(E103G, F176I)-ToMO and 3PE/(E103G, F176I)-ToMO]; oxygen atoms are shown in red, and nitrogen atoms are shown in blue. Hydrogen atoms are not shown.

which stabilize unproductive orientations of the substrate will reduce the apparent k_{cat} value. Therefore, even if all the double mutants bind the 4PE intermediate in a correct orientation and with similar noncovalent binding energies, different k_{cat} values could be obtained.

In order to predict which double mutant(s) is the best catalyst for the production of *p*-tyrosol, it is necessary to define a strategy to predict the ratio between the abundance of productive and nonproductive enzyme-substrate complexes. Monte Carlo docking of the substrate 2-phenylethanol provides a panel of possible orientations of the substrate in the active site of the double mutants, whereas comparison of the orientations of 2-phenylethanol in the complexes and the reference structure, i.e., the complex between wild-type ToMO and the arenium intermediate for the conversion of toluene to

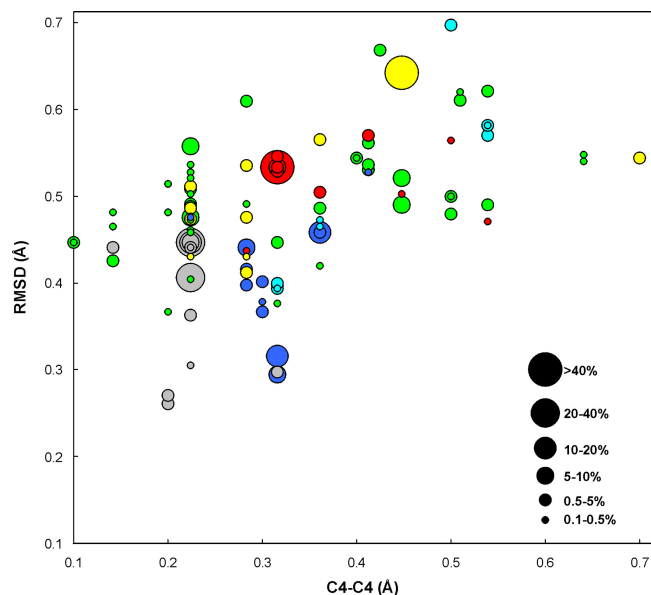


FIG. 4. Calculated relative abundance (in percent) of the ToMO-2-phenylethanol complexes as a function of the distance between the C-4 atom of the 2-phenylethanol and the C-4 atom of the reference structure and of the RMSD between the ring of 2-phenylethanol and the ring of the reference structure. Red circles, (E103G, F176A)-ToMO; gray circles, (E103G, F176I)-ToMO; cyan circles, (E103G, F176L)-ToMO; blue circles, (E103G, F176S)-ToMO; green circles, (E103G, F176T)-ToMO; yellow circles, (E103G, F176V)-ToMO.

p-cresol, helps to discriminate between productive and nonproductive enzyme-substrate complexes. Thus, we docked 2-phenylethanol into the active site of the double mutants; the total energies of the complexes were calculated and used to estimate their relative abundance at equilibrium. Finally, we compared the orientations of the substrate in these complexes with the orientation of the arenium intermediate in the reference structure. Figure 4 shows the abundance of the ToMO-phenylethanol complexes as a function of the distance between the C-4 atom of 2-phenylethanol and the C-4 atom of the reference structure (*x* axis) and of the root mean square deviation (RMSD) between the ring of phenylethanol and the arenium ring of the reference structure (*y* axis). It should be noted that as 2-phenylethanol is not covalently bound to the diiron cluster, in this case, the Fe-2-O-C-4-C-3 torsion angles, θ , are meaningless.

Data in Fig. 4 show that the double mutants dock 2-phenylethanol in slightly different orientations. (E103G, F176T)- and (E103G, F176I)-ToMO show high percentages of complexes with very short C-4-C-4 distances and RMSDs, respectively. This means that in this case 2-phenylethanol adopts in the active site orientations very similar to the orientation of the arenium ion of the reference structure, thus suggesting that the active sites of these mutants can properly orient the substrate for catalysis. On the contrary, only complexes with both relatively long C-4-C-4 distances and RMSDs are predicted for a mutant like (E103G, F176A)-ToMO, suggesting that in this mutant a larger rearrangement is necessary to switch from the enzyme-substrate complex to the transition state (the enzyme-arenium ion complex). The remaining three double mutants show an intermediate behavior. On the basis of our data,

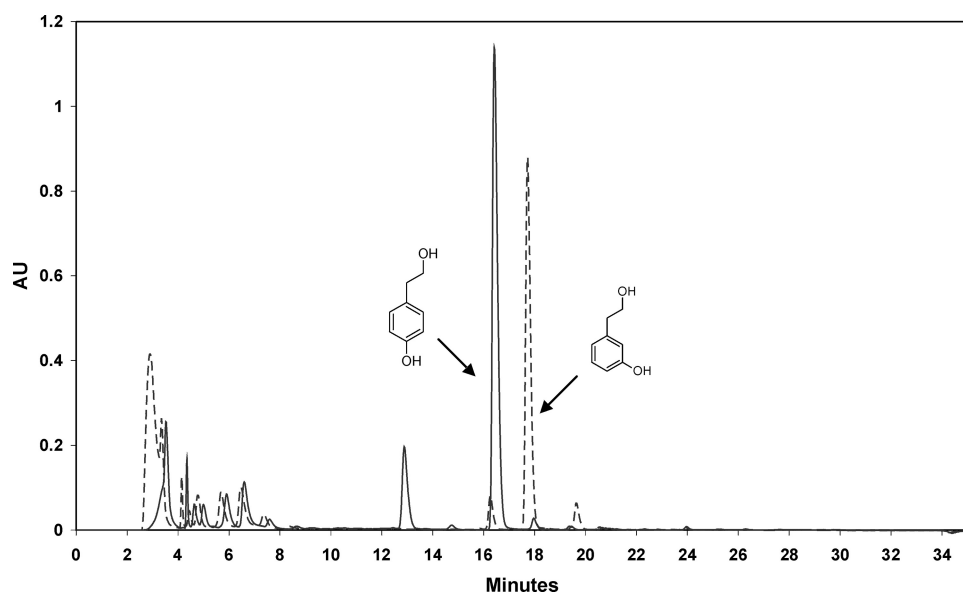


FIG. 5. Regioselectivity of ToMO/F176T-catalyzed reaction using 2-phenylethanol as a substrate (solid line). An HPLC chromatogram monitored at a λ of 276 nm shows the presence of a single product corresponding to *p*-tyrosol. The dashed-line trace is the HPLC profile monitored under the same experimental conditions using wt ToMO. Results are similar for both the F176X and E103G/F176X mutants. AU, absorbance units.

we can predict the following order of k_{cat} values: (E103G, F176T)- and (E103G, F176I)-ToMO > (E103G, F176L)-, (E103G, F176V)-, and (E103G, F176S)-ToMO > (E103G, F176A)-ToMO.

To validate our hypothesis, we prepared and characterized mutants with single mutations of ToMOA, i.e., F176I, F176L, and F176T, as well as mutants with double mutations, E103G-F176(I, L, T, A, S, V), to verify whether these changes would affect the catalytic efficiency of the enzyme on 2-phenylethanol according to our predictions.

Identification of reaction products and determination of kinetic parameters of ToMO mutant-catalyzed hydroxylation of 2-phenylethanol. Enzymatic assays on recombinant whole cells of *E. coli* strain JM109 expressing ToMOA mutants and using 2-phenylethanol as substrate were carried out as described in the Materials and Methods section. Reaction products were identified by HPLC and NMR. Our results (Fig. 5) clearly indicate that substitution of residue F176 is essential to obtain almost exclusively *p*-tyrosol from 2-phenylethanol. For all mutants with a mutation at position 176, no detectable *o*-tyrosol was observed and *m*-tyrosol yields were less than 2%. Also, double mutants produced only *p*-tyrosol, whereas ToMOA variant E103G shows the same regiospecificity as the wild-type enzyme on 2-phenylethanol (data not shown). The analysis of the kinetic parameters (Table 3) indicates that variants bearing E103G/F176X mutations have higher k_{cat} values on 2-phenylethanol than the corresponding variants with single mutations. Therefore, confirming our hypothesis, it seems that reduction of steric hindrance at position 103 (13, 37, 45) acts in a synergistic manner with mutations at position 176. Global reduction of steric hindrance inside the active site likely allows for a better fitting of 2-phenylethanol, resulting in an increase of the k_{cat} value. It should be noted, however, that the strategy of widening the active site fails to be effective when the data

obtained for mutant E103G/F176A are analyzed. In this case, in fact, an excessive broadening of the active site leads to a drastic decrease in the catalytic efficiency of the enzyme, likely due to a degree of freedom of 2-phenylethanol inside the active site of this mutant that is too high.

The higher k_{cat} value measured on 2-phenylethanol is obtained with variant E103G/F176T. The Monte Carlo-minimized models show that in this double mutant the —OH group of threonine forms an H bond with the backbone oxygen atom of Ala-172, whereas the methyl group points toward the active-site cavity and makes van der Waals interactions with the hydroxyethyl group of both 2-phenylethanol and the 4PE intermediate (see Figure S5A and B in the supplemental material). Thus, the model suggests that the active site of mutant E103G/F176T allows for the appropriate orientation of both the substrate and the intermediate. In this mutant, however, van der Waals contacts between the methyl group of the threonine residue and the hydroxyl group of 2-phenylethanol involve a partial desolvation of the hydroxyl group of the sub-

TABLE 3. Apparent K_m and k_{cat} values of ToMO and ToMO mutants using 2-phenylethanol as substrate

Mutant	K_m (μM)	k_{cat} (s^{-1})
wt	211 (± 22)	$5.4 (\pm 1.6) \times 10^{-2}$
F176I	392 (± 28)	$2.8 (\pm 0.1) \times 10^{-2}$
F176L	276 (± 52)	$3.8 (\pm 0.5) \times 10^{-2}$
F176T	662 (± 46)	$14.0 (\pm 0.5) \times 10^{-2}$
E103G/F176A	404 (± 25)	$6.0 (\pm 0.1) \times 10^{-2}$
E103G/F176I	759 (± 160)	$47.0 (\pm 4.0) \times 10^{-2}$
E103G/F176L	362 (± 44)	$18.0 (\pm 0.7) \times 10^{-2}$
E103G/F176T	1,045 (± 66)	$71.0 (\pm 1.9) \times 10^{-2}$
E103G/F176S	557 (± 42)	$14.5 (\pm 0.5) \times 10^{-2}$
E103G/F176V	435 (± 52)	$14.9 (\pm 0.6) \times 10^{-2}$

strate (see Fig. S5B in the supplemental material), thus determining a decrease of the apparent affinity for the substrate (i.e., an increase of the K_m value; Table 3).

Thus, our experimental results are in good agreement with the computational model. First, the model identified residue F176 as the major constraint for the productive orientation of the 4PE reactive intermediate. Moreover, our model correctly predicts an increase of the k_{cat} value on 2-phenylethanol when mutation F176X, responsible for the regioselectivity of the hydroxylation reaction on this substrate, is combined with mutation E103G.

This can be noticed by comparing the data in Fig. 4 and the k_{cat} values in Table 3. The two double mutants with the highest k_{cat} values, (E103G, F176T)- and (E103G, F176I)-ToMO, in fact show high percentages of complexes with very short C-4–C-4 distances and RMSDs, respectively. Mutant (E103G, F176A)-ToMO, the one with the lowest k_{cat} value among the double mutants, is instead predicted to yield only complexes with long C-4–C-4 distances and high RMSDs. The other three double mutants show an intermediate behavior for C-4–C-4 distances and RMSDs and also show intermediate k_{cat} values. We can affirm that the docking procedure that we have developed allows prediction of the relative k_{cat} values of ToMO mutants on the nonphysiological substrate 2-phenylethanol.

Finally, with the aim of investigating a future industrial application of ToMO mutants for the bioconversion of 2-phenylethanol to *p*-tyrosol, we calculated the yield of *p*-tyrosol produced by the most effective catalysts, E103G/F176I and E103G/F176T (Table 3). The yield of *p*-tyrosol produced in a minimal medium by recombinant whole cells was evaluated in batch experiments. *E. coli* strain JM109 cells harboring the plasmid coding for either the E103G/F176I or the E103G/F176T mutant were grown and induced as described in Materials and Methods. After induction, cells were harvested and suspended in M9-G medium containing 2 mM 2-phenylethanol at an OD₆₀₀ of 1. Cells were then incubated at 30°C, under constant shaking at 200 rpm. At different times a 1-ml sample was withdrawn and centrifuged at 12,000 rpm at 4°C for 10 min, and an aliquot of the cell-free supernatant was analyzed by HPLC. The amount of either 2-phenylethanol or *p*-tyrosol was determined by comparing the area of each peak with the area obtained using known concentrations of standards. *p*-Tyrosol was the only isomer produced (within the limits of our assay procedure) with mutants E103G/F176I and E103G/F176T. After 2 h of incubation, the yields of transformation obtained from 2-phenylethanol were 50.2 ± 0.2% for E103G/F176I and 56.3 ± 2.4% for E103G/F176T.

Conclusions. Both directed evolution and rational design approaches have been successfully used in numerous studies probing multicomponent monooxygenase-catalyzed reactions (10, 11, 13, 14, 24, 37, 49, 52). These studies clearly show that these monooxygenases may be considered an archive of powerful and versatile enzymes which can be used to create new catalysts useful for diverse purposes, such as bioremediation of harmful compounds and industrial biosynthesis, among others.

We have previously shown that a fine-tuning of the regioselectivity of the BMM ToMO from *Pseudomonas* sp. OX1 on natural substrates can be achieved through careful alteration of the shape of the active site and that the effects of the mutations on regioselectivity can be quantitatively predicted *a*

priori (13, 37). The computational model described in this paper and tested by its application to the synthesis of *p*-tyrosol from 2-phenylethanol, a nonnatural substrate of ToMO, improves the model previously presented for this enzyme (37). Our experimental data validate the computational model presented in this work, showing that mutation of residue F176 allows ToMO to produce exclusively *p*-tyrosol from 2-phenylethanol and that mutation E103G increases the efficiency of catalysis of the enzyme on this substrate.

REFERENCES

- Allouche, N., M. Damak, R. Ellouz, and S. Sayadi. 2004. Use of whole cells of *Pseudomonas aeruginosa* for synthesis of the antioxidant hydroxytyrosol via conversion of tyrosol. *Appl. Environ. Microbiol.* **70**:2105–2109.
- Allouche, N., and S. Sayadi. 2005. Synthesis of hydroxytyrosol, 2-hydroxyphenylacetic acid, and 3-hydroxyphenylacetic acid by differential conversion of tyrosol isomers using *Serratia marcescens* strain. *J. Agric. Food Chem.* **53**:6525–6530.
- Bailey, L. J., J. G. McCoy, G. N. Phillips, Jr., and B. G. Fox. 2008. Structural consequences of effector protein complex formation in a diiron hydroxylase. *Proc. Natl. Acad. Sci. U. S. A.* **105**:19194–19198.
- Bertoni, G., F. Bolognese, E. Galli, and P. Barbieri. 1996. Cloning of the genes for and characterization of the early stages of toluene and o-xylene catabolism in *Pseudomonas stutzeri* OX1. *Appl. Environ. Microbiol.* **62**:3704–3711.
- Bertoni, G., M. Martino, E. Galli, and P. Barbieri. 1998. Analysis of the gene cluster encoding toluene/o-xylene monooxygenase from *Pseudomonas stutzeri* OX1. *Appl. Environ. Microbiol.* **64**:3626–3632.
- Bouallagui, Z., and S. Sayadi. 2006. Production of high hydroxytyrosol yields via tyrosol conversion by *Pseudomonas aeruginosa* immobilized resting cells. *J. Agric. Food Chem.* **54**:9906–9911.
- Boyd, D. R., and T. D. Bugg. 2006. Arene cis-dihydrodiol formation: from biology to application. *Org. Biomol. Chem.* **4**:181–192.
- Boyd, D. R., N. D. Sharma, and C. C. Allen. 2001. Aromatic dioxygenases: molecular biocatalysis and applications. *Curr. Opin. Biotechnol.* **12**:564–573.
- Bradford, M. M. 1976. A rapid and sensitive method for the quantitation of microgram quantities of protein utilizing the principle of protein-dye binding. *Anal. Biochem.* **72**:248–254.
- Brouk, M., and A. Fishman. 2009. Protein engineering of toluene monooxygenases for synthesis of hydroxytyrosol. *Food Chem.* **116**:114–121.
- Brouk, M., Y. Nov, and A. Fishman. 2010. Improving biocatalyst performance by integrating statistical methods into protein engineering. *Appl. Environ. Microbiol.* **76**:6397–6403.
- Cafaro, V., et al. 2004. Phenol hydroxylase and toluene/o-xylene monooxygenase from *Pseudomonas stutzeri* OX1: interplay between two enzymes. *Appl. Environ. Microbiol.* **70**:2211–2219.
- Cafaro, V., E. Notomista, P. Capasso, and A. Di Donato. 2005. Mutation of glutamic acid 103 of toluene o-xylene monooxygenase as a means to control the catabolic efficiency of a recombinant upper pathway for degradation of methylated aromatic compounds. *Appl. Environ. Microbiol.* **71**:4744–4750.
- Cafaro, V., E. Notomista, P. Capasso, and A. Di Donato. 2005. Regioselectivity of two multicomponent monooxygenases from *Pseudomonas stutzeri* OX1: molecular basis for catabolic adaptation of this microorganism to methylated aromatic compounds. *Appl. Environ. Microbiol.* **71**:4736–4743.
- Cafaro, V., et al. 2002. Expression and purification of the recombinant subunits of toluene/o-xylene monooxygenase and reconstitution of the active complex. *Eur. J. Biochem.* **269**:5689–5699.
- Capasso, R., et al. 1995. Antibacterial polyphenols from olive oil mill waste waters. *J. Appl. Bacteriol.* **79**:393–398.
- Covas, M. I., et al. 2003. Bioavailability of tyrosol, an antioxidant phenolic compound present in wine and olive oil, in humans. *Drugs Exp. Clin. Res.* **29**:203–206.
- Deiana, M., et al. 1999. Inhibition of peroxynitrite dependent DNA base modification and tyrosine nitration by the extra virgin olive oil-derived antioxidant hydroxytyrosol. *Free Radic. Biol. Med.* **26**:762–769.
- de la Puerta, R., V. Ruiz Gutierrez, and J. R. Hout. 1999. Inhibition of leukocyte 5-lipoxygenase by phenolics from virgin olive oil. *Biochem. Pharmacol.* **57**:445–449.
- Dordick, J. S., Y. L. Khmelnsky, and M. V. Sergeeva. 1998. The evolution of biotransformation technologies. *Curr. Opin. Microbiol.* **1**:311–318.
- Espin, J. C., C. Soler-Rivas, E. Cantos, F. A. Tomas-Barberan, and H. J. Wichers. 2001. Synthesis of the antioxidant hydroxytyrosol using tyrosinase as biocatalyst. *J. Agric. Food Chem.* **49**:1187–1193.
- Etchmann, M. M., W. Bluemke, D. Sell, and J. Schrader. 2002. Biotechnological production of 2-phenylethanol. *Appl. Microbiol. Biotechnol.* **59**:1–8.
- Feingersch, R., J. Shainsky, T. K. Wood, and A. Fishman. 2008. Protein engineering of toluene monooxygenases for synthesis of chiral sulfoxides. *Appl. Environ. Microbiol.* **74**:1555–1566.
- Fishman, A., Y. Tao, L. Rui, and T. K. Wood. 2005. Controlling the regio-

- specific oxidation of aromatics via active site engineering of toluene para-monooxygenase of *Ralstonia pickettii* PKO1. *J. Biol. Chem.* **280**:506–514.
25. Gao, F., and A. J. Daugulis. 2009. Bioproduction of the aroma compound 2-phenylethanol in a solid-liquid two-phase partitioning bioreactor system by *Kluyveromyces marxianus*. *Biotechnol. Bioeng.* **104**:332–339.
26. Ishige, T., K. Honda, and S. Shimizu. 2005. Whole organism biocatalysis. *Curr. Opin. Chem. Biol.* **9**:174–180.
27. Kelsey, N. A., H. M. Wilkins, and D. A. Linseman. 2010. Nutraceutical antioxidants as novel neuroprotective agents. *Molecules* **15**:7792–7814.
28. Laemmli, U. K. 1970. Cleavage of structural proteins during the assembly of the head of bacteriophage T4. *Nature* **227**:680–685.
29. Lazaridis, T., and M. Karplus. 1999. Discrimination of the native from misfolded protein models with an energy function including implicit solvation. *J. Mol. Biol.* **288**:477–487.
30. Lazaridis, T., and M. Karplus. 1999. Effective energy function for proteins in solution. *Proteins* **35**:133–152.
31. Leahy, J. G., P. J. Batchelor, and S. M. Morcomb. 2003. Evolution of the soluble diiron monooxygenases. *FEMS Microbiol. Rev.* **27**:449–479.
32. Lippard, S. J. 2005. Hydroxylation of C-H bonds at carboxylate-bridged diiron centres. *Philos. Trans. A Math. Phys. Eng. Sci.* **363**:861–877.
33. Loughlin, W. A. 2000. Biotransformations in organic synthesis. *Biores. Technol.* **74**:49–62.
34. Manna, C., V. Migliardi, F. Sannino, A. De Martino, and R. Capasso. 2005. Protective effects of synthetic hydroxytyrosol acetyl derivatives against oxidative stress in human cells. *J. Agric. Food Chem.* **53**:9602–9607.
35. Merx, M., et al. 2001. Dioxygen activation and methane hydroxylation by soluble methane monooxygenase: a tale of two irons and three proteins. *Angew. Chem. Int. ed. Engl.* **40**:2782–2807.
36. Murray, L. J., and S. J. Lippard. 2007. Substrate trafficking and dioxygen activation in bacterial multicomponent monooxygenases. *Acc. Chem. Res.* **40**:466–474.
37. Notomista, E., V. Cafaro, G. Bozza, and A. Di Donato. 2009. Molecular determinants of the regioselectivity of toluene/o-xylene monooxygenase from *Pseudomonas* sp. strain OX1. *Appl. Environ. Microbiol.* **75**:823–836.
38. Notomista, E., A. Lahm, A. Di Donato, and A. Tramontano. 2003. Evolution of bacterial and archaeal multicomponent monooxygenases. *J. Mol. Evol.* **56**:435–445.
39. Owen, R. W., et al. 2000. Olive-oil consumption and health: the possible role of antioxidants. *Lancet Oncol.* **1**:107–112.
40. Parales, R. E., N. C. Bruce, A. Schmid, and L. P. Wackett. 2002. Biodegradation, biotransformation, and biocatalysis (b3). *Appl. Environ. Microbiol.* **68**:4699–4709.
41. Park, J., et al. 2007. The analysis and application of a recombinant monooxygenase library as a biocatalyst for the Baeyer-Villiger reaction. *J. Microbiol. Biotechnol.* **17**:1083–1089.
42. Petroni, A., et al. 1995. Inhibition of platelet aggregation and eicosanoid production by phenolic components of olive oil. *Thromb. Res.* **78**:151–160.
43. Rietjens, S. J., A. Bast, and G. R. Haenen. 2007. New insights into controversies on the antioxidant potential of the olive oil antioxidant hydroxytyrosol. *J. Agric. Food Chem.* **55**:7609–7614.
44. Sambrook, J., E. F. Fritsch, and T. Maniatis. 1989. *Molecular cloning: a laboratory manual*, 2nd ed. Cold Spring Harbor Laboratory Press, Cold Spring Harbor, NY.
45. Sazinsky, M. H., J. Bard, A. Di Donato, and S. J. Lippard. 2004. Crystal structure of the toluene/o-xylene monooxygenase hydroxylase from *Pseudomonas stutzeri* OX1. Insight into the substrate specificity, substrate channeling, and active site tuning of multicomponent monooxygenases. *J. Biol. Chem.* **279**:30600–30610.
46. Sazinsky, M. H., and S. J. Lippard. 2006. Correlating structure with function in bacterial multicomponent monooxygenases and related diiron proteins. *Acc. Chem. Res.* **39**:558–566.
47. Singleton, V. L., R. Orthofer, and R. M. Lamuela-Raventós. 1999. Analysis of total phenols and other oxidation substrates and antioxidants by means of Folin-Ciocalteu reagent. *Methods Enzymol.* **299**:152–178.
48. Straathof, A. J., S. Panke, and A. Schmid. 2002. The production of fine chemicals by biotransformations. *Curr. Opin. Biotechnol.* **13**:548–556.
49. Tao, Y., A. Fishman, W. E. Bentley, and T. K. Wood. 2004. Altering toluene 4-monooxygenase by active-site engineering for the synthesis of 3-methoxycatechol, methoxyhydroquinone, and methylhydroquinone. *J. Bacteriol.* **186**:4705–4713.
50. Torres Pazmino, D. E., M. Winkler, A. Glieder, and M. W. Fraaije. 2010. Monooxygenases as biocatalysts: classification, mechanistic aspects and biotechnological applications. *J. Biotechnol.* **146**:9–24.
51. Vardar, G., Y. Tao, J. Lee, and T. K. Wood. 2005. Alanine 101 and alanine 110 of the alpha subunit of *Pseudomonas stutzeri* OX1 toluene-o-xylene monooxygenase influence the regiospecific oxidation of aromatics. *Biotechnol. Bioeng.* **92**:652–658.
52. Vardar, G., and T. K. Wood. 2005. Protein engineering of toluene-o-xylene monooxygenase from *Pseudomonas stutzeri* OX1 for enhanced chlorinated ethene degradation and o-xylene oxidation. *Appl. Microbiol. Biotechnol.* **68**:510–517.
53. Viggiani, A., et al. 2004. The role of the conserved residues His-246, His-199, and Tyr-255 in the catalysis of catechol 2,3-dioxygenase from *Pseudomonas stutzeri* OX1. *J. Biol. Chem.* **279**:48630–48639.
54. Visioli, F., A. Poli, and C. Gall. 2002. Antioxidant and other biological activities of phenols from olives and olive oil. *Med. Res. Rev.* **22**:65–75.
55. Watanabe, K., H. Futamata, and S. Harayama. 2002. Understanding the diversity in catabolic potential of microorganisms for the development of bioremediation strategies. *Antonie Van Leeuwenhoek* **81**:655–663.
56. Waterman, E., and B. Lockwood. 2007. Active components and clinical applications of olive oil. *Altern. Med. Rev.* **12**:331–342.